Investigating the Role of RAP2.12 and GAPDH in Photosynthetic CO_2 Fixation to Improve Drought Tolerance

Mohammed Khader Alqurashi

A thesis submitted for the degree of Doctor of Philosophy

School of Biological Sciences

University of Essex

Date of submission

January 2019

Abstract

Manipulation of photosynthetic processes offers an opportunity to increase food production in plants. Current and previous studies have shown that various efforts have been made towards manipulation of photosynthesis to increase crop yield. VBSSM Modelling has been used to identify critical genes involved in the regulation of photosynthetic carbon assimilation. Three highly connected genes were identified as being important in influencing drought-induced transcriptional responses of the genes that encode for enzymes of the Calvin cycle. These genes are the drought-inducible transcription factor RAP2.12, the Calvin cycle gene GAPA-2 and a putative transcription factor (At1g16750) (Bechtold et al., 2016). The first objective was to investigate this model prediction and to determine if GAPA-2 and *RAP2.12* are playing essential roles in the regulation of Calvin cycle enzymes under drought and non-drought condition. The single and double mutant lines of *RAP2.12* with OE GAPA-2 showed highly variable, and there is no significant difference in growth analyses. Furthermore, it is evident that in the *RAP2.12* mutant that the expression of the Calvin cycle genes is altered, predominately under drought stress conditions. Although these changes were not exactly as expected by the modelling these data provide new information on this gene network. Moreover, it has been revealed that the relative amounts of GAPDH plastids subunit (A2B2) and (A4) vary between species, but almost always the A2B2 form is predominant (Howard et al., 2011b). Previously, plants without A4 have been recognised, but no plants without A2B2 have been identified. The second hypothesis was to study the role of GAPB subunit in determining the photosynthetic rate in plants. Arabidopsis and tobacco plants with reduced the protein level of GAPA and GAPB were produced. Transgenic Arabidopsis lines of GAPA and GAPB showed a significant decrease in leaf number and rosette dry weight together with a reduction in photosynthetic capacity.

Table of Contents

Acknowledgements

I would like to express my sincere gratefulness to my supervisors Professor Christine Raines and Dr Ulrike Bechtold for all of the support and encouragement. Also thank you to Prof Tracy Lawson for the comments and suggestions given at all board meetings during my PhD studies. Additionally, I would like to thank my family and all lab members especially, Dr Andrew Simkin for producing and some transgenic Arabidopsis plants and help throughout this study.

List of abbreviations

°C – degree Celsius

µg – microgram

µl – microliter

µmol – micromoles

cm – centimetre

Col-0 – Columbia-0

DNA – Deoxyribonucleic acid

g – relative centrifugal force

rSWC – relative soil water content

T-DNA – Transfer DNA

VBSSM – Variational Bayesian State Space Modelling

WT – wild-type

ATP- Adenosine triphosphate

°C- Temperature

CO_2- Carbon dioxide

PPFD- Photosynthetic Photon Flux Density

RNA- Ribonucleic acid

dNTP -Deoxynucleoside- 5'- phosphate

EDTA -Ethylenediaminetra-acetic acid (disodium salt)

HCL- hydrochloric acid

H-hours

LB media- Luria Agar Media

DDH2O- Double-distilled water

DNase- A deoxyribonuclease

cDNA- Complementary DNA

HEPES- (4-(2-hydroxyethyl)-1-piperazineethanesulfonic acid)

$MgCl_2$ - Magnesium chloride

EGTA- (ethylene glycol-bis(β-aminoethyl ether)-N,N,N',N'-tetraacetic acid)

PMSF- phenylmethane sulfonyl fluoride

DTT- Dithiothreitol

NaCl- Sodium chloride

KCL- Potassium Chloride

Na2HPO4- sodium hydrogen phosphate

KH2PO4- Monopotassium phosphate

G3P-Glyceraldehyde 3-phosphate

ml- Millilitre

RNase- Ribonuclease

APS- Adapter protein with a PH and SH2 domain

NADP- Nicotinamide adenine dinucleotide phosphate

NADPH-Reduced nicotinamide adenine dinucleotide phosphate

NADH-Nicotinamide adenine dinucleotide (reduced form)

PCR- Polymerase Chain Reaction

QPCR- quantitative polymerase chain reaction

mM-millimole

RT-Room Temperature

RuBP-Ribulose 1,5-bisphosphate

S- Second

SDS-Sodium dodecyl sulfate

TAE-TRIS-base, acetic acid and edta

TBA-Tris-base, B orate and EDTA

Temed-Tetramethylethylenediamine

TK-Transketolase

Tris- 2-amin0-2(h ydroxymethyl) propene 1,3-diol

Tween-20-Polysorbate 20

UTR- Untranslated region

V- Volt

List of Figures

List of Tables

Chapter 1: Literature review

1.1 General background

A steadily increasing global population has led to an ever-increasing claim for food and fuel resources. However, annual increases in agricultural yields have reached a plateau and in some species are declining (Fischer and Edmeades, 2010; Ray et al., 2013; Long et al., 2015; Ort et al., 2015). There is an urgent requirement to improve crop yields to ensure the continuing availability of food. The world-wide requirement for cereal production is predicted to rise by 60% when the global population reaches 9.6 billion. It has been expected that by 2050, the food requirement will be almost double what it is today (FAO (Food & Agriculture Organisation), 2012; FAO, 2013; Horton, 2000; Fischer and Edmeades, 2010; Uematsu et al., 2012). It is a known fact that drought stress reduces the photosynthetic rate per unit leaf area as well as the leaf area itself, consequently reducing photosynthesis. The key means by which the photosynthetic rate is reduced is through metabolic impairment or stomatal closure (Tezara et al., 1999). Changes within the photosynthetic carbon metabolism are the principal cause of the metabolic damage in the drought stress (Lawlor and Cornic, 2002). Under drought stress, the principal dependence of the biochemical effectiveness of photosynthesis is upon ribulose-1,5-bisphosphate (RuBP) regeneration as well as the ribulose-1,5-bisphosphate carboxylase/oxygenase (RuBisCO) activity (Medrano et al., 1997; Lawlor, 2002). There has been much development in the enhancement of metabolic changes, photosynthetic light reaction as well as the CO_2 stomatal components. These include the photosynthesis-related expression to control photosynthesis under drought conditions in order to enhance the grain yield (Chaves et al., 2009). It has been implied that the carbon assimilation C4 pathway is the primary C3 pathway adaptation to restrict water loss, develop

photosynthetic efficiency and decrease photorespiration under drought stress (Cockburn, 1983). Nevertheless, the photosynthesis C3 pathway is present significant crops such as potato, soybean, wheat and rice (Black, 2003; South et al., 2019). Despite the fact that the C4 pathway is being transferred into C3 crops, it makes only a minimal contribution to growth in grain yield (Gowik and Westhoff, 2011). When plants are photosynthetically adapted to drought stress, there is a complicated interaction of sugars, ROS, hormones as well as other metabolic occurrences (Pinheiro and Chaves, 2011). Combined computational paradigms which assimilate with the metabolic and physiological procedures and gene expression data together with transgenic and breeding tools have considerable potential to enhance photosynthesis, and consequently, crop yields in both drought stress and normal conditions. Photosynthesis, therefore, represents an unexploited chance in research planning to increase crop yields. For instance, there increase crop yields using genetic manipulation to improve photosynthetic carbon fixation (Horton, 2000; Sharma and Dubey, 2005; Raines, 2006; Feng et al., 2007; Rosenthal et al., 2011).

1.2 The Photosynthetic Process

Photosynthesis is a complex process by which the sun's energy is changed to ATP and NADPH, and CO_2 is fixed into organic molecules using this energy. This process adds compounds to carbon backbones used for biosynthesis and metabolic energy in all cellular procedures and generates the oxygen molecules essential to all aerobic organisms. The photochemical process consists of two different and associated stages. Light-dependent reactions take place in the plant's thylakoid membranes, where a photon is absorbed by chlorophyll electron, leading to the flow of electrons down an electron transport chain resulting in the reduction of NADP to NADPH and the release of O_2. In light-independent or "dark" reactions, the enzyme RuBisCO captures CO_2 from the

atmosphere and uses NADPH to generate three-carbon sugars in a process known as the Calvin–Benson or C3 cycle in the chloroplast stroma. ATP and NADPH formed from light reactions are used to fix inorganic CO_2 to organic compounds. This results in the biosynthesis of the carbohydrates that are essential for plant's growth; this process is often referred to as carbon fixation or assimilation (Bassham *et al.*, 1950; Bassham, 2003; Raines and Paul, 2006; Stitt, Lunn and Usadel, 2010; Kramer and Evans, 2011).

1.3 The Calvin-Benson cycle

Photosynthetic CO_2 assimilation takes place in the chloroplasts of plants, and inorganic carbon is assimilated via the Calvin-Benson, C3 cycle. This cycle of photosynthetic carbon reduction is the primary method of carbon fixation, and it occurs in the stroma of chloroplasts. This cycle also plays an essential role in plant metabolism and carbon flux (Geiger and Servaites, 1994). The cycle involves enzymes that act to catalyse reactions and manipulate their kinetic properties was studied elucidated in the 1950s by Melvin Calvin and his colleagues. The net products of CO_2 assimilation are the triose phosphates, which are the main intermediates of the Calvin-Benson cycle and an important supply of starch, shikimate, thiamine nucleotides, isoprenoids, and sucrose for the other biosynthetic pathways contained therein (Bassham *et al.*, 1950; Raines, 2003b; Lefebvre *et al.*, 2005). The Calvin-Benson cycle involves eleven enzymes that act to catalyse thirteen different reactions (Figure1.1). It takes place in three distinct phases, which occur continuously. These three phases are the fixation of carbon dioxide, reduction, and regeneration of RuBP. The first phase involves carboxylation of the CO_2 acceptor molecule RuBP by RuBisCO; consequently, two molecules of a unchanging three carbon product acknowledged as 3-PGA are formed, leading some to refer to it as the "C3 cycle." Next, the NADPH and ATP products of photosynthetic light reactions are

used in the reductive stage through two reactions utilising 3-PGA for atmospheric CO_2 fixation into carbon backbones, triose phosphate, glyceraldehyde 3-phosphate (G3P), and dihydroxyacetone phosphate (DHAP); this results in the production of fuel for higher metabolic processes. Lastly, the CO_2 acceptor molecule (RuBP) is formed via triose phosphates in the regenerative stage. Carbon compounds created by the C3 cycle serve as metabolites for plant growth (Geiger and Servaites, 1994; Lichtenthaler, 1999 Raines, Lloyd and Dyer, 1999; Raines, 2003a; Raines, 2011). Calvin cycle enzymes require a pH of 8, and stromal pH is thought to increase from 7 to 8 upon exposure to light (Nishizawa and Buchanan, 1981; Heldt et al., 1973; Werdan, Heldt and Milovancev, 1975). Light regulation via a ferredoxin/thioredoxin system helps to establish the interface between light reactions in the thylakoid membranes and use of the resultant metabolites for downstream biosynthetic purposes. In terrestrial plants, hexose phosphates are transformed by the OPP pathway into pentose phosphates producing NADPH in the plastids. These reactions are different from the Calvin-Benson cycle, also known as the reductive pentose phosphate pathway; both pathways being active simultaneously in the same compartment would use of three ATPs per fixed molecule of CO_2. As a result, a number of Calvin-Benson cycle enzymes are stimulated by light, as previously explained, whereas the Glc-6-P dehydrogenase (G6PDH), which catalyses the first oxidative reaction of the OPP, is controlled and congested following thioredoxin reduction in light conditions (Wenderoth, Scheibe and Von Schaewen, 1997; Michels, 2005). The activities of Calvin-Benson cycle enzymes such as SBPase, FBPase, PRK, and GAPDH are controlled by the ferredoxin/thioredoxin system during the day. Certain compounds, such as the CP12 protein, have been discovered to control definite enzymes in the Calvin-Benson cycle such as PRK and GAPDH by complexing with these enzymes. The 12 kDa CP12 protein can be found in all photosynthetic, chloroplastic organisms. Other studies

have suggested that Calvin-Benson cycle enzymes could be controlled via an NADPH-mediated, alterable reaction of the complex of PRK/CP12/GAPDH (Wedel, Soll and Paap, 1997; Wedel and Soll, 1998; Graciet et al., 2003).

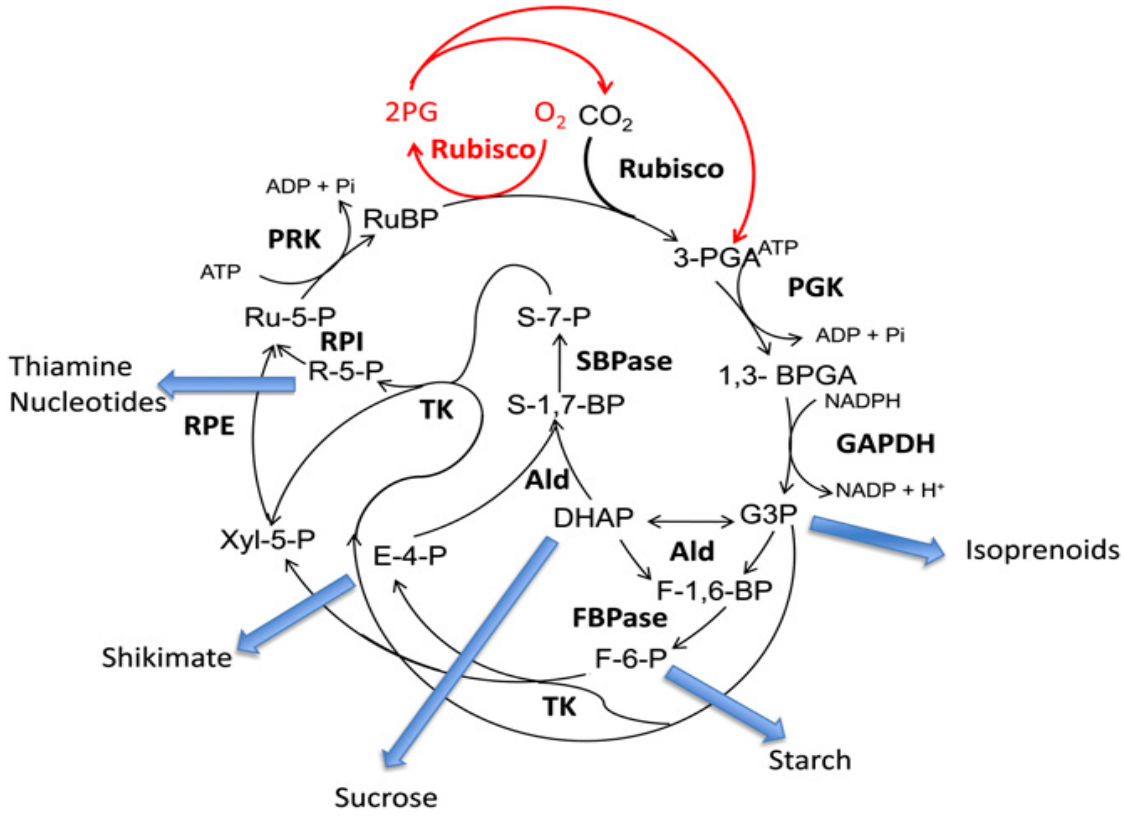

Figure1.1: The Calvin cycle adapted from (Raines, 2011b), starting point with the Rubisco carboxylation reaction of the CO_2 acceptor molecule RuBP, and succeeded in 2 molecules of three stable carbon product phosphoglycerate (3- PGA), sequenced by the reductive phase of the cycle with two reactions catalysed by 3-PGA kinase (PGK) and GAPDH, generating G3P. Followed by the entry of the G-3-P to the regenerative phase, catalysed by aldolase (Ald) and either FBPase or SBPase, creating Fru-6-P (F-6-P) and sedoheptulose-7-P (S-7-P). Then, Fru-6-P and sedoheptulose-7-P are usually attempted in reactions catalysed by TK, R-5-P isomerase (RPI), and ribulose-5-P (Ru-5-P) epimerase (RPE), creating Ru- 5-P. Followed finally by the of Ru-5-P to RuBP, catalysed by PRK. The reaction of Rubisco oxygenation to fixes O_2 into the acceptor molecule RuBP resulted in PGA and 2- phosphoglycolate (2PG), and CO_2 and PGA are released through the photorespiration process (red).Consequently, of this cycle, five significant products are created (blue)

1.4 Improving photosynthesis

In the 1990's analysis of transgenic Arabidopsis and tobacco plants in which the levels of individual proteins or enzymes were manipulated altered the view that there was a single restrictive step in photosynthetic carbon assimilation. These studies were based on metabolic control analysis (MCA) where changes in single enzyme activities were used to perturb the system and the impact of this change measured. This work revealed that control of carbon assimilation was shared between numbers of enzymes, but that the share of control assigned to an individual enzyme was not equal or fixed and varied with environmental conditions. Antisense plants with reductions in the Rieske iron sulphur protein of the cytochrome *b6f* (Cyt *b6f*) complex correlated linearly with reduced rates of carbon assimilation (Price et al., 1995; Yamori et al., 2011). Interestingly, it has been shown recently that the introduction of the Porphyra Cyt c6 gene into Arabidopsis increased rates of electron transport and plant growth providing support that electron transport through the Cyt *b6f* complex can increase photosynthesis and growth (Chida et al., 2007). Similarly, small reductions in either sedoheptulose-1,7-bisphosphatase (SBPase) or plastid aldolase in the Calvin cycle impacted negatively on carbon fixation (Harrison et al., 1998; Haake et al., 1999) indicating that these enzymes had significant over the rate of carbon assimilation. These experiments suggested that improvements in photosynthetic carbon fixation may be achieved by increasing the activity of these enzymes independently. Evidence supporting this hypothesis came from transgenic tobacco plants in which the levels of the enzyme SBPase were increased. This single manipulation resulted in an increase in photosynthesis of 10% leaf area, and total biomass were up 30% in plants grown under high light conditions (Lefebvre et al., 2005). However, the growth of SBPase overexpressing plants in greenhouse conditions in the winter, when light levels were lower, resulted in only minimal increases in growth.

Interestingly, increased levels of SBPase in rice did not improve photosynthesis under non-stress conditions; this manipulation helped to maintain photosynthesis at non-stress levels when plants were grown exposed to heat or osmotic stress (Feng et al., 2007). In plants that fix atmospheric CO_2 using RuBisco, the theoretical greatest energy conversion efficiency achievable is 4.6%, however, in the field, efficiencies of less than 50% of this are recognised. The kinetic models based on ordinary differential equations (ODEs) have been improved to explain the responses of photosynthetic carbon assimilation (Poolman et al., 2000). Additional development of these models to involve not only the reactions in the Calvin cycle but, essentially, those in the pathways of sucrose and starch biosynthesis and photorespiration has led to the structure of a dynamic model of carbon metabolism (Zhu et al., 2007). The outputs of this modelling work recommended that an increase in the Calvin cycle enzymes sedoheptulose-1,7-bisphosphatase (SBPase) and fructose-1,6-bisphosphate aldolase (FBPA) and the starch biosynthesis enzyme ADP-glucose pyrophosphorylase (AGPase), together with a reduction in the photorespiratory enzyme glycine decarboxylase (GDC), might increase photosynthetic carbon assimilation.

More recently, the overexpression of FBPA in transgenic tobacco plants caused an increase in photosynthesis and biomass, but only at elevated levels of CO_2 (Uematsu et al., 2012). According to Simkin et al. (2015), over-expression of two C3 cycle enzymes leads to a rise in photosynthesis and a cumulative increase in total biomass yield. It is also revealed that over-expression of ictB, a protein thought to be involved in inorganic carbon transport, in combination with SBPase (ictB and SBPase) or SBPase and FBPA (SBPase, FBPA, and ictB) brought about a further important improvement in both of these parameters.

Although changes in the expression of a single gene has resulted in improved photosynthesis and growth in plant grown under laboratory conditions, it is clear that in order to design plants with improved photosynthetic performance, that is sufficiently robust to be maintained under a range of environmental conditions, will require more complex manipulations of metabolism.

1.5 The effect of drought on photosynthesis and how plants adapt to drought

Reduced water availability leads to drought stress, which is a main limitation on the physiology, growth, development, and productivity of plants (Boyer, 1970; Lobell and Field, 2007; Roberts and Schlenker, 2009; Skirycz et al., 2010; Lobell et al., 2011; Verelst et al., 2013). Consequently, understanding how plants respond to drought stress is vital in protecting natural vegetation and stabilizing crop performance under drought conditions. Drought affects photosynthesis either directly, via decreased CO_2 availability caused by diffusion restriction through the stomata and mesophyll (Chaves et al., 2003a; Chaves et al., 2009) or the variations of photosynthetic metabolism. The secondary effects specifically called oxidative stress which is an element of many abiotic stress conditions such as drought, high temperature stress, salinity and heavy metal stress and biotic stress conditions such as herbivory and plant-pathogen interactions (Moran et al., 1994; Larkindale, 2002; Hernández et al., 1993; Sytar et al., 2013; Orozco-Cardenas and Ryan, 1999; Grant et al., 2000). Plants are frequently subjected to drought throughout their lifetime and hence have involved several adaptation mechanisms to deal with drought stress (Chaves, Maroco and Pereira, 2003; Greco et al., 2013). Responses include escape, avoidance, or tolerance of reduced water availability (Levitt, 1985; Blum, 2005; Aguirrezabal et al., 2006; Franks, 2011). Drought escape, plants complete their lifecycle before the start of drought, whereas water is still available, and therefore ensure

reproduction is effective. Drought avoidance includes the plants conserving higher cellular water potential in the existence of decreasing levels of soil humidity (Chaves et al., 2009). To do this, plants make adjustments to reduce the loss of water from the leaves,wheras trying to raise the increase of water uptake from the soil over the roots (Chaves et al., 2009; Chaves et al., 2003b). Water shortfall causes a loss of turgor due to a decrease in cellular water content. Turgor damage in leaves because of decreased stock of water straight causes a drop in the growth rate of cells, which leads to a reduction in leaf area. Decreased stomatal conductance happens in response to increasing water insufficiency to diminish, water-loss through of transpiration. As drought, older leaves are hut to further save water by reducing transpiration, whereas plus approving that plant resources are transferred to younger leaves for growth. The separating of water resources away from the shoot and leaves is to allow rise in the water source to roots to help their growth bigger into the moister areas of soil (Chaves et al., 2003b; Chaves et al., 2009). In drought tolerance, the cell modifies to the lower water possible via producing some of the expression of genes wanted for the adaptation process. The Osmolytes and sugars are created to assistance equilibrium the alteration in water potential (Serraj and Sinclair, 2002), the Late Embryogenesis Abundant (LEA) proteins support to safeguard cellular structure from crystallisation throughout drought stress (Bravo et al., 2003) and ROS detoxifying enzymes are made to adapt the synthesis of ROS (Sharma and Dubey, 2005). The Stomatal close, and therefore photosynthesis, is additionally regulated by the hormone Abscisic Acid (ABA) and a few changing genes that control stomatal function and photosynthetic capacity under stress (Murata et al., 2001). At the cellular level, plants react to drought with modifications in gene expression, protein and metabolite abundances (Charlton et al., 2008; Harb et al., 2010; Wilkins et al., 2010; Baerenfaller et al., 2012), which are part of resistance mechanisms and detoxification processes

(Shinozaki and Yamaguchi-Shinozaki, 2007; Begcy et al., 2011; Ozfidan et al., 2012). Previously, has been shown two targets of AGL22, DREB1A and FBH3 that regulation of abiotic stress responses. Overexpression of DREB1A leads to drought, salt, and freezing tolerance (Kasuga et al., 1999; Kasuga et al., 2004), whereas FBH3 has been indicated to control stomata opening (Takahashi et al., 2013) and roles in ABA signalling in response to osmotic stress (Yoshida et al., 2015). From this AGAMOUS-LIKE22 (AGL22; also known as SHORT VEGETATIVE PROTEIN), from the GRNs. AGL22 has an established function in plant development (Gregis et al., 2013; Méndez-Vigo et al., 2013), However in study by Bechtold et al. (2016), it was shown AGL22 to play for undiscovered role in the critical early stages of the plant's response to drought. This study showed the potential value of experimental strategies that combine time-series transcriptomics data with dynamic modelling as a gene discovery tool promotes the selection of unknown, yet highly connected genes for further phenotypic evaluation and identifying stress-responsive genes (Bechtold et al., 2016).

The recent approach in genomics, transcriptomics, and bioinformatics has lined the way for explaining drought-response mechanisms and has allowed the targeted modification of drought-responsive genes in plants for instance, the overexpression of some of genes that code for transcription factors (TFs) indications to drought resistance (Sakuma, 2006; Nelson et al., 2007; Chen et al., 2008; Quan et al., 2010; Tang et al., 2012).

In many reports to identify genes essential in the regulation of drought responses, the effects of water limitation at the transcriptional level have been studied by exposing plants to severe dehydration. This includes treatments such as cutting and air-drying leaves and or roots or induction of osmotic shock throughout the application of highly concentrated osmotica such as polyethylene glycol or mannitol (Kreps, 2002; Seki et al., 2002; Kawaguchi et al., 2004; Kilian et al., 2007; Weston et al., 2008; Fujita et al., 2009; Abdeen

et al., 2010; Deyholos, 2010; Mizoguchi et al., 2010). These experiments indicated the molecular responses under severe drought stress. However, they do not always reflect physiological conditions practised by drought-stressed soil-grown plants (Bechtold et al., 2010; Bechtold et al., 2013; Harb et al., 2010; Wilkins et al., 2010; Lawlor, 2013). Physiological responses such as stomatal conductance, photosynthetic performance, and metabolic changes are usually not measured during the development of the drought stress, and the altered nature of the stress induction treatments makes a comparative analysis between experiments difficult. Slow developing soil water deficits have different physiological concerns than those encouraged by rapid tissue dehydration and consequently perhaps use different gene networks (Chaves et al., 2003a; Chaves et al., 2009; Pinheiro and Chaves, 2011). From these findings, an overall integrative image of the temporal responses to drought is developing slowly, and it is pure that use of a single or a small number of time points and different types of experimental conditions lead to very different results. One consequence of this is that very little is known about the primary events in the understanding of drought stress signals (Ueguchi et al., 2001; Wohlbach et al., 2008; Pinheiro and Chaves, 2011). To address the issue of drought and produce plants with improving photosynthesis and resistance to drought, we carried out reverse engineering based on a transcriptional network of the Calvin cycle generated from a microarray time series data and Variational Bayesian State Space modelling (VBSSM). Gene regulatory networks (GRNs) were modelled using Variational Bayesian State Space Modelling (Beal et al., 2005) is a dynamic Bayesian algorithm that uses time-series transcriptomics data to produce models of gene regulation. These models might help identify possibly essential drought-responsive regulatory genes. VBSSM has been used earlier to generate gene regulatory networks for senescence (Breeze et al., 2011).

VBSSM has good potential in identifying new connections between genes that would not normally be assumed based on transcriptome data only.

1.6 Exploitation of transcriptional network modelling

19 Calvin cycle genes that showed altered expression during drought stress, and a subset of the 80 responding TFs were included in the initial model. Subsequent models contained several different sub-sets of TFs to test all 150-drought responsive transcriptional regulators (Bechtold et al 2016), with the exception that hub TFs were retained in subsequent iterations of the models.

Several studies have quantified transcriptome alterations during drought (Seki et al., 2002; Harb et al., 2010), however these have only examined a single time-point after the plant has been subjected to severe drought stress and have not quantified the changing dynamic as the drought developed. The work presented in this thesis is based on the work of Bechtold et al. (2016) in which a time-series of transcriptional analyses during development of drought stress was performed. Differentially expressed genes from this analysis were used to model gene regulatory networks (GRNs) using Variational Bayesian State Space Modelling (Beal et al., 2005) GRNs are generated that contain of highly connected genes that are shown to have a collaboration, either directly or indirectly, with other genes in the model, and therefore the model is based around the highly connected genes gene. VBSSM has good potential in identifying novel collaborations between genes that would not generally be realised based on transcriptome data only. One difficulty of VBSSM is that only a restrict number of genes not more than 100 can be modelled at a time, and hence it is helpful to cluster the list of differentially expressed genes into groups of slight numbers of genes.

The application of high-density DNA microarray technology to gene transcription analysis has stimulated the enhancement of algorithms to catalogue and define the complex transcriptional response of a biological system and to show interactions among the factors of a cellular system. Many of the methods that have been applied in an examining approach to the problem of reverse engineering genetic regulatory networks from gene expression data have been newly changed by Someren et al. (2005). Murphy and Mian (1999) were the first to suggest the use of a general class of graphical models known as Dynamic Bayesian Networks (DBNs) to model time series gene expression data. Bayesian networks have a number of features that make them attractive candidates for modelling gene expression data, such as their ability to handle missing data, to handle unknown variables such as protein levels that might have an effect on mRNA expression levels, to explain locally interacting processes and the possibility of making causal inferences from the derived models. Gene regulatory networks show the communication among different genes and afford a larger view of gene networks that can possibly show novel connections. Moreover, statistical algorithms might be used to reverse-engineer gene regulatory networks established on transcriptomics data and the greatest common types of mathematical models used are ordinary differential equations, Boolean networks and Bayesian networks (Bansal et al., 2007). Ordinary differential equations characterise the alteration in the level of a transcript as a function of the alteration in the amounts of all other transcripts and additionally due to the effect of an outside perturbation. Boolean networks characterise the expression levels of genes as any ‘0’ or ‘1’ i.e. unexpressed formal or expressed formal. Together of these approaches can only be advantageous to steady-state data and cannot be used on dynamic in (time-series) data. Bayesian networks can any be static or dynamic, and dynamic Bayesian networks are used time-series data by operating Bayesian statistics to reverse-engineer the fundamental

relationship between two ‘nodes’ or genes. (Gardner and Faith, 2005; Bansal et al., 2007). One Dynamic Bayesian method called Variational Bayesian State Space Modelling VBSSM (Beal et al., 2005), was used by Breeze et al. (2011) to classic entire transcriptome data from a time-series senescence experiment. VBSSM builds network models approximately genes of interest using the Metropolis algorithm. At each step in the Metropolis algorithm, a Bayesian state space model is fixed to the time series gene expression contours for the chosen genes, and the low probability used as the selection criteria to determine the best fit (Beal et al., 2005). VBSSM was used to classical Gene Regulatory Networks in the drought response. A number of such networks were produced, and special note was taken of the highly connected genes in each network, as these could be theoretically vital regulatory genes during drought stress response via the direct or indirect control of the expression of genes within a given network. VBSSM model has been used successfully to develop a realistic network associated with T-cell activation in mammalian systems (Rangel et al., 2004). More recently, VBSSM has also been used to identify novel highly connected genes in Arabidopsis that result in phenotypes in knockout insertion mutants subjected to environmental stresses (Bechtold et al., 2016). Prior to this project, a microarray time series was generated from mRNA collected from soil-grown Arabidopsis plants subjected to progressive water deficit (from 100% – 18% relative soil water content) that resulted in a 30% reduction in carbon assimilation at 50% relative soil water content (Bechtold et al., 2016). Analysis of these time series data using a VBSSM simulation has identified three hubs (Figure 2.1, green circles) that may be important determinants of drought-induced transcriptional responses of genes encoding Calvin cycle enzymes. These genes were identified RAP2.12 (a member of the ERF subfamily of the ERF/AP2 transcription factor family and has been found to be involved in response to hypoxia AT1G53910 (Licausi et al., 2011a), a Calvin cycle enzyme of

GAPDH family GAPA-2 (At1g12900), and an unknown protein Atg16750. With the exception of RAP2.12 (Licausi et al., 2011; Papdi et al., 2015) none of the other genes have been shown to have a role in drought or any other stress response. Thus, VBSSM has the possible to isolate genes and gene networks that are not usually known to be stress-responsive. Nevertheless, the theoretical isolation of these potentially vital genes must be proved experimentally by analysing the role of these proteins in plants during drought stress in mutant plants.

Although transgenic antisense studies did not identify GAPDH as a target for manipulation to increase photosynthesis, no plants have been produced with increased levels of the GAPA subunit or have plants with reduced levels of GAPDH been tested under abiotic stress. Recent studies in wheat showed a coordinated down-regulation of a number of Calvin cycle genes in response to drought (Xue et al., 2008) and analysis of publicly available microarray data revealed that GAPA-1 is particularly sensitive to drought. Furthermore, unpublished data from the Raines' lab has shown that in drought-tolerant wheat GAPDH levels are maintained in contrast to other Calvin cycle enzymes. Taken together these results provide support for the outputs of the model, and that expression of the GAPA-2 genes may be an important target for manipulation to avoid a decrease in photosynthesis under mild water stress. To produce plants with improved performance of the Calvin cycle under drought, we will manipulate genes identified by VBSSM simulations. An initial VBSSM model containing only Calvin cycle genes predicted positive interactions of GAPA-2 (At1g12900) with most other genes in this cycle, suggesting that over-expression of this gene could improve Calvin cycle performance. The outputs from the model suggest that increasing the levels of expression of the GAPA-2 (At1g12900) gene and decreasing the levels of both transcription factors *RAP2.12* (At1g53910) and (At1g16750), will have a positive effect on the expression of a number of Calvin cycle

genes in plants grown under drought (orange and yellow circles, Figure 2.1). Further simulations of the VBSSM model including various combinations of transcription factors with the Calvin cycle genes, consistently identified *RAP2.12* (At1g53910) as a negative regulator of Calvin cycle enzymes and GAPA-2 as a positive regulator of other Calvin cycle genes and this is only the hypothesis of modelling may not be exactly as predicted by the modelling. Subsequently, the putative transcription (At1g16750) factor was identified from a simulation that included a subset of transcription factors directly linked to Calvin cycle genes and differentially expressed during drought. As the VBSSM model does not provide quantitative information, we produced plants with different amounts of these proteins. Therefore, reduced the expression levels of *RAP2.12* (At1g53910) and the putative transcription factor (At1g16750) using antisense technology and overexpress GAPA-2 (At1g12900) in individual plants and also in combination.

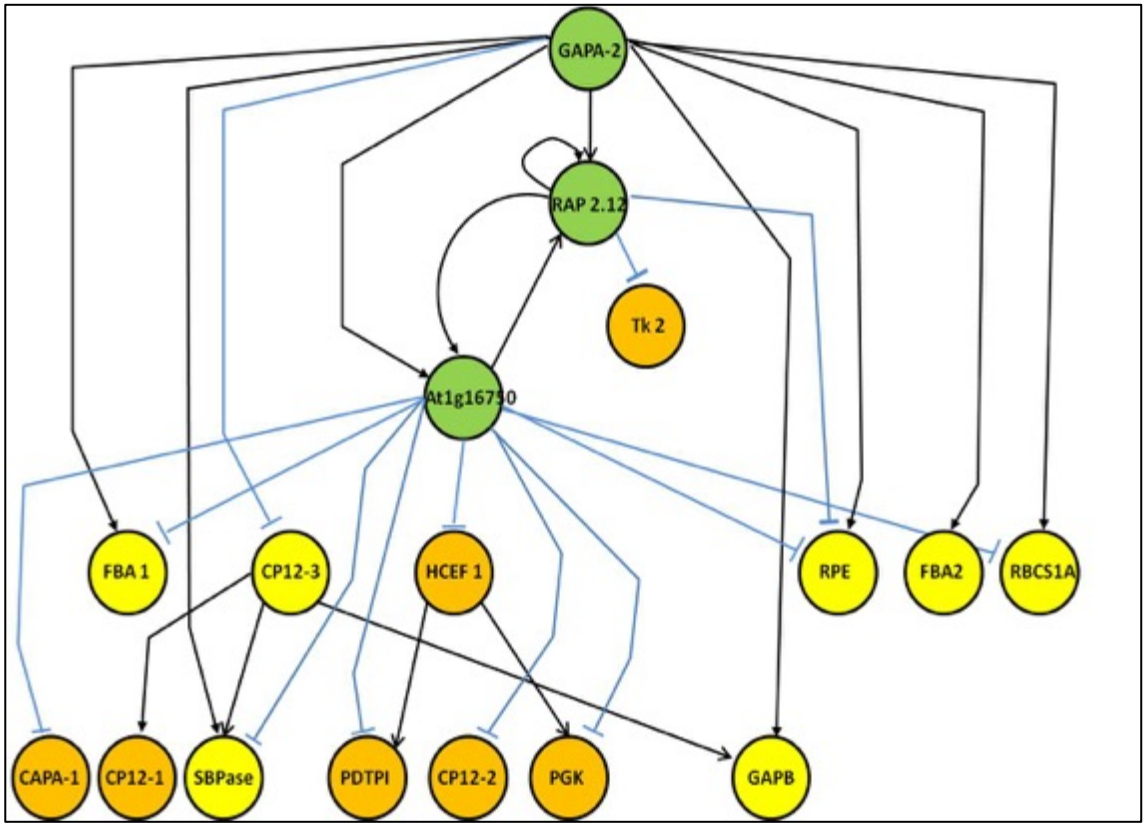

Figure2.1: VBSSM model output, including transcription factors and Calvin cycle genes: Glyceraldehyde-3- phosphate dehydrogenase A subunit (GAPA-2); Phosphoribulokinase (PRK); Glyceraldehyde-3-phosphate dehydrogenase B subunit (GAPB); Phosphoglycerate kinase (PGK1); Ribulose bisphosphate carboxylase small subunit 1A (RBCS1A); CP12-3; Triose phosphate isomerase (PDTPI); Fructose-bisphosphate aldolase 1 (FBA1); Rubisco activase (RCA); Transketolase (TKx); CP12-1; Ribose 5-phosphate isomerase (RPI); Glyceraldehyde-3-phosphate dehydrogenase (GAPA-1); High cyclic electron flow 1 (HCEF1); Sedoheptulose-1,7-bisphosphatase (SBPase); Transketolase (TK2); CP12-2 ; Fructose-bisphosphate aldolase (FBA2); Ribulose-5-phosphate-3- epimerase (RPE); putative transcription factor (At1g16750); RAP2.12. Black arrows – positive interaction, blue bars – negative interaction.

1.7 The Ethylene response factors family

The ERF-VII family of Arabidopsis transcription factors comprises five members: ERF71 (hypoxia responsive ERF1 (HRE1), At1g72360); ERF72 (related to AP2.3 (RAP2.3, At3g16770); ERF73 (HRE2, At2g47520); ERF74 (RAP2.12, At1g53910); and ERF75 (RAP2.2, At3g14230) (Nakano et al., 2006). These ERF-VII transcription factors have been implicated in plant responses to hypoxia (Xu et al., 2006; Hattori et al., 2009; Hinz et al., 2010; Licausi et al., 2011a), with similar N-terminal degron motifs, MCGGA-I/V, controlled by the N-end rule pathway of protein degradation (Gibbs et al., 2011; Licausi et al., 2011a). In addition to hypoxia, ERF71 - ERF75 also play roles in the management of other stresses. In rice (*Oryza sativa*), SUB1A, the expression of which has been found to confer submergence tolerance, is also expressed in response to oxidative stress and drought (Fukao et al., 2011). Moreover, *35S::ERF75* transgenic plants and *erf75* T-DNA insertion mutants demonstrated insensitivity and sensitivity, respectively, to necrotrophic Botrytis as compared to wild type (Zhao et al., 2012). Furthermore, the ERF gene *RAP2.4* was found to be excited by drought, and overexpression of this gene has been shown to rise drought tolerance in plants compared to their wild type counterparts (Lin et al., 2008). Finally, ERF72 - ERF75 have also been found to modulate oxidative and osmotic stress tolerance (Park et al., 2011; Papdi et al., 2015).

1.8 Studies of RAP2.12 gene

Oxygen is a major limiting substrate in aerobic organisms. Aerobic organisms such as plants need molecular oxygen for production of ATP during respiration. The ethylene-responsive transcription factor RAP2.12 is encoded by the RAP2.12 gene in Arabidopsis

thaliana and is a member of the ethylene response factor (ERF) subfamily B-2. RAP2.12 has been shown to modulate the plant's ability to withstand hypoxic stress (Hinz et al., 2010). Overexpression of RAP2.12 improves the ability of plants to survive during periods of low oxygen. Plants often encounter low oxygen conditions during waterlogging and flooding. Unlike animals, plants have no active mechanisms for the distribution of oxygen to internal tissues, instead of depending on diffusion for oxygen transport. However, diffusion is limited in that it may cause steep oxygen gradients in multi-layered tissues (Kosmacz et al., 2015). Low oxygen limits aerobic metabolism and subsequent availability of ATP, lowering the production of storage products such as proteins, starches, and lipids (Geigenberger, 2003). Plants activate a variety of acclimation responses during hypoxic conditions to reduce the detrimental effects of energy depletion (Licausi et al., 2011b). When oxygen is limited, ATP for oxidative phosphorylation is generated through fermentation. The activation of fermentative metabolism involves strong up-regulation in the expression of fermentative genes and those encoding transcription factors and hypoxia-induced proteins. Control of adaptive responses under low oxygen conditions is mediated by a sensing mechanism involving oxygen-dependent localization of the transcription factor RAP2.12 via the N-end rule pathway.

RAP2.12 is a transcription factor belonging to the ethylene responsive factor (ERF-VII) group that acts as an activator for anaerobic responses (Licausi et al., 2011b). ERF-VII proteins have a highly conserved N-terminal motif, which is recognized as a degradation signal; in the presence of NO and oxygen; the N-terminal motif results in entrance into the protease-dependent N-end rule pathway. According to Kosmacz et al. (2015), the terminal methionine is initially cleaved by Met-aminopeptidase attachment to a cysteine residue at the second position of the N-terminus. This is followed by oxidation of exposed cysteine amino acids by plant cysteine oxidases (PCOs), which triggers conjugation of

the N-terminus to arginine residues by Arg-tRNA protein transferases (ATEs). Among the members of the ERF-VII group in Arabidopsis, RAP2.12 is expressed in many cell types, and the RAP2.12 transcription factor is degraded in the presence of oxygen (Licausi et al., 2011b).

The increasing oxygen concentration in the plant environment can increase plant yield. Various studies have explored the role of RAP2.12 in mediating oxygen concentration and possible manipulation of oxygen response mechanisms to improve plant yields. One study by Gibbs et al. (2011) demonstrated substantial evidence for the role of the N-end rule pathway in facilitating homeostatic responses to changes in oxygen concentrations, providing a basis for further exploration of the genes involved in this process. Gibbs and his colleagues investigated hypoxia regulation by the N-end rule pathway and found that this pathway acted as a homeostatic sensor mechanism enabling plants to adapt to changes in oxygen levels. Transgenic plants were then subjected to periods of oxygen deprivation followed by phenotypic analysis with Western blot. The findings of this study found that plants deficient components of the N-end rule pathway constitutively express essential hypoxia-response genes and are additional tolerant of hypoxic stress. Furthermore, identify the hypoxia-associated ethylene response factor group VII transcription factors of Arabidopsis like substrates of this pathway (Gibbs et al., 2011).

In another study, Licausi et al. (2011) also studied the oxygen sensing mechanism in plants in the N-end rule pathway by subjecting *A. thaliana* plants to oxygen stress by growing them in 1% oxygen. Flooding tolerance was assayed using independent transgenic lines. Licausi et al. (2011) uncovered a ubiquitin-dependent N-end rule pathway that mediated protein degradation. The pathway was shown to act as an oxygen

sensing mechanism in A. thaliana. Licausi et al. (2011) further demonstrated that a conserved amino acid sequence in the ERF-transcription factor RAP2.12 was oxygen-dependent and subject to post-translational modifications that led to RAP2.12 degradation under aerobic conditions. These studies found that in low oxygen environments such as during flooding, the plasma membrane releases RAP2.12, which accumulates in the nucleus and activates hypoxia acclimation gene expression. Such findings suggest the possibility of improving yield and flood tolerance by modifying oxygen-sensing mechanisms.

A recent study by Kosmacz et al. (2015) corroborates evidence for the role of the transcription factor RAP2.12 in the regulation of oxygen concentration in plants. In their study, transgenic A. thaliana plants overexpressing RAP2.12 were developed. Two-week-old plants were subjected to low oxygen levels of 1-21% v/v followed by re-oxygenation treatments. Microscopic observations using confocal laser-scanning microscopy were conducted on leaves following hypoxic stress. Investigators discovered that reduced oxygen concentration triggered the reallocation of RAP2.12 into the nucleus. The presence of RAP2.12 in the nucleus appeared to be dependent on the localisation of existing proteins as well as the de novo synthesis of the transcription factor RAP2.12. The study further demonstrated that RAP2.12 present in the nucleus was degraded soon after tissue re-oxygenation, typically within three hours (Kosmacz et al., 2015). Furthermore, hypoxia response attenuator-1 (HRA1), is highly up-regulated by hypoxia. HRA1 induces the expression of fundamental low oxygen-responsive genes and the transcriptional activation of hypoxia-responsive promoters by RAP2.12.

1.9 GAPDH Family

Glyceraldehyde-3-P dehydrogenases (GAPDHs) are enzymes well-preserved in all living organisms, where they play a fundamental role in the carbon of the cells. In plants are four distinct isoforms of GAPDHs: GAPC, a cytosolic, phosphorylating, NAD-specific GAPDH catalyzing the conversion of glyceraldehyde-3-P (Ga3P) to 1,3-bisphosphoglycerate; NP-GAPDH, a cytosolic non-phosphorylating NADP-dependent GAPDH that catalyzes the oxidation of Ga3P to 3-phosphoglycerate (3PGA) (Valverde et al., 2005); GAPA, and GAPB, a phosphorylating, NADP-specific GAPDH involved in photosynthetic CO_2 fixation in chloroplasts (Cerff, 1979) and GAPCp, involved in glycolytic energy making, in non-green plastids (Petersen et al., 2003).

In current years, detailed studies have been carried out on the structure-function associations (Habenicht et al., 1994; Petersen et al., 2003; Anderson et al., 2004; Hancock et al., 2005) and kinetic properties (Gómez Casati et al., 2000; Bustos and Iglesias, 2002; Bustos and Iglesias, 2003; Iglesias et al., 2002) of the cytosolic GAPDHs. But, only a few studies have been focused on their in vivo functions (Hajirezaei et al., 2006; Rius et al., 2006; Wang et al., 2007). It has been suggested that the NP-GAPDH isoform plays an essential role in a shuttle system mechanism for the moving of the NADPH produced by photosynthesis from the chloroplast to the cytosol and in providing NADPH for gluconeogenesis (Kelly and Gibbs, 1973; Rumpho et al., 1983; Habenicht, 1997).

In a study by Marri et al. (2005) investigators used the RT-PCR method to clone whole coding sequences for *gapA-1*, *gapB*, *gapC-1*, and *gapCp-1* from Arabidopsis; expression

parameters for cytosolic *gapC* and plastid *gapCp,* which do not cooperate with the CP12 protein, were additionally tested for comparison. The expression of *CP12-2*, but not *CP12-1*, was realised to be co-regulated alongside *gapA1*, *gapB*, and *PRK* under all conditions tested. Conversely, the expressions of *gapC-1* and *gapCp-1* did not associate with known photosynthetic genes (Marri et al., 2005a). The organised regulation of *gapA-1*, *gapB*, *CP12-2*, and *PRK* at the genetic level underscores the presence and physiological relevance of a supramolecular complex involving GAPDH, CP12, and PRK proteins in chloroplasts (Wedel and Soll, 1998b; Scheibe et al., 2002; Graciet et al., 2004).

1.9.1 GAPC structure and function

The importance of GAPC in photosynthetic tissues has been extensively studied; but, only a few studies have described its function in heterotrophic tissues (Fernie et al., 2004; Hajirezaei et al., 2006). Moreover, GAPC-1 is cytoskeletally connected in many organisms including plants (Chuong et al., 2004). Furthermore, it was found associated with other glycolytic enzymes, both in the cytoskeleton and in the mitochondria (Giege, 2003; Holtgräwe et al., 2005). Therefore, it was hypothesized that glycolytic proteins might be essential in energetic mitochondrial metabolism and in regulating mitochondrial functions (Giege, 2003). Moreover, the coexistence of GAPC and NP- GAPDH in the cytosol establishes a bypass of carbon flux during the glycolysis, which very likely recovers the flexibility to respond to environmental stresses. Its physiological function and full importance within plant metabolism is not yet clear, and new studies propose that this enzyme could be involved in additional cellular functions as, in Arabidopsis, its lack of GAPCP leads to modification in carbon flux and mitochondrial dysfunction, which in turn appears to lead to modifications in plant growth and seed production (Rius et al., 2008a).

In Study by Rius et al. (2008) isolated and characterized two lines exhibiting a GAPC-1 deficiency: a null mutant line of Arabidopsis deficient in GAPC-1 expression (*gapc-1*, SALK_010839) and a transgenic line expressing the antisense version of the *GAPC-1* gene (At3g04120, *as- GAPC1*). Both lines showed defects in fertility, with alterations in seed and fruit development, advising that GAPC-1 is vital in these tissues. The molecular, biochemical, and physiological studies of these lines show that this enzyme plays critical and pleiotropic roles, being essential for the maintenance of cellular ATP levels and carbohydrate metabolism and required for full fertility.

1.9.2 GAPCP structure and function

In Arabidopsis, at least two genes encode GapCp proteins, *gapCp1* and *gapCp2* (Petersen et al., 2003). Although this enzyme was first discovered in the 1990s, its physiological function and full importance with regards to plant metabolism remain unclear. Recent studies have proposed that it could be involved in additional cellular functions; in Arabidopsis, a lack of GapCp leads to modifications in carbon flux and mitochondrial dysfunction, which in turn appears to have consequences felt in plant growth and seed production (Rius et al., 2008b). Despite the low gene expression level of GAPCps in Arabidopsis, *gapcp* double mutants (*gapcp1-gapcp2*) indication great alterations of plant development, mainly arrested root improvement and sterility (Munoz-Bertomeu et al., 2009; Muñoz-Bertomeu et al., 2010). The strategic situation of GAPCp in the glycolytic pathway could make this enzyme an essential player not only for glycolysis but however also for the generation of metabolites for other anabolic pathways (Plaxton, 1996; Ho and Saito, 2001; Andre et al., 2007; Baud et al., 2007).

1.9.3 The GAPDH chloroplast oligomers (A2B2) and (A4)

GAPDH multimeric forms have been described in spinach, pea, and maize (Trost et al., 1993). The PRK/GAPDH/ CP12 complex has also presented in these three higher plants (Wedel et al., 1997; Wedel and Soll, 1998a; Scheibe et al., 2002), in a cyanobacterium, (Tamoi et al., 2005), and some algal species (Avilan et al., 1997; Boggetto et al., 2007). Recently it was suggested that regulation of PRK and GAPDH activity by CP12 and by redox varies among different algal species (Maberly et al., 2010); similarly, the activity of GAPDH in dark leaves of spinach versus maize are also disparate (Trost et al., 1993). Two GAPDH subunits referred to as GAPA and GAPB have been found in higher plants, the main difference between them being the presence of the C-terminal extension on the GAPB peptide that confers thioredoxin-mediated redox regulatory capacity to the GAPDH enzyme and plays a fundamental role in GAPDH protein-to-protein interactions (Baalmann et al., 1996; Fermani et al., 2007). There are two isoforms of GAPDH, a homotetramer and a heterotetramer. The heterotetramer isoform containing two GAPA and two GAPB subunits (A_2B_2) is the predominant isoform. The homotetramer (A4**)**

isoform as detected in spinach chloroplast preparations has been shown to account for 15–20% of total GAPDH activity (Scagliarini et al., 1998) (Table1.1). This form of GAPDH has been determined to be non-regulatory due to a lack of the C-terminal extension. It has been proposed, however, that the PRK/GAPDH/CP12 complex permits regulation of this GAPDH isoform (Trost et al., 2006). Some studies have suggested that PRK/GAPDH/CP12 can associate with the A2B2 heterotetramer alone (Wedel et al., 1997; Scheibe et al., 2002; Howard et al., 2008), as well as a complex with combined A4 and A2B2 isoforms (Clasper et al., 1991).

Fermani et al. (2007) explored the mechanism of thioredoxin regulation of A2B2-GAPDH in photosynthesis. Mutants of A2B2-GAPDH involving Site-Specific Mutants of B4

GAPDH and Chimeric [A+CTE]4–GAPDH were purified from spinach chloroplasts. Purified [A+CTE]4–GAPDH and A2B2-GAPDH were oxidized in the presence of thioredoxin from E.coli. The findings of the study demonstrated that the C-terminal extension is a redox-sensitive regulatory domain with the ability to force AB-GAPDH into a kinetically inhibited conformation under oxidized conditions. The work by Fermani et al. (2007) contributed significantly to the understanding of the molecular mechanism of photosynthetic GAPDH in plants.

The study by Howard et al. (2011b) attempting to define relations of GAPDH with itself and with PRK in dark conditions, stromal extracts were derived from the leaves of dark-adapted species from the *Leguminosae* family (pea, Medicago, broad bean, and French bean), the *Solanaceae* group, (potato, tomato, and tobacco), the *Amaranthaceae* (spinach), and the *Brassicaceae* (*Arabidopsis*). BN-PAGE was used to isolate native proteins. Bands representing GAPDH and PRK were identified following Western blot and immunolocalization with polyclonal antibodies against the GAPDH holoenzyme containing both the A and B subunits and PRK. Results showed a variety of GAPDH oligomeric statuses in extracts from the leaves. Bands demonstrated by GAPDH antibodies were observed at 150, 160, 300, 600, and 700 kDa. PRK bands presented at 70 kDa and 600 kDa, indicating the dimeric, active form of PRK and the PRK/GAPDH/CP12 complex, respectively. All species having a band indicating a GAPDH multimer at 160 kDa. Second-dimension, Tricine-SDS-PAGE of lanes cut from the gels revealed that this GAPDH band contained both GAPA and GAPB subunits, indicative of the A2B2 heterotetramer (Howard et al., 2008). The lowest kDa GAPDH band at 150 kDa in Medicago, tobacco, and potato was found only to comprise the GAPA subunit. Investigators concluded that this small GAPDH complex likely represented the A4

GAPDH tetramer. The capacity to identify this isoform in spinach correlated to the levels of illumination the leaves were exposed to prior to extraction.

Overall, GAPDH in the plastid forms either a heterotetramer comprised of two distinct subunits produced from separate genes, the stoichiometry of the functional enzyme and is A2B2, but this can also form multimeric forms of (A2B2) that are inactive. This form of GAPDH is activated by thioredoxin mediated by the C-terminal extension on the B subunit which contains two cysteine residues. The second form of GAPDH in the chloroplast is in the form of a homotetramer A4. It has been revealed that the relative amounts of these two complexes vary among species, but almost always the A2B2 form is predominant, some plants have no detectable levels of A4, but no plants without the A2B2 have been identified (Howard et al., 2011b). The relative importance of these different forms of plastid GAPDH A4 and A2B2 has not been determined and given the data emerging from modelling to investigate the role of A2B2 in growth under normal and drought condition and photosynthesis capacity in higher plants.

1.9.4 GAPDH Forms

Table1.1: Tables showed the different GAPDH isoform with **Characteristics** and their functions.

GAPDH form	Characteristics	Regulation
A4	This only form presents in organisms 'cyanobacteria and green algae.	The non-regulatory isoform because of its insensitivity to the factors and metabolites that modulate A2B2 activity (Scagliarini et al., 1998). The only known regulation approach for this isoform is the collaboration with CP12 form the GAPDH/CP12/PRK complex.
A2B2	It is the main isoform in plant chloroplast. It can aggregate to form the hexadecamer (A2B2)4 it's exciting to point out that A4 and A2B2 isoforms, although of their alterations, have same kinetic properties (Scagliarini et al., 1998).	Highly vulnerable to regulation by redox potential of the environment through the action of thioredoxins (TRXs). Moreover, its activity seems to be affected by NADPH and BPGA (Scagliarini et al., 1998). It can furthermore cooperate with CP12 and PRK to form the regulatory GAPDH/CP12/PRK complex. (Howard et al., 2008; Howard et al., 2011b; Howard et al., 2011a).
A8B8	It Is the largest isoform identified, roughly 600 kDa	Is thought to be a regulatory relatively inactive form that has high NADH related and small NADPH dependent activities (Sparla et al., 2002).

1.10 Aims

The overall aim of this project to take an integrated approach using the knowledge gained from network modelling VBSSM to produce plants with enhanced photosynthetic performance and increased yield under drought stress. A second aim is to gain a better understanding of the roles of the GAPDH isoforms in photosynthetic carbon fixation.

`1.11 Objectives

1-Identify double mutant lines (homozygous) of the overexpressed GAPA-2 gene with the null expression of RAP2.12, (rap2.12-1 &GAPA-2 (13), and rap2.12-2 & GAPA-2 (29) plus single mutant of RAP2.12 and GAPA-2 genes to test the hypothesis that these two proteins play an important role in the regulation of Calvin cycle enzymes under drought and non-drought conditions.

2-To study the relative role of the different forms of the plastid GAPDH enzyme in determining the rate of photosynthetic carbon assimilation using antisense technology and T-DNA knock out insertion Arabidopsis mutants of GAPA and GAPB.

Chapter 2: Materials and Methods

2.1 Materials

2.1.1 Chemicals, antibiotics and molecular biology reagents

All chemicals and antibiotics used in this study were purchased from Sigma Furthermore, the optimal concentrations of antibiotics were determined to select for transformed plants or bacteria. The antibiotics were added to bacteria growing media at the concentrations given in (Table 2.1).

2.1.2 Enzyme

Restriction enzymes were purchased either from Invitrogen or Fermentas and used with the suitable buffers suggested by the manufacturer. All other enzymes were purchased from Invitrogen, Roche, Sigma, Biolabs and Echelon Biosciences Inc and TheromFisher Scientific and stored as recommended by the company (Table 2.2).

Table 2.1. Antibiotics used during this study.

Antibiotic	**Stock concentration**	**storage**	**Concentration on working with bacteria**
Ampicillin	100 mg mL-¹ in H²O	-20 ºC	100µg mL-¹
Kanamycin	100 mg mL-¹ in H²O	-20 ºC	100µg mL-¹
Hygromycin	100 mg mL-¹ in H²O	-20 ºC	100µg mL-¹
Gentamycin	100 mg mL-¹ in H²O	-20 ºC	100µg mL-¹
Rifampicin	100 mg mL-¹ in H²O	-20 ºC	100µg mL-¹

Table 2.2. Enzymes purchased plus their details

Enzymes	Company	Catalogue Numbers
Taq DNA Polymerase PCR Buffer (10X)	TheromFisher Scientific	18067017
PhusionHigh-Fidelity DNA Polymerase	BioLabs	F-530
Dream *Taq* DNA Polymerase	Fermentas	EP0401
RevertAid Reverse Transcriptase	TheromFisher Scientific	EP0441
5X Reaction Buffer	TheromFisher Scientific	EP0442

2.1.3 Plasmid vectors and primers

All plasmid expression vectors were used throughout this research is detailed in (Table 2.3) with matching antibiotic resistance. All primers used in this project were synthesised by Invitrogen and detailed with sequences in (Table 2.4). Primers stock concentration was 100 pmole µl-1, and the operating concentration of primers for PCR was 10 pmole µl-1, hence, to make an suitable working concentration, the stock primers were diluted ten times.

2.1.4 Plant material

Wild-type Columbia (Col-0) Arabidopsis was used for the cloning both GAPA and GAPB genes using antisense technology. Also, GAPB antisense tobacco plants were constructed in our lab previously.

2.1.5 Gas exchange apparatus

For Tobacco plants, an open infra-red gas analysis (IRGA) of photosynthesis rate was done using the gas exchange system with an integral blue-red LED light source (LI-COR 6400; LI-COR, Lincoln, Nebraska). For Arabidopsis plants using CIRAS-1 portable gas exchange system (PP Systems, CIRAS-1, PP Systems Ltd.).

Table 2.3. Plasmid vectors, bacteria cell strain and suitable resistance antibiotic

Plasmids	Antibiotic resistance	Working concentration	Vectors Supplier
pENTR™ Directional TOPO®	Kanamycin	100 µg mL-¹	Invitrogen
PGWB2 vector	Kanamycin and Hygromycin	100 µg mL-¹	Nakagawa et al. (2007)
GV1301	Rifamycin, Kanamycin, Hygromycin and Gentamycin	100 µg mL-¹	Prepared in the lab
rbcG2	Kanamycin and Hygromycin	100 µg mL-¹	

Table 2.4: Primers used in this study

Primer sequence was used to identify plants with T-DNA insert of rap2.12-*1* and *rap2.12-2* with GAPA-2 OE lines (13, 29).

Name of primer	Sequences	AGI code	Expected size
rap2.12-1 F	TGGCTACTCCTGAATGCAAAC	AT1G53910	1490bp
rap2.12-1 R	CTCAGCTGTCTTGAACGTTCC	AT1G53910	1490bp
rap2.12-2 F	AAAGTTACTGGCTTGGATGGG	AT1G53910	1494bp
rap2.12-2 R	AATTTACGAGAACCGGTTTGG	AT1G53910	1494bp
Insertion primer (Gabi-Kat)	ATATTGACCATCATACTCATTGC	-	
GAPA-2 Forward	CACCATGAGAAGCAATGGTGGATACAGG	At1g12900	1140bp
Nos primer	TGCCAAATGTTTGAACGATCG	-	1140bp

Primer sequences were used to study network connections of gene regulatory networks (VBSSM) direct and indirect targets of *RAP2.12* and GAPA-2

Name of primer	Sequences	AGI code	Expected size
TK2 F	TCATCATCATCTCAGCCGCT	AT5G23070	97bp
TK2 R	GGCGGAGAAGTGTTGTTGTT	AT5G23070	97bp
FBA1 F	TCCCTGGCATCAAAGTCGAC	AT2G21330	141bp
FBA1 R	TGCTCACAACAGTACGCCAT	AT2G21330	141bp
HCEF1 F	GGCATCATCATCCCAGCCTT	AT3G54050	118bp
HCEF1 R	GGCCATACACCTCACTCCAC	AT3G54050	118bp
SBPase F	TCTCTCTCTCGCCCAATTGC	AT3G55800	88bp
SBPase R	AAGGCTGTTCACGGTCAGAG	AT3G55800	88bp
PDTPI F	CTACCTCTCTCACTGCCCCT	AT2G21170	114bp
PDTPI R	TAGAGGAATTGACGCGGTGG	AT2G21170	114bp
PGK F	AGCCTCTTGTGCCCAGATTG	AT1G79550	150bp
PGK R	CTTCCTCGGCGTAGAACCTC	AT1G79550	150bp
RPE F	TTGTCAAGGCCTCATCTCGG	AT5G61410	110bp
RPE R	CACTGCTTTTACCTGCTCGC	AT5G61410	110bp
FBA2 F	GTCCTCGTCGAGCAGAACAT	AT4G38970	94bp
FBA2 R	GTCCTTGGCACCATGACTCA	AT4G38970	94bp
RBCS1A F	TTAAGTCCTCCGCTGCCTTC	AT1G67090	83bp
RBCS1A R	GTTAACTCTTCCGCCGTTGC	AT1G67090	83bp
Actin2 F	ACCTTGCTGGACGTGACCTTACTGAT	AT3G18780	
Actin2 R	GTTGTCTCGTGGATTCCAGCAGCTT	AT3G18780	
CP12 (1) F	GAAGCGGATGGTTGTGGTT	AT2G47400	63bp
CP12 (1) R	CTCTTCTCCACCTTCTCCGA	AT2G47400	63bp
CP12 (2) F	TTCACAGGCTGCCGTGTACC	AT3G62410	85bp

CP12 (2) R	GACGAAGACACGCTGGGTTG	AT3G62410	85bp
CP12 (3) F	AGCCTGATGATGGTGACGAAGG	AT1G76560	113bp
CP12 (3) R	TCGCAAACCTCTGTCGCTTCC	AT1G76560	113bp
RAP2.12 F	ATGTGTGGAGGAGCTATAATATCCGA	AT1G53910	93bp
RAP2.12 R	ATTCTTCTTCAGATCCGGCCAAA	AT1G53910	93bp
16750 F	GCTTCACTGTTTCGCCAAGA	AT1G16750	132bp
16750 R	CCCAGAAAACCCCACCATTG	AT1G16750	132bp
GAPA-1 F	TCACAGAGAGTTGTTGACTTGGC	AT3G26650	149bp
GAPA-1 R	TACTACAATTATACAGTCTTCACCG	AT3G26650	149bp
GAPA-2 F	ATGGTTATGGGAGATGATATGG	AT1G12900	142bp
GAPA-2 R	ATGGAGCAGACATCAAGAGGTTG	AT1G12900	142bp
GAPB F	TTCAGGTGCTCTGATGTCTCTACC	AT1G42970	142bp
GAPB R	TAGCCACTAGGTGAGCCAAATCCACC	AT1G42970	142bp
PRK F	GCTCATTGCCAACAAAGCCA	AT1G32060	90bp
PRK R	AAATCCGCGGTAAACAACGC	AT1G32060	90bp

Primers were used for cloning (GAPA, GAPB, and Atg16750 unknown protein)

Primer name	**sequences**	**Locus ID**
GAPA F	CACCTATCGAAGGAACCGGAGTGTT	AT1G12900
GAPA R	TCCTGTAGATGTTGGAACAATG	AT1G12900
GAPB F	CACCTTGATGGTAAGCTCATCAAAGTT	AT1G42970
GAPB R	GGTGTAGGAGTGTGTGGTTGT	AT1G42970
16750 F	CACCCAACCTAGAAGCAAAGTGGC	AT1G16750
16750 R	ACATTGAAGCCACTTCAGTTGC	AT1G16750
M13 F	GTAAAACGACGGCCAGT	
M13 R	AACAGCTATGACCATG	
PGWB2 F	ATCGTTGAAGATGCCTCTGCC	

Primers were used to identify plants with T-DNA insert of GAPDH

Name of Primer	Sequences	AGI code	Expected Size
GAPB(Sail_267) F	GAATGGTGCAGCTCTAAGCAC	AT1G42970	968bp
GAPB(Sail_267) R	CCTACCAATCCTTCCAAAACC	AT1G42970	968bp
Insert Primer Sail LB3	TAGCATCTGAATTTCATAACCAATCTCGATACAC		460bp
GAPB Full-length F	ATGGCCACACATGCAGCTCTCGC	AT1G42970	2463bp
GAPB Full-length R	TCAGTCATAGACTTTGCATTCCTCATCAGC	AT1G42970	2463bp
GAPA-1 Salk138567C F	TGATAACCTTCTTGGCACCAG	AT3G26650	1207bp
GAPA-1 Salk 138567C R	GTCAGACAAATGGAGAGCAGC	AT3G26650	1207bp
GAPA-1 Sail 1293 F	GTTGGTGTCTTTGCCTCTGTC	AT3G26650	1088bp
GAPA-1 Sail 1293 R	GCTGCTCTCCATTTGTCTGAC	AT3G26650	1088bp
Insert Primer Sail LB1	TGATAACCTTCTTGGCACCAG		490bp
Insert Primer Salk LB1	GTCAGACAAATGGAGAGCAGC		750bp

2.2 Methods

2.2.1 Molecular biology approaches

2.2.1.1 DNA extraction

(Edwards et al., 1991) described the method for DNA extraction. Genomic DNA was arranged by grinding a plant leaf with Pastel using a 1.5-mL micro-centrifuge tube in 200 ul of extraction buffer (200 mM Tris-HCl, pH 7.5, 250 mM NaCl, 25 mM EDTA, 0.5% SDS). This sample was then stored for 2 minutes at room temperature, after which it was centrifuged for 5 minutes at maximum speed. The supernatant was wisely transferred to a new tube and precipitated. For this, 500 µl of isopropanol was added and mixed, followed by centrifuging for 10 minutes at maximum speed. Subsequently, the supernatant was discarded, and 500 µl of 70% ethanol was added, followed by centrifuging for 5 minutes at maximum speed to clean the pellet. Next, the supernatant

was removed, and the samples were left on a bench or in a hood cupboard to air dry (roughly 30 minutes). Finally, the DNA was re-suspended in 50 µl of TE buffer (10 mM Tris-cl, pH 7.5, 1 mM EDTA) or water. The resulting DNA was either used immediately or stored at -20 °C (the method can be altered depending on the plant materials).

2.2.1.2 Polymerase chain reaction (PCR)

The PCR reaction was achieved in PCR plates using the following master mix: 10x polymerase reaction buffer made of Dream Taq (Fementas) or Phusion High-Fidelity DNA polymerase (New England Biolabs), dNTPs and water. The PCR reaction comprised 1.5 µl of 10 pmol ul stock primer solution per each PCR reaction, 1.5 10X polymerase reaction buffer 0.3 µl of Dream Taq enzyme, 0.5 µl of dNTPs, 2 µl of DNA and 9 µl of water for each reaction. The capacity of the reactions varied between 10–50 µl. The PCR settings were: 30 seconds at 98°C, followed by 35 cycles of 15 seconds at 98°C, 30 seconds at 60-68°C (established on primers temperature), 2 min/kbp elongation stage at 72°C and finally 10 minutes at 72°C, before the incubation at 4°C.

2.2.1.3 Agarose gel electrophoresis and visualisation of PCR products

To envisage the PCR product, about 1 µl of 6x DNA loading dye (10 mM Tris-HCl, pH 7.6, 0.03% bromophenol blue, 0.03% xylene cyanol FF, 60% glycerol, 60 mM EDTA) was mixed with the PCR product. Then, the PCR product was separated for study using gel electrophoresis: 0.5-1% agarose gel was run at 100 V for 45 minutes (150-mL gel) or 85 V for 20 minutes (50-mL gel). Make the gels and the PCR product Tris-borate buffer was used to run the study (TBE: 89 mM Tris, 89 mM boric acid, 2 mM EDTA). SafeView from NBS Biologicals was added to the gels for nucleic acid envisaging below UV or blue light.

2.2.1.4 Primer design

The primers for gateway cloning and identified plants with T-DNA insert of *RAP2.12* and GAPDH and expression analysis were designed and formatted using the primer extension analyses Primer3 plus software (https://primer3plus.com) (Table 2.4).

2.2.1.5 Quantification of nucleic acids (plasmid, DNA, RNA)

To quantify the plasmids, RNA and DNA were measured, and their pureness was determined by spectrophotometry using the Nano DropTM ND-1000 Spectrophotometer (Thermo Fisher Scientific) as described the company's instructions.

2.2.1.6 Seed sterilisation

Seed sterilisation was achieved by using a modified protocol established on Aronsson and Jarvis (2002) and Singh, Nath and Sharma (2007). First, the seeds were soaked in a solution comprising 95% ethanol + 0.1% Tween and left in a shaker for 10 minutes to be mixed well. Then, the solution was removed, and the seeds were rinsed 4–6 times with 75% ethanol. Finally, the seeds were placed in filter paper and left to dry inside a cabinet for about 1 hour, after which they were directly sown in MS plates, which were located in a dark, cold room at 4 °C for 2-3 days before being transferred to a growth room, either a short- or long-day room.

2.2.1.7 Plasmid DNA preparation

To obtain the high-purity plasmid DNA used for sequencing, plasmid DNA was extracted from E.coli cells using the Qiagen Mini plasmid preparation kit according to the manufacturer's instructions. For this, a single colony from the plate was used to inoculate in 10 mL of LB plus antibiotics (50 µg/mL kanamycin or 30 µg/mL hygromycin, depending on the plasmid) and left overnight at 37 °C to grow. The next day, 3–10 mL of the culture

was reduced with a large centrifuge for 15 minutes. The cells were re-suspended with 250 µl of P1 buffer containing RNase A and then transferred to a microcentrifuge tube. Afterwards, 250 µl of P2 buffer was added, and the substances of the tube were mixed thoroughly by inverting the tube 3–6 times. Subsequently, 350 µl of N3 buffer was added and mixed directly by again inverting the tube 3–6 times. Then, the lysed cells were centrifuged for 10 minutes at maximum speed in a conventional table-top micro-centrifuge. Next, the supernatant was transferred to the QIAprep spin column by pipetting. The column was then centrifuged at maximum speed for 45 seconds, and the flow-through discarded. After that, the column was washed with 0.75 mL of PE buffer and centrifuged for 30–60 seconds; again, the flow-through was discarded, and the column was centrifuged for 1 minute to remove residual wash buffer. At this step, the column was transferred into a clean 1.5-mL tube, and 50 µl of EB buffer (10 mM Tris, pH 8.5) or sterilised water was added to the centre of the column. This sample was then incubated for 1-2 minutes at room temperature. Finally, the sample was centrifuged for another 1 minute, and the plasmid DNA was stored at -20 ° C.

2.2.1.8 Preparation of Agrobacterium competent cells and transformation by electroporation

The preparation of *Agrobacterium tumefaciens*-competent cells of the AGL1, LBA 4404 and GV3101 strains and their transformation operating electroporation are defined by Sambrook and Russell (2001). A single colony from the plate was inoculated in 10 mL of LB plus antibiotics (50 µg/mL rifampicin for all strains, 25 µg/mL gentamicin for GV3101, 50 µg/mL and 30 µg/mL streptomycin for LBA 4404). Then, the colony was left in a shaker and allowed to grow for 48 hours at 28 °C. After that, the culture was ice-cold on ice and centrifuged for 15 minutes at 4 °C and 3000 g of speed. Next, the cells were re-suspended in 10 mL of cold sterilised water and centrifuged again for 15 minutes at 4 °C with 3000 g

of speed. The wash was repeated 3-4 times. Finally, the cells were re-suspended in 200 µl of cold sterilised 10% glycerol. The competent cells were aliquoted 50 µl in 1.5-mL tubes for immediate use or were stored at -80 °C. For Arabidopsis plant transformation using competent cells, 1-2 µl of previously extracted plasmid was gently mixed into the electroporation cuvette. Then, the cells were electroporated at 2500 V using the EasyJect Prima electroporator from Equibio. Next, the cuvette tube was removed and 1 mL (1000 µl) of cold Luri media (LB) was added in cuvette tube, before being transferred again to a 1.5-mL tube and left in a gentle shaker for approximately 2 hours at 28 °C: 100–200 µl of cells were spread on LB plates containing the antibiotics (50 µg/mL rifampicin, 25 µg/mL gentamicin, 50 µg/mL kanamycin and 30 µg/mL hygromycin), which were then left in a cupboard at 28 °C to grow for 48–72 hours.

2.2.1.9 Arabidopsis plant transformation

Arabidopsis plant transformation via the floral dipping method was explained by Clough SJ and Bent A (1998). Arabidopsis plants were grown in a growth chamber for approximately 4 weeks in a short-day growth room (photoperiod: 8 h light / 16 h dark, RD 50%), followed by roughly 4 weeks in a long-day growth room (photoperiod: 16 h light / 8 h dark), which is the time needed for the plants to flower. The first bolts were clipped to encourage the proliferation of numerous secondary bolts (the optimal plants are assumed to have many immature flower clusters and not many fertilised siliques). Ten-ml cultures of strains carrying the genes of interest were grown in a shaker at 28 °C in LB media with the following antibiotics: 50 µg/mL rifampicin, 25 µg/mL gentamicin, 50 µg/mL kanamycin and 30 µg/mL hygromycin. The next day, bacterial cells were centrifuged with 3000 g for 15–20 minutes, and the cells were re-suspended in a 5% sucrose solution with an OD of approximately 0.5 before dipping; then, 0.05% Sliwet L-77 (500 µl/L) was added to encourage the transformation. After that, pipetting transformed the solution to un-opened

blots. The plants were next placed in large autoclave bags to preserve their humidity and left in a dark room overnight. Afterwards, the plants were moved to a greenhouse and allowed to grow generally; and for high-quality transformation, the process was repeated after 1 week for new un-opened blots. Finally, the seeds were harvested when the plants were dried, and the transformed plants were selected using 50 µg/mL kanamycin or 10 µg/mL hygromycin, or a herbicide-selectable marker. For chosen transformed plants, the seeds were sown in MS plates having the antibiotics for 15 days in a long-day growth room. Then resistance positive transformed plants were transferred to individual pots to allow further growth and seed production.

2.2.1.10 RNA extraction (Tri-reagent)

After the plant tissue had been collected and stored at -80 °C, TRI reagents from the Sigma Company were used to isolate RNA from the tissue. The plant tissue was ground using the mortar and cold pestles (stuck in dry ice) with liquid nitrogen, and then the powder was transferred to 1.5-mL tubes for immediate use or storage at -80 °C. Then, 1 mL (1000 µl) of TRI reagent was added, and the tube was thoroughly mixed using a rotator before being incubated at room temperature for 5 minutes. Next, the samples were centrifuged at 4 °C with 12,000 g for 10 minutes, and the supernatant was transferred into new 1.5-mL tubes. Next, 200 µl of chloroform was added by inversion to the samples 20 times, and the tubes were left standing at room temperature for 5 minutes. Then, the samples were centrifuged at 4 °C with 12,000 g for 15 minutes. The aqueous phase was then carefully transferred to new 1.5-mL tubes, and 500 µl of isopropanol was added before the mixture was gently blended by inversion; afterwards, the mixture was left to stand at room temperature for 10 minutes. Then, the samples were centrifuged at 4 °C with 12,000 g for 15 minutes, and the supernatant was then discarded; and should be in this point see the pellet of RNA. Following this, 1 ml of 75% ethanol was added to wash

the pellet, and the samples were then centrifuged at 4 °C with 12,000 g for 5 minutes. The supernatant was then removed, and the tubes were left to stand at room temperature for approximately 15 minutes to allow the pellet to air dry. When the pellet was dried, 400 µl of DDH2O was added to re-dissolve the pellet, and 400 µl of chloroform was added; the samples were then shaken for 15 seconds. After that, the samples were centrifuged at 4 °C with 12,000 g for 5 minutes. Afterwards, 300 µl of the upper phase was carefully transferred into new 1.5-mL tubes, and 30 µl of 3M sodium acetate with 750 µl of cold 100% ethanol were added. The samples were then centrifuged at 4 °C with 12,000 g for 15 minutes, after which they were chilled in dry ice for 20 minutes or stored at -20 °C for 40 minutes; then, the samples were spun down at 4 °C with 12,000 g for 15 minutes. Afterwards, the supernatant was discarded, and the pellet was recovered and washed with 500 µl of 75% ethanol. Finally, the samples were centrifuged at 4 °C with 12,000 g for 5 minutes, after which the supernatant was removed, and the tubes were left to stand at room temperature for roughly 15 minutes to allow the pellet to air dry. After that, 43 µl of DDH2O was added to re-dissolve the pellet, and the samples were stored at -80 °C or used immediately.

2.2.1.11 DNase treatment of RNA

DNase treatment was used to check the nonappearance of genomic DNA in the RNA samples. The RNA samples should be 1 µg that is mean 4 µl of the 250 ng µ-1 produced from the extraction; 1 µl of 10x DNase I reaction buffer and 1µl of DNase I, Amp Grade, were then added (the buffer from Thermo Fisher Scientific). Next, 4 µl of water was added, and the samples were stored at 37 °C for 15 minutes. To deactivate the DNase, 1 µl of 25-mM EDTA solution was added to the mixture and incubated at 65 °C for 10 minutes; then, the samples were put on ice.

2.2.1.13 RNA extraction from Kit

After the plant tissues were collected and stored at -80 °C, approximately 0.8 mg of tissue was ground with the mortar and ice-cold pestles (stuck in dry ice) with liquid nitrogen, and then the powder was transferred to 1.5-mL tubes for immediate use or was stored at -80 °C. Then, 350 µl of RP1 and 3.5 µl of B-mercaptoethanol for example (10 samples = 4 mL RP1 + 40 µl B-ME) were added and vigorously spun, and the samples were then centrifuged at maximum speed for 30 seconds. Next, in the filtration step, the supernatant was transferred to the purple column, and the samples were centrifuged at maximum speed for 75 seconds. Subsequently, the flow-through (avoiding the pellet) was carefully transferred to a new tube containing 350 µl of 70% ethanol and mixed well by pipetting up and down 5 times; afterwards, all mixtures were transferred to the blue column, and the samples were centrifuged at maximum speed for 2 minutes. Next, all flow-through was transferred to new 1.5-mL tubes, and the protein samples were put back into dry ice (DNA and RNA are bound to the blue column); after that, 350 µl of MDB solution was added in the same blue column and centrifuged at maximum speed for 75 seconds. Then, the samples were treated with DNase by adding 95 µl of DNase mix, and the samples were left at room temperature for 15–20 minutes. Subsequently, the samples were washed using 200 µl of RA2 buffer and centrifuged at maximum speed for 45 seconds. After this, the flow-through was discarded, and the samples were washed using 600 µl of RA3 buffer and centrifuged at maximum speed for 45 seconds. Then, the samples were washed using 250 µl of RA3 and centrifuged at maximum speed for 2 minutes. Following this, the samples were transferred from the blue column to new 1.5-mL tubes for RNA, careful not to let the flow-through touch the column, if this occurs, the samples will need to be centrifuged again. Finally, 25–50 µl of sterilised water was added to the blue column and centrifuged at maximum speed for 1-2 minutes, then removed and stored at -80 °C.

2.2.1.14 Revert Aid first strand cDNA synthesis

To synthesise the cDNA, each sample was diluted to 1 µg of RNA (11 µl total) using RNase-free water. One µl of oligo primer (dT) was added and incubated at 65 °C for 5 minutes. Next, the samples were chilled on ice and centrifuged quickly. Finally, 2 µg of DNA-free RNA, 2 µl of 10 mM dNTPs, 4 µl 5x reaction buffer, and 1 µl of water were added to make a final volume of mixture 12 µl. Finally, the samples were incubated in a PCR machine at 42 °C for 60 minutes, followed by 10 minutes at 70 °C, and then the cDNA samples were stored at -20 °C or used immediately.

2.2.1.15 Gene expression analysis using q-PCR

Study the genes expression, the produced cDNAs were amplified using quantitative PCR (qPCR) to recognise whether or not the transformed genes were expressed. A mix containing 7.5 µl of Sybre, 1 µL of forward primer (10 pmol) and 1 µL of 10 pmol reverse primer were fixed. The total 9 µL of the master mix were added in triplicate into 96 wells plates involving 6 µL of cDNAs and mixed together by manual centrifugation. Following, the q-PCR cycling conditions were carried out as following: 95°C for 3 min, (95°C for 10 sec, 62°C for 30 sec) (45 cycles). qPCR reactions were completed using SensiFast SYBR No-ROX mix (Bioline Reagents Ltd, London, UK) as detailed by the manufacturer.

2.2.1.16 Cloning GAPA and GAPB and Atg16750 genes using gateway technology

The GAPB and GAPA gene sequences of Arabidopsis *thaliana* were used from the TAIR database. Then, the forward and reverse primers for those genes were designed according to the pENTRTM Directional TOPO® Cloning guidelines. The PCR primers for gene amplification, with the addition of 4-nucleotide CACC at the 5' end of the forward

primer (for more details, please refer to the pENTRTM Directional TOPO® Cloning Kit Manual, pp. 8-9, for diagrams of the TOPO® cloning site for pENTRTM/D-TOPO® and pENTRTM/SD/D-TOPO®; Afterwards, PCR was performed to amplify the gene of interest with high-fidelity DNA polymerase. Then, the TOPO cloning reaction was set up using pENTRTM/D-TOPO®. Next, LR recombination reaction was performed. The Gateway® LR ClonaseII enzyme mix kit (Invitrogen) was used to perform the LR recombination reaction. The destination vector used in this experiment was the PGWB2 antisense vector for knockdown expression of GAPA and GAPB genes. Finally, after verifying the plasmid sequences, the transformation was achieved by the *Agrobacterium tumefaciens* strain carrying the gene of interest on a binary vector.

2.2.1.17 Colony PCR to verify positively transformed plants

The colony PCR was performed to confirm positively transformed plants (the PCR was conducted as described above in the PCR reaction section). The colonies were selected with sterilised tips and slipped into the PCR mixture. M13 forward and gene-specific reverse primers were used for the reaction. The PCR condition used for the annealing temperature for M13 primers was 60 °C.

2.2.1.18 PCR to identify T-DNA insertion mutants of GAPDH and RAP2.12

The identification and locations of T-DNA insertion mutant lines of GAPA and GAPB were chosen from the TAIR website. Seeds were directly sown in soil pots and germinated in a long-day growth room (photoperiod: 16 h light / 8 h dark) until the plants matured, after which the tissues were collected and used for genomic DNA extractions. Then, PCR analysis was conducted using the specific primer of the T-DNA insertion mutant, plus the left border depending on the kind of insertion mutant (SAIL, SALK, Gabi-kat); primer

sequences are indicated in (Table 2.4).

2.2.1.19 Protein extraction

After the plant tissues were collected and stored at -80 °C, they were ground using a cold pestle with mortar, after which 1 ml (1000 µl) of extraction buffer was added (the recipe for the extraction buffer is indicated in the table below).

	gram to add for			
Concentration	**50 ml**	**250 ml**	**500 ml**	**1 litre**
50 mM HEPES pH 8.2 (KOH)	0.5958	2.979	5.958	11.916
5 mM $MgCl_2.6H_2O$	0.0508	0.254	0.508	1.016
1 mM EDTA	0.0186	0.093	0.186	0.372
1 mM EGTA	0.019	0.095	0.19	0.38
10% Glycerol	5 ml	25 ml	50 ml	100 ml
0.10% Triton X-100	50 µl	250 µl	500 µl	1 ml
2 mM Benzamidine *	0.0158	0.079	0.158	0.316
2 mM Aminocaproic acid *	0.0132	0.066	0.132	0.264
0.5 mM PMSF * (dissolved in isopropanol)	0.0044	0.022	0.044	0.088
10 mM DTT	0.0772	0.386	0.772	1.544

The samples were then centrifuged at 4 °C with 14,000 g to remove all debris. Next, the supernatant was carefully transferred into new 1.5-mL tubes.

	gram to add for		
Concentration	**20 ml**	**50 ml**	**100 ml**
313 mM Tris-HCl pH 6.8	0.7584	1.896	3.792
10% SDS	2	5	10
25% Glycerol	5 ml	12.5 ml	25 ml
25% 2-Mercaptoethanol	5 ml	12.5 ml	25 ml

Then, the samples were boiled in a heater for 5 minutes and stored at -80 °C or used immediately.

2.2.1.20 Preparation of SDS-PAGE electrophoresis and polyacrylamide gels

Polyacrylamide gels (resolving and stacking gels) were produced as follows:

	1 Gel		2 Gels		3 Gels	
	resolving (mL)	stacking (mL)	resolving (mL)	stacking (mL)	resolving (mL)	stacking (mL)
H2O	1.633	1.511	3.265	3.023	4.898	4.534
Tris PH 8.8	1.266	-	2.532	-	3.798	-
Tris PH 6.8	-	0.169	-	1.239	-	1.858
30% Acrylamide	1.999	0.330	3.998	0.659	5.998	0.989
10% SDS	0.05	0.025	0.100	0.050	0.150	0.074
10% APS	0.05	0.012	0.100	0.025	0.150	0.037
TEMED	0.002	0.002	0.004	0.005	0.006	0.007
Total	5	2.5	10	5	15	7.5

Before being loaded onto the polyacrylamide gels, the protein samples were heated for 10 minutes at 80 °C to confirm correct migration on the gel. The gels were then inserted into the Bio-Rad electrode assembly, and the running buffer (25 mM Tris-HCl, 192 mM glycine) was used to fill the tank. Afterwards, a molecular weight marker was used to approximate the protein's molecular weight, and the protein samples were loaded onto the gels; the gels were then run for 90 minutes at 110 V.

2.2.1.21 Protein transfer

When the gels were entirely run, they were removed from the casting plates and sited in transfer buffer (25 mM Tris-HCl, 192 mM glycine and 20% methanol). The transfer sandwich contained sponges, blotting papers, protein gel and a PVDF membrane: these elements were soaked in transfer buffer. Next, the cassette sandwich was set in the following order: on the black side of the cassette sponge, filter paper, gel, membrane, filter paper, and sponge and close the cassette. The tank was filled with cold transfer buffer, and runs were set at 66 V for 66 minutes.

2.2.1.22 Blocking and gel staining

Once the transfer was complete, the membrane was transferred in 6% milk in 1x PBS solution phosphate-buffered saline (PBS containing 137 mM NaCl, 2.7 mM KCl, 10 mM Na2HPO4, 2 mM KH2PO4) (3 g in 50 mL per gel) and left in a gentle shaker (45 rpm) for 1 hour or overnight in a cold room (it is best to leave the membranes with their protein side facing up). The gels were then transferred into a coomassie stain to observe protein loading.

2.2.1.23 Washing and antibodies

The milk was washed from the membranes with 1x PBS with Tween (300 ml 1XPBS plus 150 µl Tween 20) for 20 minutes on the shaker table (repeat 3x). Then, the primary antibody was added of the protein of interest and left on a shaker table for 1 to 1.5 hours (For best signal and detection it is best to leave the membranes overnight in a cold room). Next, the membranes were washed with 1x PBS with Tween (300 ml 1XPBS plus 150 µl Tween 20) for 30 minutes on the shaker table (repeat 3x), and the secondary antibody was prepared with 50 ml 1x PBS, 3% milk and 20 µl of antibody; the membranes were then left in the secondary antibody for 1 to 1.5 hours (or overnight at 4 °C) on the shaker table. Finally, the membranes were washed with 1x PBS with 0.05% Tween 20 for 10 minutes, three times, on the shaker table.

2.2.1.24 Detection

The membranes were transferred to fresh plastic paper, and a Mix ECL solutions kit was used to mix 1.5 ml of each solution (1:1, v:v to a volume of 3 ml). Then, by pipetting transfer the ECL solution to cover all the membrane before taking a picture.

2.2.1.25 Coomassie Brillant Blue staining

To estimate the transfer productivity of proteins, gels were incubated in 0.1% Coomassie Blue (250R) solution organised in 50% (w/v) methanol and 10% (v:v) acetic acid for about 20 minutes. Next, the gels were de-stained in a destaining solution (10% acetic acid and 50% methanol) for roughly 40 min till the background of the gel was clear, with changing the solution frequently.

2.2.1.26 Protein Extraction by kit

For protein perception, approximately 700 µl of extractions were transferred to new 1.5-mL tubes. Then, 1 volume of PP solution was added (700 µl), and the samples were centrifuged at 11,000 g for 5 minutes. Afterwards, the supernatants were discarded, and 500 µl of 50% ethanol was added; all samples were then centrifuged at 11,000 g for 1 minute. Next, the supernatants were discarded, and the samples were left at room temperature to dry the pellet for 15–20 minutes. Subsequently, 20–100 µl of PSB-TCEP was added and incubated at 95–98 °C for 3 minutes and the samples were then centrifuged at 11,000 g for 1 minute.

2.2.2 Growth and Physiological analyses

2.2.2.1 Plant growth condition

Plants were grown in growth chambers at 22 °C under short-day (photoperiod: 8 hours light / 16 hours dark, virtual humidity [RD] 50%) or long-day conditions (photoperiod: 16 hours light / 8 hours dark), or in a greenhouse.

2.2.2.2 Calculation of rosette area

Plant images were examined using the image processing software ImageJ (https://imagej.nih.gov/ij/) to calculate the rosette area of the plants, as described by (Bechtold et al., 2010).

2.2.2.3 Drought stress experiment

The drought experiment was achieved as defined by Bechtold et al. (2016). To achieve the drought experiment, 7-8-cm pots (Desch Plantpak, Maldon, UK) were filled with an identical amount of compost and vermiculite mixture (Verve; B&Q, Colchester, UK), and 2–4 seeds were sown per pot. The controller pots were filled to the same weight with soil, and then soaked in water for 2-3 hours or overnight until saturation. The pots were then weighed to estimate 100% relative soil water content (rSWC). Six weeks after sowing the seeds, one-half of the plants were maintained in well water condition, whereas stop water the half staying plants to start drought experiment. The pots exposed to drought were weighed every day, and their relative soil water content (rSWC) was measured using the formula equation:

$$\frac{\text{Pot weight – Empty pot weight – Dry soil weight x 100 Saturated}}{\text{Pot weight – Dry soil weight}}$$

The drought condition was constant until the rSWC of plants reached 20%. Then, the plants were harvested for molecular analysis (qPCR, western blot).

2.2.2.4 Photosynthetic light response curves (CIRAS-1) for Arabidopsis

The *A/Ci* response curves were measured by using a CIRAS-1 portable gas exchange system (PP Systems, CIRAS-1, PP Systems Ltd.). The measurement procedure was performed as described by Simkin et al. (2017), with some modifications. Leaves were

irradiated with an integral red-blue LED light source (PP Systems Ltd.) attached to the gas exchange system, and light levels were maintained at a saturating photosynthetic photon flux density (PPFD) of 1000 µmol m^{-2} s^{-1} for the duration of the *A/C*i response curve. Measurements of *A* were made at ambient CO_2 concentrations (*C*a) at 400 µmol mol–1, before *C*a was decreased to 300, 200, 100, and 50 µmol mol–1. Following this, the *C*a was increased stepwise to 1500 µmol m^{-2} s^{-1} for completion of the curve in 11 steps (550, 350, 215, 60, 550, 740, 900, 1140, 1340, 1640 and 1850 µmol m^{-2} s^{-1}). Measurements were recorded after *A* reached a new steady state (1-2 minutes) and before stomatal conductance (gs) changed to the new light levels. The maximum carboxylation rates of Rubisco- (Vc_{max}) and the maximum rate of electron transport for RuBP regeneration (J_{max}) were determined and identical to a leaf temperature of 25 °C based on equations by von Caemmerer and Farquhar (1981) and Sharkey et al. (2007).

2.2.2.5 Photosynthetic light response curves (LI-COR) for Tobacco

An open infrared gas analysis (IRGA) of the photosynthesis rate was achieved using the gas exchange system with an integral red-blue LED light source (LI-COR 6400; LI-COR, Lincoln, Nebraska). The measurement procedure was done as defined by Simkin et al. (2015). Photosynthesis measurements were performed on young, fully expanded leaves. The response of the assimilation rate of CO_2 (*A*) to a variety of concentrations of intercellular CO_2 (*Ci*) was determined at a maintained level of saturated light at 1500 µmol m^{-2} s^{-1} using an open infrared gas exchange system and a 2 cm^2 leaf chamber with an integral red-blue LED light source (LI-COR 6400; LI-COR, Lincoln, Nebraska). Leaf temperature was fixed at 25 °C, and the moisture was maintained around 20 µmol m^{-2} s^{-1}. An outside gas cylinder provided the CO_2. The measurements were done at different CO_2 concentrations (150, 250, 150, 100, 50, 400, 550, 700, 900, 1100, 1300, 400). The

maximum carboxylation rate (Vc_{max}) and maximum electron transport flow (J_{max}), and the C3 photosynthesis model (Farquhar et al., 1980) were fitted to the *A/Ci* data using a spreadsheet provided by Sharkey et al. (2007).

2.2.2.6 Chlorophyll fluorescence imaging (Arabidopsis)

Images of Chl a fluorescence were obtained in 2-week-old Arabidopsis seedlings after sowing that had been grown in a controlled environment chamber providing 130 µmol m–2 s–1 and ambient (400 µmol m^{-2} s^{-1}) CO_2 were imaged. Chlorophyll fluorescence parameters were obtained using a chlorophyll fluorescence (CF) imaging system (Technologica, Colchester, UK; (Barbagallo et al., 2003; Baker and Rosenqvist, 2004).

2.2.2.7 Chlorophyll fluorescence imaging (Tobacco)

The chlorophyll fluorescence measurements were made on 3-week-old tobacco seedlings and plants grown in a controlled environment chamber at 130 µmol mol–2 s–1 and ambient (400 µmol m^{-2} s^{-1}) CO_2. Three-four days before chlorophyll fluorescence imaging, the plants were transferred to the greenhouse and grown in natural irradiance with additional light to maintain levels between 400–600 µmol m^{-2} s^{-1} PPFD at bench level. Chlorophyll fluorescence parameters were obtained using a chlorophyll fluorescence (CF) imaging system (Technologica, Colchester, UK; (Barbagallo et al., 2003; Baker and Rosenqvist, 2004).

Chapter 3: Investigating the role of manipulating RAP2.12 and GAPA-2 on Calvin cycle enzymes under drought and non-drought condition using modelling network (VBSSM)

3.1 Introduction

Yield enhancement and the maintenance of crops' yield stability are necessary for the increasing world population's food security. There are approximately 850 million starving people in the world, mostly living in developing countries, and by the year 2050, the global demand for cereal production is expected to increase by 60% as the global population rises to about 9.6 billion (Fischer and Edmeades, 2010; Bruinsma, 2009; FAO (Food & Agriculture Organisation), 2012; FAO, 2013). The most widespread environmental side which restricts the production of crops is drought stress (Bray, 1997; Chaves et al., 2003). According to Passioura (2007), drought has a wide variety of frequently quite dissimilar meanings. Even in the world of cultivated and plant science functioning definitions vary deeply, mostly because of the time balances of the events being considered. A study that objects to improve water-limited yields on farms should finally make sense on farms. For the many of us whose research takings place mostly in laboratories and which deals with event that take place in hours, or days, the task is to clear the connections among what the scientists are doing and what farmers do, and, what agronomists and plant breeders do. To clear these contacts requires some public of language, of the terms that they use, and of the concepts that such terms represent. Regularly the expression is best done in steps.

For instance, if 'drought resistance', as understood by a molecular biologist or biochemist, does not make greatly sense to a plant physiologist and it will have no opportunity at all of creating sense to an agronomist or a farmer. Agronomists and breeders can help improve workings of seasonal water balance in the field, for instance, by minimising evaporative losses from the soil surface, or by recovering coordinating the development of a crop with its environment. Physiologists, biochemists, and molecular biologists can

help by identifying methods of improving the ability of particular organs. Changes within the photosynthetic carbon metabolism are the principal cause of the metabolic impairment in the drought stress (Lawlor and Cornic, 2002) Under drought stress, the major dependence of the biochemical effectiveness of photosynthesis is upon ribulose-1,5-bisphosphate (RuBP) regeneration as well as the ribulose-1,5-bisphosphate carboxylase/oxygenase (RuBisCO) activity (Lawlor, 2002; Medrano et al., 1997). There is required sign from transgenic studies that manipulation of the Calvin cycle will donate to closing this gap in efficiency and that this could increase yield in the absence of significant stress (Zhu et al., 2010; Raines, 2011). Opportunities include improving the present of leaves in crop canopies to avoid light saturation of individual leaves and additional study of a photorespiratory via that has already improved the productivity of model species. In the longer-term chances include manufacturing into plants carboxylases that are develop adapted to current and coming CO_2 concentrations, and the use of modelling to director molecular optimization of supply investment between the machineries of the photosynthetic apparatus, to increase carbon gain without increasing crop inputs. (Zhu et al., 2010; Raines, 2011). Manipulation of the C3 cycle a chance to increase photosynthesis and yield. Enhancement of the C3 cycle is not just about raising CO_2 fixation , however should also aim to increase together nitrogen use efficiency and water use effectiveness whereas preserving high yield. The variety of genetic and molecular techniques that are currently available, together with the improvement and application of fast *in vivo* techniques to permit in field analysis of a larger variety of species in their natural environments, will assist the wider study of natural variation in photosynthetic carbon assimilation. (Zhu et al., 2010; Raines, 2011). However, to fully maximise any efficiency gains through the manipulation of this pathway, it will also be essential to develop approaches that will reduce the negative impact of stress responses, such as

drought. There has been much development in the enhancement of metabolic changes, photosynthetic light reaction as well as the CO_2 stomatal components. These include the photosynthesis-related gene expression to control photosynthesis under drought conditions to enhance the grain yield (Chaves et al., 2009).

To address the issue of drought and produce plants with improving photosynthesis and resistance to drought, we carried out reverse engineering based on a transcriptional network of the Calvin cycle generated from a microarray time series data (Bechtold et al., 2016) and Variational Bayesian State Space modelling (VBSSM). Gene regulatory networks (GRNs) were modelled using Variational Bayesian State Space Modelling (VBSSM; Beal et al., 2005) as described in Chapter 1 (Figure 1.2). The model output suggests that increased levels of GAPA-2 (AT1G12900) gene expression and decreased levels of the transcription factor *RAP2.12* (AT1G53910) may have a positive effect in the expression of Calvin cycle genes under drought conditions (Figure 1.2). Prior to this project, two T-DNA insertion lines of RAP2.12 (*rap2.12-1*, and *rap2.12-2*) have been identified by Dr Subramaniam (PhD thesis, Figure 3.1). Furthermore, GAPA-2 overexpression was constructed by Dr Simkin (Figure 3.2), and analysis to identify the overexpression lines of GAPA-2 (line 13, and 29) and crossing *rap2.12-1*, *rap2.12-2* with GAPA-2 (13, and 29) has previously been done by Dr Andrew Simkin (Figure 3.3). This chapter aimed to:

1. Identify double mutant lines *rap2.12-1* and *rap2.12-2* with GAPA-2 OE lines (GA-13, and GA-29).

2. To carry out preliminary growth analysis and drought stress phenotyping for single and double mutant lines *rap2.12-1* and *rap2.12-2* with GAPA-2 OE lines (GA-13, and GA-29).

3. To test predicted network connections of the gene regulatory network under drought conditions.

Identification of T-DNA insertion lines for RAP2.12

Single T-DNA insertion mutants were previously isolated, and seeds were provided by Dr Subramaniam (University of Essex, PhD thesis).

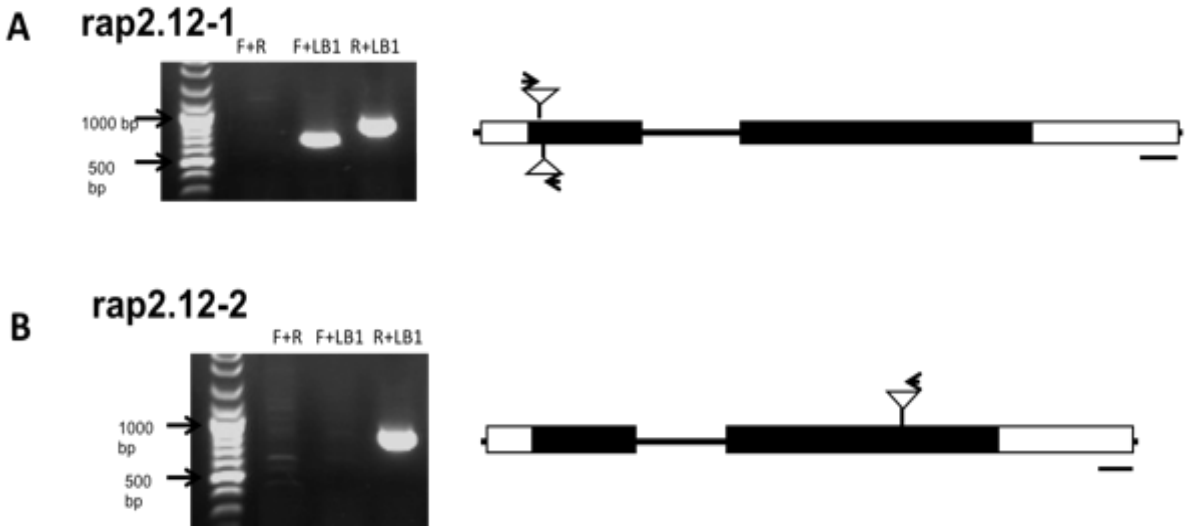

Figure 3.1: Homozygous single mutants, along with the position and orientation of the insertions **(A)** Identified T-DNA insertion homozygous line of *rap2.12-1* by PCR. (B) Identified T-DNA insertion homozygous line of *rap2.12-2* by PCR. (Identification Insertion mutant has been done by Dr Subramaniam.

Production of plants with GAPA-2 overexpression

The over-expression construct of GAPA-2 full-length coding sequence of under the control of the Rubisco small subunit 2B (rbcS2B 1150bp; AT3G26650) promoter was cloned out by Dr Andrew Simkin**.** The rbcS2B promoter directs high-level photosynthetic tissue specific transcription of the transgene. The full-length coding sequence of the Glyceraldehyde- 3-phosphate dehydrogenase A subunit 2 (GAPA-2: At1g12900) was

amplified by RT-PCR (Primers sequences can be found in table 2.4 in materials and methods chapter 2).The resulting amplified product was cloned into pENTR/D (Invitrogen, UK) to make pENTR-*AtGAPA-2*, which was subsequently introduced into the destination vector pGWPTS1 to make pGWPTS1-rbcS2B: AtGAPA-2 (PTS1-G2, Figure 3.2). This construct was created and analysis transgenic lines over express GAPA-2 by Dr Andrew Simkin (Figure 3.2 and 3.3).

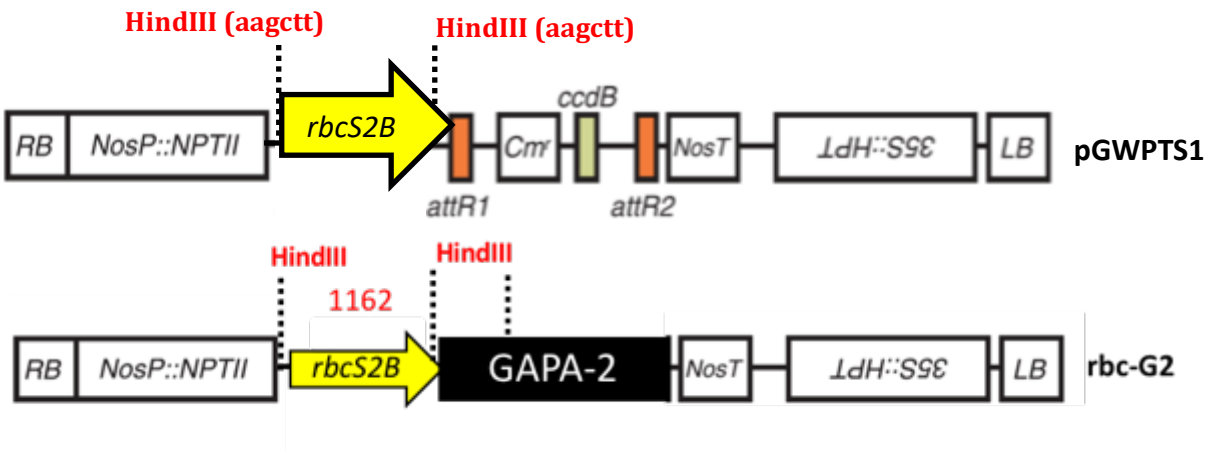

Figure 3.2: GAPA-2 overexpression constructs. The full-length coding sequence of glyceraldehyde-3- phosphate dehydrogenase A subunit 1 (GAPA2: At1g12900) under the transcriptional control of the rbcS2B (1150bp; At5g38420) promoter (NPTII and the 35:: HTP genes which confer resistance to the Kanamycin antibiotic and allow for selection in both bacteria and plants). **The construct was created by Dr Andrew Simkin.**

The resultant transformants were subsequently analysed by Western blot using GAP antibodies (Figure 3.3). Two lines with elevated GAPA proteins levels (13 and 29) were selected for crossing with both *rap2.12* single mutants.

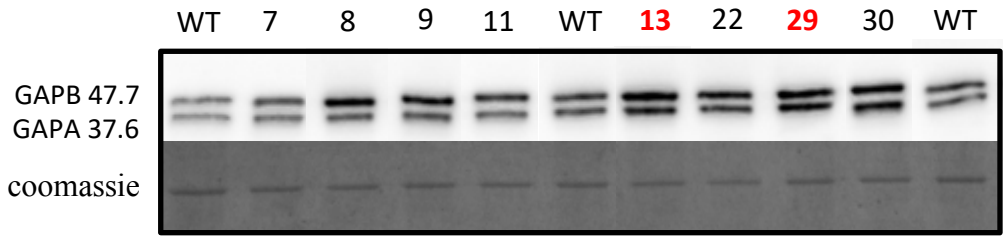

Figure 3.3: Protein levels GAPA transgenic lines over-expressing GAPA-2 (13, 29). This western blot has been done by Dr Andrew Simkin.

3.2 Results

3.2.1 Screening for double mutant plants (*rap2.12 -1+2* & GAPA-2) by PCR

To test the successful outcome of the crosses to produce double mutants over-expressing GAPA-2 in *rap2.12-1* and *rap2.12-2* mutant background, PCR analysis was conducted using gene-specific primers for *rap2.12-1* and *rap2.12-2* with the left border Gabi-kat primer. The first PCR was conducted for 24 plants to identify plants with a T-DNA insertion in *rap2.12-1,* and most plants in this PCR amplified at 1490bp using forward and reverse primers. The majority of the plants were identified as WT (Figure 3.4). The second PCR was conducted for 24 plants to identify plants with T-DNA insertions for *rap2.12-2.* Five plants amplifying approximately 750bp using the reverse primer of *rap2.12-2* and Gabi-kat left border were identified as homozygous plants (Figure 3.5). In addition, PCR was conducted using GAPA-2 Forward with Nos terminator primer to check that the homozygous *rap2.12-2* plants contained the GAPA-2 and all five plants amplifying approximately ~ 1140bp (Figure 3.6).

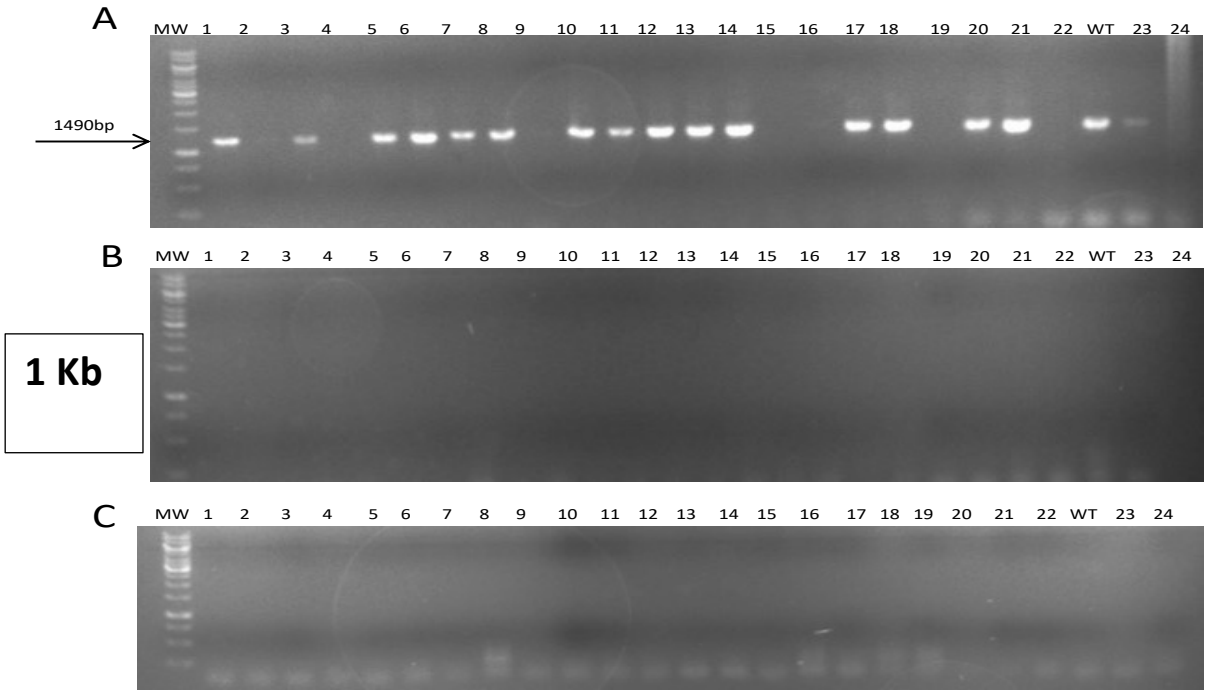

Figure 3.4: PCR analyses to identify homozygous plants with an insert of *rap2.12-1*.

(A) PCR analysis using a gene-specific primer (Forward + Reverse) for *rap2.12-1*.

(B) PCR analysis using Forward primer of *rap2.12-1* and left boarder (Gabi-kat).

(C) PCR analysis using Reverse primer of *rap2.12-1* and left boarder (Gabi-kat).The marker used in this PCR was 1 Kb.

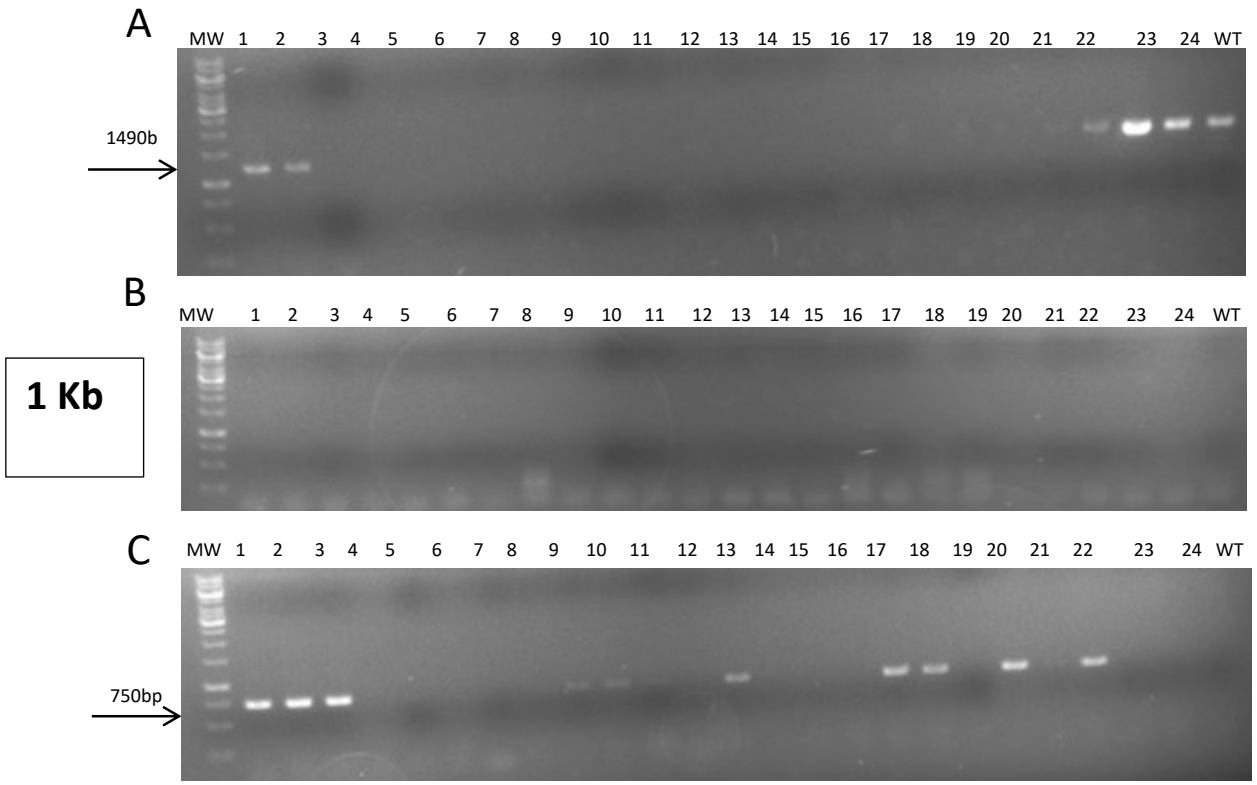

Figure 3.5: PCR analyses to identify homozygous plants with an insert of *rap2.12-2*.

(A)PCR analysis using a gene-specific primer (Forward + Reverse) for *rap2.12-2*.

(B)PCR analysis using Forward primer of *rap2.12-2* and left boarder (Gabi-kat).

(C)PCR analysis using Reverse primer of *rap2.12-2* and left boarder (Gabi-kat). PCR analysis showed that plants 3, 13, 17, 18 and 20 contained the T-DNA insertion with an insert of *rap2.12-2*. The marker used in this PCR was 1 Kb.

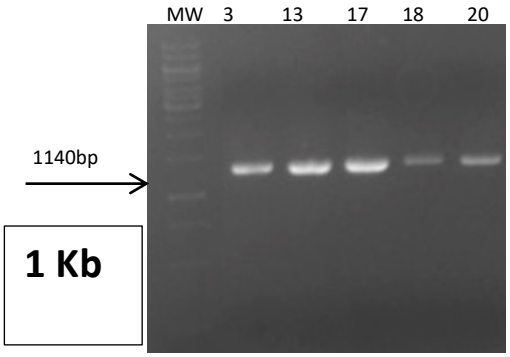

Figure 3.6: PCR analyses using a gene-specific primer of GAPA-2 to check the presence of the transgene GAPA-2 construct in the identified homozygous lines for *rap2.12-2*.PCR analysis indicated that the five plants had the insert of *rap2.12-2* and GAPA-2 OE. (The number of samples indicated the plants identified with an insert of *rap2.12-2* in figure 3.5). The marker used in this PCR was 1 Kb.

3.2.2 Screening for double mutant plants (*rap2.12 -1+2* & GAPA-2) by PCR

Molecular analysis by PCR was repeated to try to identify the plants with *rap2.12-1* insert. Transgenic seeds were sown in sterile agar medium containing Murashige and Skoog salts supplemented with 1% (w/v) Sucrose and were selected using 50 µg/mL kanamycin. Resistant plants were transferred to soil after 14 days of germination (Figure 3.7). The First PCR was conducted for 12 plants to identify plants with a T-DNA insertion in *rap2.12-1,* and five plants were amplifying approximately 750bp using the reverse, and forward primers of *rap2.12-1* and Gabi-kat left border were identified as homozygous (Figure 3.8). The second PCR was conducted for 12 plants to identify plants with a T-DNA insertion in *rap2.12-2,* and three plants were amplifying approximately 750bp using the reverse primer of *rap2.12-2* and Gabi-kat left border were identified as homozygous (Figure 3.9). In addition, PCR was conducted using GAPA-2 Forward with Nos primer to check these homozygous plants of *rap2.12-1* and *rap2.12-2* contained the GAPA-2 transgene, and all plants had the insert of *rap2.12-1* and *rap2.12-2* amplifying approximately ~ 1140bp (Figure 3.10A and 3.10B).

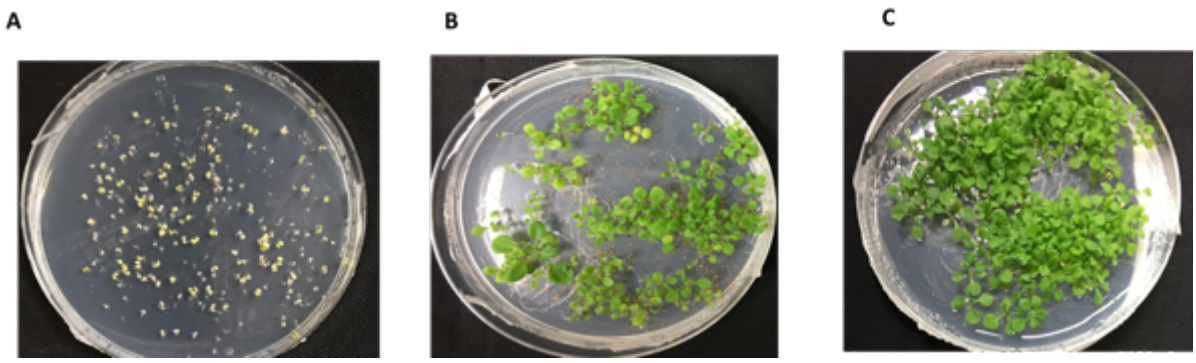

Figure 3.7: Example of screening the double mutant lines *rap2.12-1* and *rap2.12-2* & GAPA-2 OE construct by kanamycin **(A)** Screening col-0 WT plants as a control. **(B)** Screening double mutant line *rap2.12-1* & GAPA-2 OE construct. **(C)** Screening double mutant line *rap2.12-2 &* GAPA-2 OE construct.

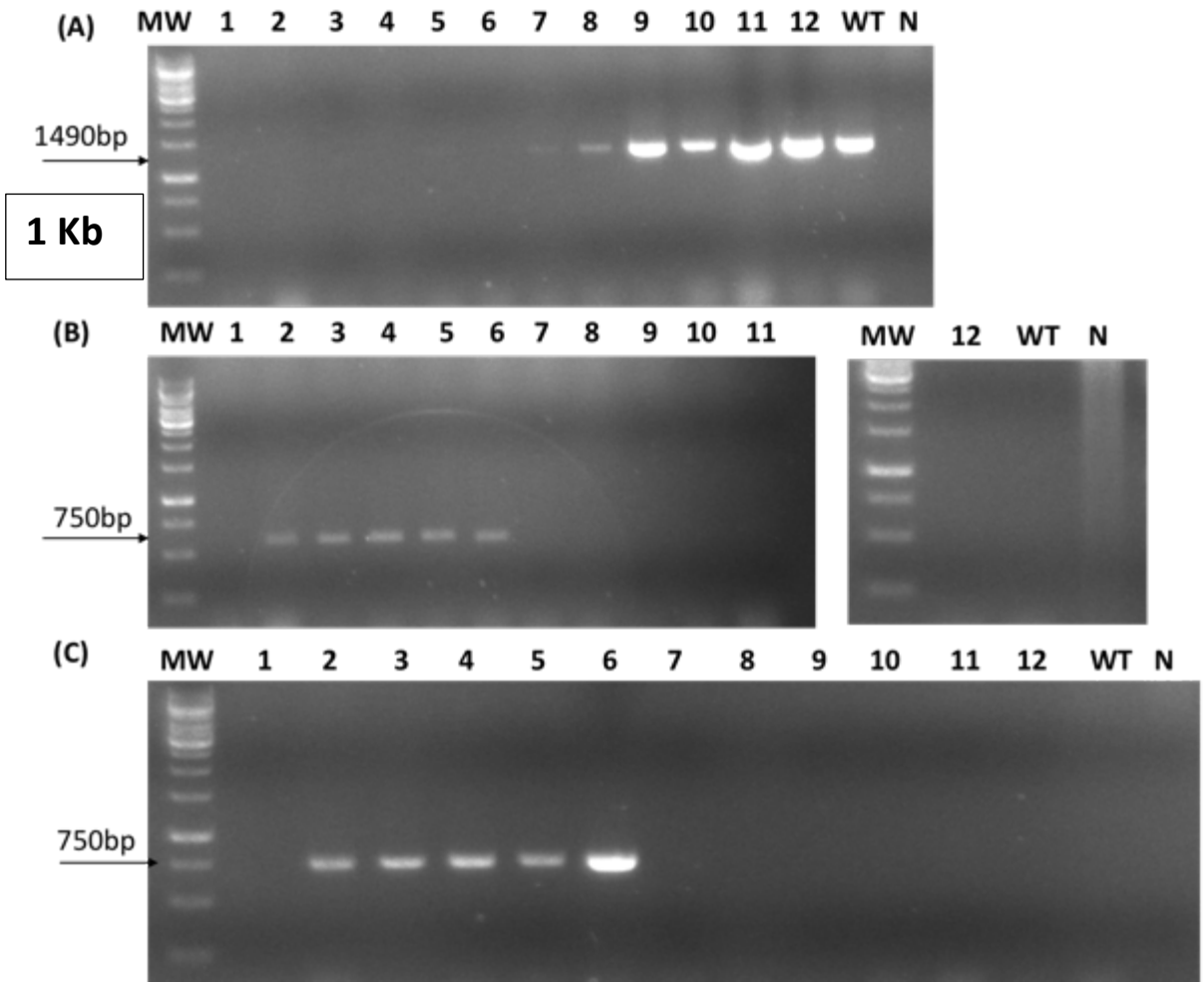

Figure 3.8 PCR analyses to identify homozygous plants with an insert of *rap2.12-1*.

(A) PCR analyses by using a gene-specific primer (Forward + Reverse) for *rap2.12-1.*

(B) PCR analyses by using a forward primer of *rap2.12-1* and left boarder (Gabi-kat).

(C) PCR analyses by using a reverse primer of *rap2.12-1* and left boarder (Gabi-kat). PCR indicated that plants 2,3,4,5 and 6 contained the T-DNA insertion with an insert of *rap2.12-1.* The marker used in this PCR was 1 Kb.

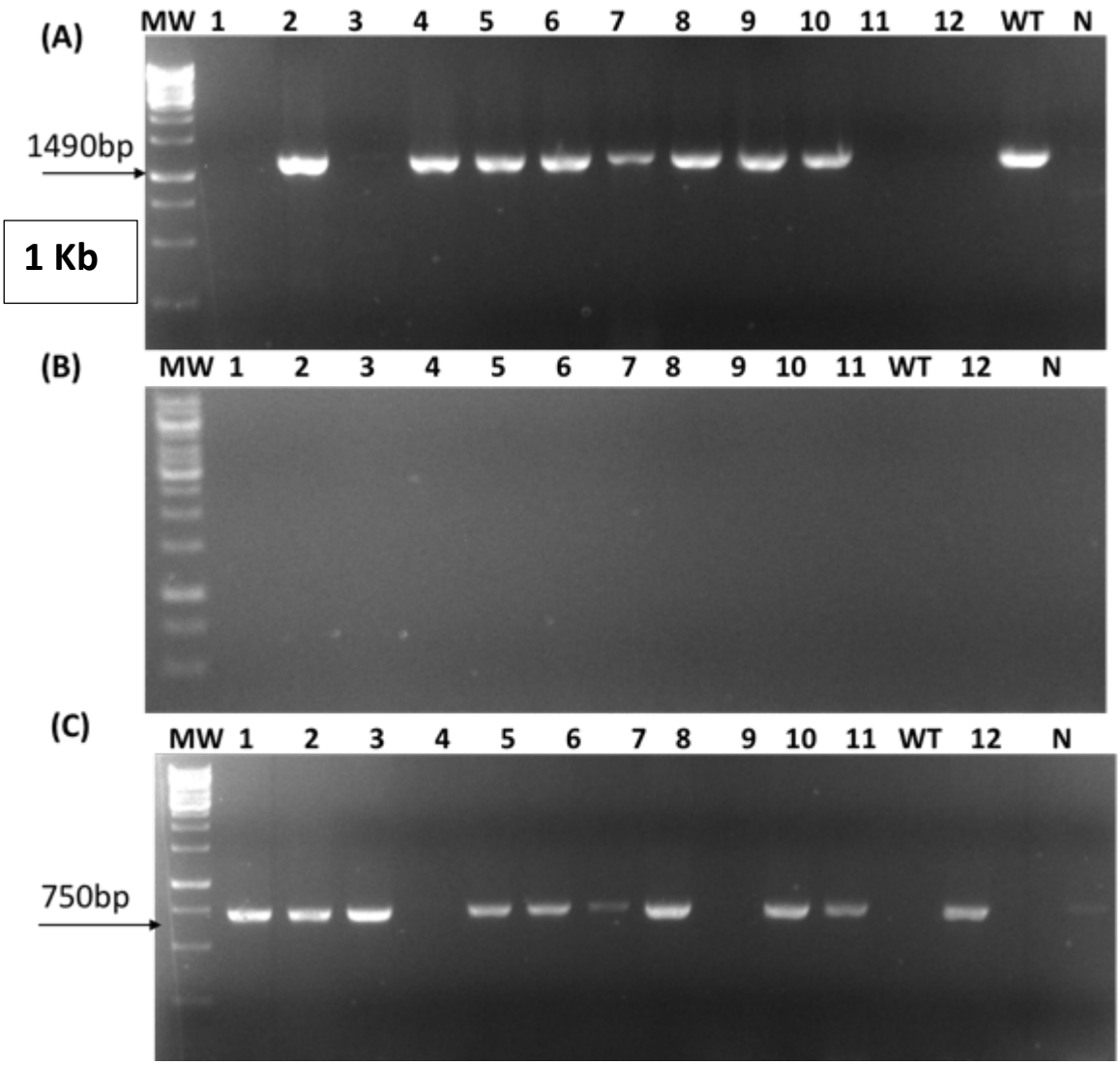

Figure 3.9: PCR analyses to identify homozygous plants with an insert of *rap2.12-2*

(A) PCR analyses by using a gene-specific primer (Forward + Reverse) for *rap2.12-2.*

(B)PCR analyses by using a forward primer of *rap2.12-2* and left boarder (Gabi-kat).

(C)PCR analyses by using a reverse primer of *rap2.12-2* and left boarder (Gabi-kat).PCR analysis indicated that plants 1, 3 and 11 contained the T-DNA insertion of *rap2.12-2.* The marker used in this PCR was 1 Kb.

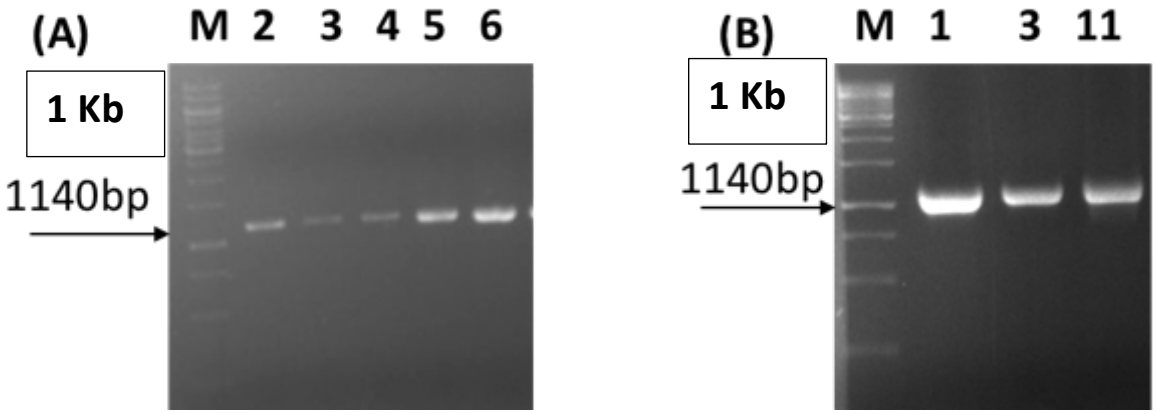

Figure 3.10: PCR analyses using a gene-specific primer of GAPA-2 to confirm the presence of the GAPA-2-OE construct in the identified homozygous lines for *rap2.12-1* and *rap2.12-2* **(A)** PCR analysis showed that plants contained T-DNA insertion of *rap2.12-1* and GAPA-2 OE using GAPA-2 forward primer with Nos primer. **(B)** PCR analysis indicated that plants contained T-DNA insertion of *rap2.12-2* and GAPA-2 OE. The marker used in this PCR was 1 Kb.

3.2.3 Assessing the expression level of single and double mutant lines of *rap2.12-1*, *rap2.12-2* and GAPA-2 OE

To assess the level of expression for both *RAP2.12* and GAPA2 genes in the double mutants, the qPCR analyses was performed using *RAP2.12* and GAPA-2 primers. The first qPCR showed that all five double mutant plants had reduced the expression level of *RAP2.12* compared to WT plants, but not significantly, with the exception of line 4. Moreover, qPCR analysis using GAPA-2 primers did not show increased GAPA2 expression levels for all five double mutant lines, which suggests that the GAPA-2 OE could have been silenced or was still segregating (Table 3.1) and (Figure 3.11 and 3.12). The subsequent growth analysis was therefore performed on plants with decreased expression levels of *rap2.12-2* and potentially segregating for the GAPA-2 OE construct. The experiment was repeated to identify plants with both insertions in*rap2.12-1*, *rap2.12-2* and increased expression levels of GAPA-2. QPCR was carried out on both single mutants of *rap2.12-1,* and *rap2.12-2* double mutant lines (*rap2.12-1*/GAPA-2 13), (*rap2.12-2*/GAPA-2 29) and GAPA-2 OE lines GA-13 and GA-29. The expression level of *RAP2.12* was significantly reduced in both the single and double mutant lines compared to WT plants, however using GAPA-2 primers there was no significant difference compared to WT plants (Table 3.2). The GAPA-2 OE line 13 again showed no significant difference in the expression level of GAPA-2; however, the GAPA-2 OE line 29 had significantly increased expression levels of GAPA-2 and *RAP2.12* compared to WT plants (Table 3.2) and (Figure 3.13 and 3.14).

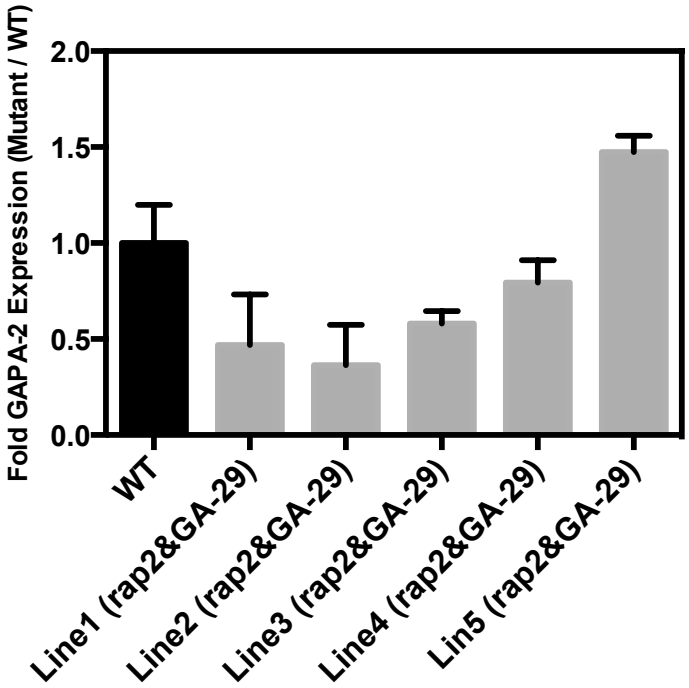

Figure 3.11: Fold expression of GAPA-2 for five double mutant lines of *rap2.12-2* with GAPA-2 OE (line 29) Values are mean ± standard error (no. of biological replicates, n=3). Stars showed the significant transgenic lines compare to WT control ($P<0.05$) one-way ANOVA, post-hoc test).

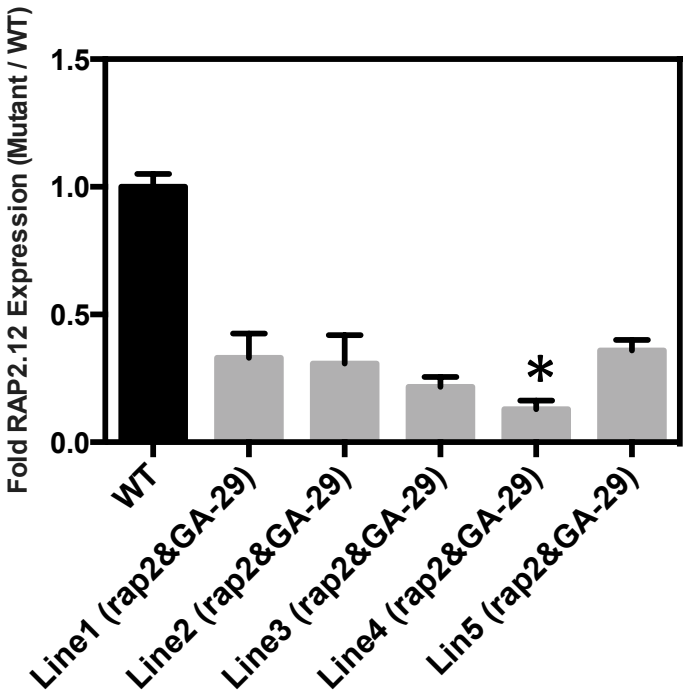

Figure 3.12: Fold expression of *RAP2.12* for five double mutant lines of *rap2.12-2* with GAPA-2 OE (line 29) Values are mean ± standard error (no. of biological replicates, n=3). Stars showed the significant transgenic lines compare to WT control ($P<0.05$) one-way ANOVA, post-hoc test).

Table 3.1

Name of line	Features	*rap2.12* Expression level	GAPA-2 Expression level
Line 1	*rap2.12-2* & GAPA-2 OE (29)	0.264429	0.469644
Line 2	*rap2.12-2* & GAPA-2 OE (29)	0.308702	0.363402
Line 3	*rap2.12-2* & GAPA-2 OE (29)	0.216777	0.580877
Line 4	*rap2.12-2* & GAPA-2 OE (29)	0.012937	0.793502
Line 5	*rap2.12-2* & GAPA-2 OE (29)	0.359555	1.4739
WT	Col-0	1	1

Table 3.1: Indicated the features of five double mutant lines of *rap2.12-2* with GAPA-2 OE (line 29) and the expression level for both *RAP2.12* and GAPA-2 genes. Values are mean ± standard error (no. of biological replicates, n=3).

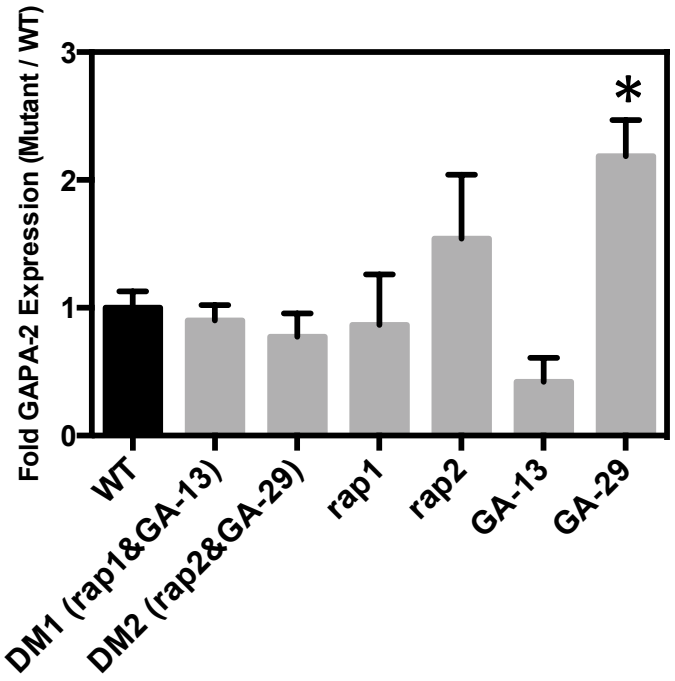

Figure 3.13: Fold expression of GAPA-2 for two single mutant lines of *rap2.12 (1-2),* two overexpression lines of GAPA-2 (13-29), two double mutant lines of *rap2.12 (1-2)* with overexpression of GAPA-2 (13-29), and WT Columbia (Col-0). Values are mean ± standard error (no. of biological replicates, n=3). Stars showed the significant transgenic lines compare to WT control ($P<0.05$) One-way ANOVA, post-hoc test).

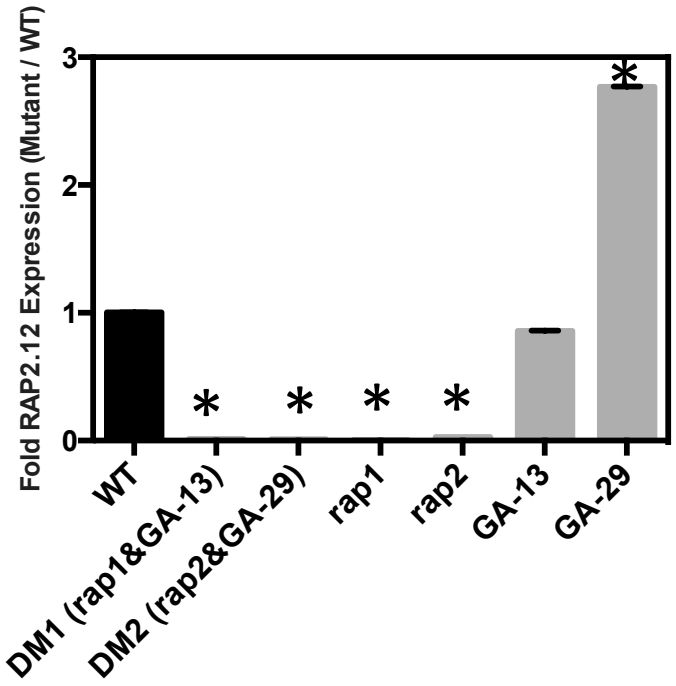

Figure 3.14: Fold expression of *RAP2.12* for two single mutant lines of *rap2.12 (1-2),* two overexpression lines of GAPA-2 (13-29), two double mutant lines of *rap2.12 (1-2)* with overexpression of GAPA-2 (13-29), and WT Columbia (Col-0). Values are mean ± standard error (no. of biological replicates, n=3). Stars showed the significant transgenic lines compare to WT control ($P<0.05$) one-way ANOVA, post-hoc test).

Table 3.2

Name of line	Features	RAP2.12 Expression level	GAPA-2 Expression level
DM1	*rap2.12-1* & GAPA-2 (13)	0.015 *	1.0030318
DM2	*rap2.12-2* & GAPA-2 (29)	0.012 *	0.8599512
rap1	*rap2.12-1*	0.006 *	0.9639518
rap2	*rap2.12-2*	0.028 *	1.7162966
GA-13	GAPA-2 OE line (13)	0.859	0.468378
GA-29	GAPA-2 OE line (29)	2.77 *	2.088898 *
WT	Col-0	1	1

Table 3.2: Indicated the features of two single mutant lines of *rap2.12 (1-2),* two overexpression lines of GAPA-2 (13-29), two double mutant lines of *rap2.12 (1-2)* with overexpression of GAPA-2 (13-29) and the expression level for both *RAP2.12* and GAPA-2 genes. Values are mean ± standard error (no. of biological replicates, n=3). Stars showed the significant transgenic lines compare to WT control ($P<0.05$) one-way ANOVA, post-hoc test).

3.2.4 Protein expression analysis (Western Blot)

To investigate protein expression for drought and well-watered samples of two single mutant lines of *rap2.12 (1-2)*, two overexpression lines of GAPA-2 (13-29) and the two double mutant lines of *rap2.12 (1-2)* with overexpression of GAPA-2 (13-29), protein was extracted from leaves of the transgenic plants and was analysed using immunoblotting. Immunoblotting was carried out using the total extractable protein of 1.5 µg and loaded onto 12% SDS-polyacrylamide gels. The proteins were run and separated by electrophoresis, transferred onto PVDF membranes, probed with GAPDH antibody. A band at about 37.6 kDa indicates the GAPA gene, and at about 47.7 kDa indicates the GAPB gene. Under well-watered condition both double mutant lines (Table 3.2), and GA-29 showed increased protein levels of both GAPA and GAPB compared to WT plants; however, GA-13 only showed increased protein levels for GAPB (Figure 3.15A). Both single mutant lines *rap2.12-1* and *rap2.12-2* showed no difference in GAPA and GAPB protein level compared to WT plants (Figure 3.15A). Under drought conditions, DM2, both single mutant lines of *rap2.12* and both GAPA-2 OE (13-29) showed slightly increased the protein level of GAPA and GAPB compared to WT plants (Figure 3.15B).

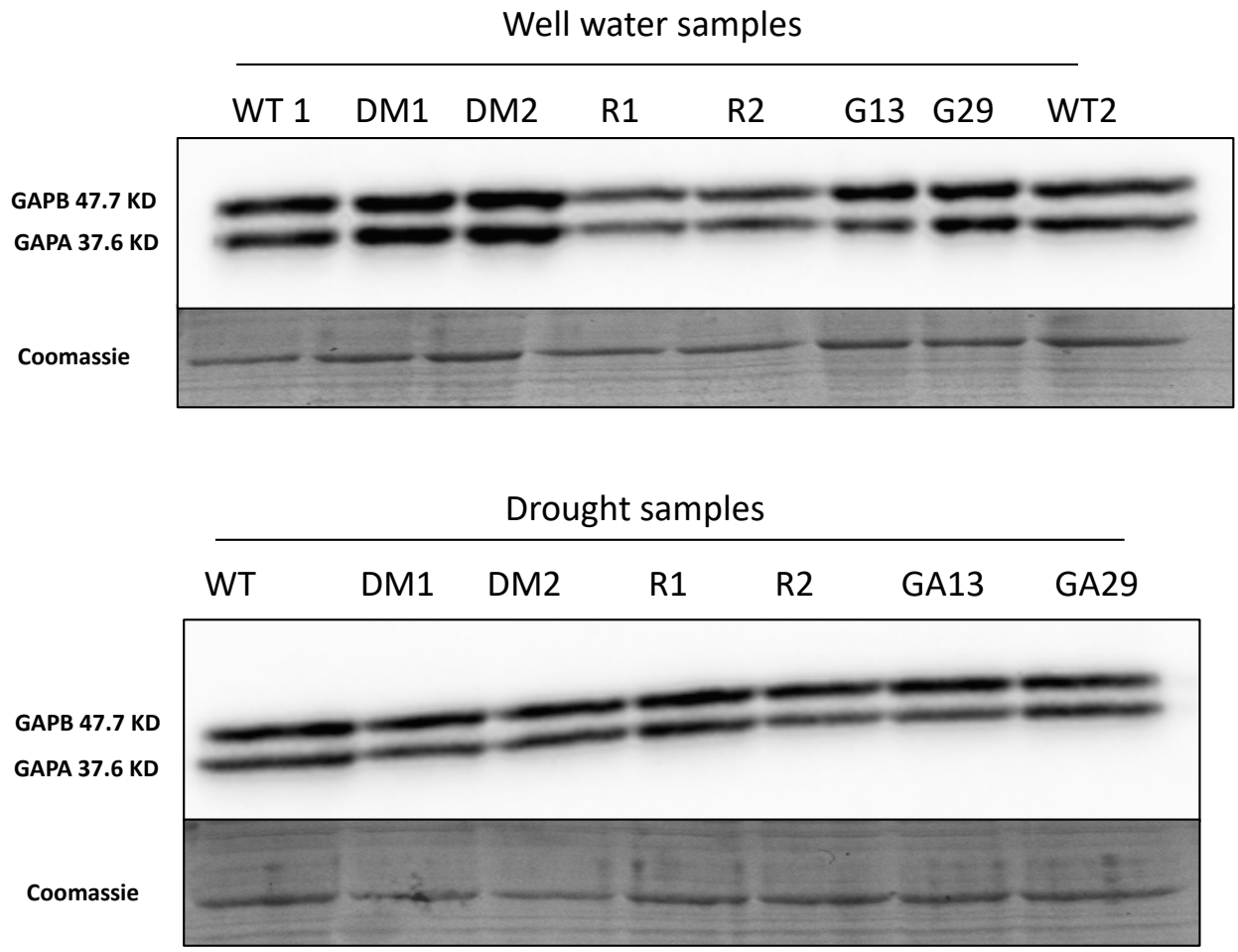

Figure 3.15: Immunoblot analysis of transgenic two single mutant lines of *rap2.12 (1-2)*, two overexpression lines of GAPA-2 (13-29), two double mutant lines of *rap2.12 (1-2)* with overexpression of GAPA-2 (13-29). **(A)** Western blot for watered samples and the loading indicated in coomassie stain. **(B)** Western blot drought for drought samples and the loading indicated in coomassie stain. The numbers indicated the loading in each well by microliter. And the letters showed the name of samples *rap2.12-1* (R1), *rap2.12-2* (R2), DM1 (*rap2.12-1*/GAPA-2), DM2 (*rap2.12-2*/GAPA-2), G13 (GAPA-2 line 13), and G29 (GAPA-2 line 29).

3.2.5 Plant growth and development

3.2.5.1 Rosette area

The first growth analysis was performed using WT Columbia (Col-0) and five independent double mutant lines of *rap2.12-2* with GAPA-2 OE line 29 (Table 3.1). Arabidopsis plants were grown in growth chambers at 22 °C under short day (Photoperiod: 8 hours' light / 16 hours' dark), and relative humidity (RD) 60%. Photographs of the plants were taken three times per week starting after 18 days of germination. Rosette area of plants was measured using ImageJ. Rosette area measurements 18 days after germination indicated that the lines 2, 4 and 5 were significantly larger compared to WT plants, while lines 1 and 3 showed no difference (Figure 3.16A). Rosette area measurement after 25 days of germination showed that lines 4 and 5 were significantly larger compared to WT plants (Figure 3.16B). However, lines 1, 2 and 3 showed no differences compared to WT plants. Rosette area measurement after 32 days of germination which showed lines 1, 2, 3, 4, and 5 were significantly larger compared plants (Figure 3.16C). Rosette area measurement after 41 days of germination presented lines 1, 2, 4 and 5 were significantly larger compared to WT plants. However, line 3 showed no difference compared to WT plants (Figure 3.16D). In conclusion lines 4 and 5 exhibited consistently larger rosette areas throughout this growth analysis, while the remaining lines showed highly variable results.

The growth analysis was subsequently repeated to include the single mutants as well as the double mutants and WT (Table 3.2). Rosette area measurements 18 days after germination indicated that the *rap1*, *rap2* lines, and two double mutant lines were smaller compared to WT plants, while both GAPA-2 OE lines, GA-13, and GA-29 showed no difference compared to WT plants (Figure 3.17A). After 25 days of germination, all single and double mutant lines showed no significant difference, except *rap1* which was

significantly larger compared to WT plants (Figure 3.17B). After 32 days of germination, all single and double mutant lines indicated no difference, with the exception of line DM2 (Table 3.2), which was significantly larger compared to WT plants (Figure 3.17C). After 39 days of germination, all single and double mutant lines showed no difference compared to WT plants (Figure 3.17D). In conclusion, no consistent pattern was observed for any of the transgenic plants, which suggest that altering *RAP2.12* and GAPA-2 levels did not affect rosette growth or development.

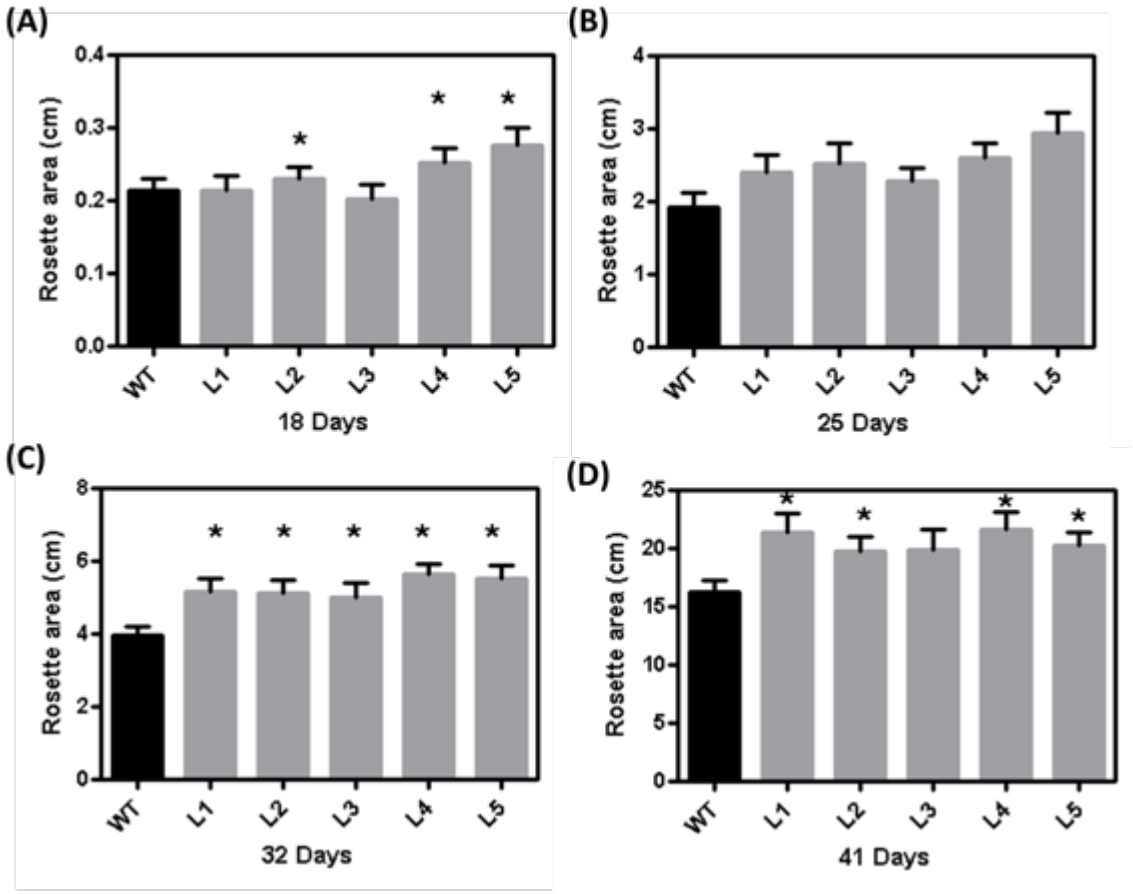

Figure 3.16: Comparison of the average rosette area of WT Columbia (Col-0) and five independent lines of double mutant (*rap2.12-2* & OE GAPA-2). Plants were grown in short day room (photoperiod: 8 hours' light / 16 hours dark). **(A)** Rosette area of plants after 18 days of germination. **(B)** Rosette area of plants after 25 days of germination. **(C)** Rosette area of plants after 32 days of germination. **(D)** Rosette area of plants after 41 days of germination. Error bars represent SE, n=20 replicates. Stars showed the significant transgenic lines compare to WT control ($P<0.05$) one-way ANOVA, post-hoc test).

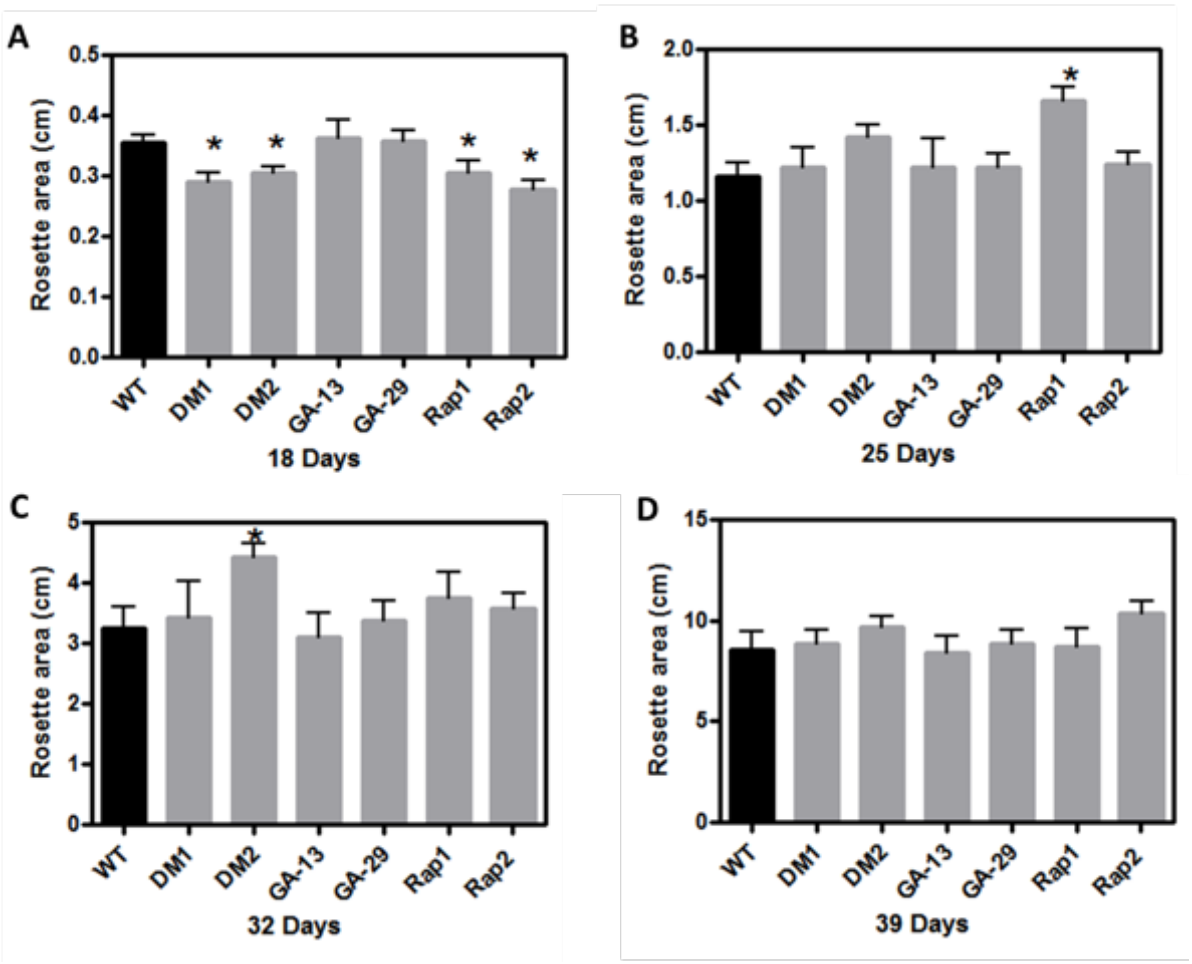

Figure 3.17: Comparison the average of rosette area of WT (Col-0), two single mutant lines of *rap2.12 (1-2)*, two lines of GAPA-2 overexpression (GA-29 and-GA13), and two lines of double mutant *rap2.12 (1-2)* Knockout with GAPA-2 OE expression construct. Plants were grown in short day room (photoperiod: 8 hours' light / 16 hours dark). **(A)** Rosette area of plants after 18 days of germination. **(B)** Rosette area of plants after 25 days of germination. **(C)** Rosette area of plants after 32 days of germination. **(D)** Rosette area of plants after 39 days of germination. Error bars represent SE, n=20 replicates. Stars showed the significant transgenic lines compare to WT control ($P<0.05$) one-way ANOVA, post-hoc test).

3.2.5.2 Seed weight

From the first growth analyses, the average total seeds of the five independent double mutant lines (Table 3.1) showed no significant differences compared to WT plants (Figure 3.18A). Similarly, results were obtained for the second growth analysis, where the average total seeds of double mutant lines (Table 3.2) showed no significant difference. Two of the single mutants, *rap2.12-2* and GA-29, however, produced significantly more seeds compared to WT (Figure 3.18B).

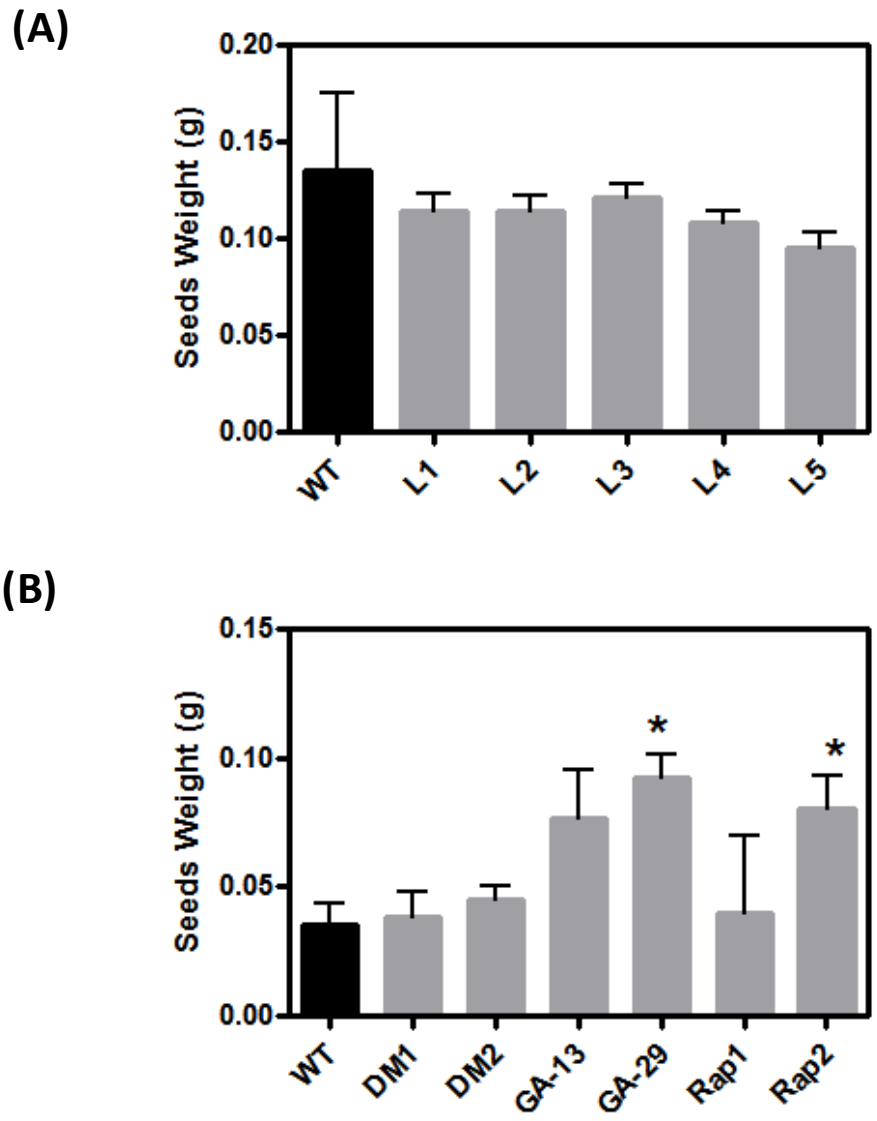

Figure 3.18: Comparison of the average of the seeds yields. **(A)** The of total seeds per lines of WT Columbia (Col-0) and five independent lines of double mutant (*rap2.12-2* & OE GAPA-2). Error bars represent SE n=20 replicates. Stars showed the significant transgenic lines compare to WT control (P<0.05). **(B)** The of total seeds per lines of WT (Col-0), two single mutant lines of *rap2.12 (1-2)*, two lines of GAPA-2 overexpression (GA29 -GA13), and two lines of double mutant *rap2.12 (1-2)* with GAPA-2 OE expression construct. Error bars represent SE, n=6 replicates. Stars showed the significant transgenic lines compare to WT control (P<0.05) one-way ANOVA, post-hoc test).

3.2.5.3 Number Of Leaves

Rosette leaf numbers of five independent double mutant lines were counted at 38 days after potting. The five double mutant lines showed no significant difference compared to WT plants (Figure 3.19).

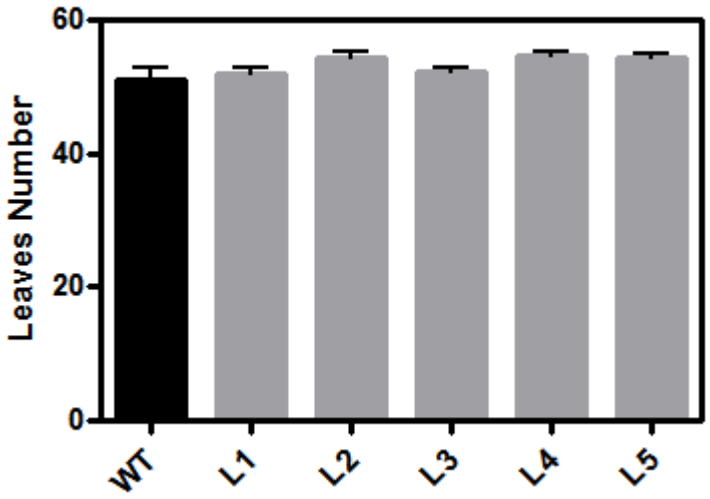

Figure 3.19: Comparison, the average count, leaves a number of WT Columbia (Col-0) and five independent lines of double mutant (*rap2.12-2* & OE GAPA-2). Plants were grown in short day room (photoperiod: 8 h light / 16 h dark). Count leaves numbers were taken at 53 days of germination (38 days after potting). Error bars represent SE n=20 replicates. Stars showed the significant transgenic lines compare to WT control ($P<0.05$).

3.2.6 Drought experiment

A drought experiment was performed for all single and double mutant lines plus WT plants (Table 3.2). A progressive slow-drying experiment starting at 100% relative gravimetric soil water content (rSWC), drying down to 20% rSWC was performed on 5-week-old Arabidopsis plants (Figure 3.20). Six weeks after sowing, one-half of the plants were maintained under well-watered conditions, whereas the remaining half plants were induced for drought stress by with holding water. The pots subjected to drought were weighed daily, and their relative soil water content (rSWC) was calculated (as described

in materials and methods chapter). Leaf material was harvested at 20% rSWC for gene expression analysis. The qPCR analysis was performed to study the expression level of the genes from the network model shown in (Figure 1.2 in Chapter 1 with details).

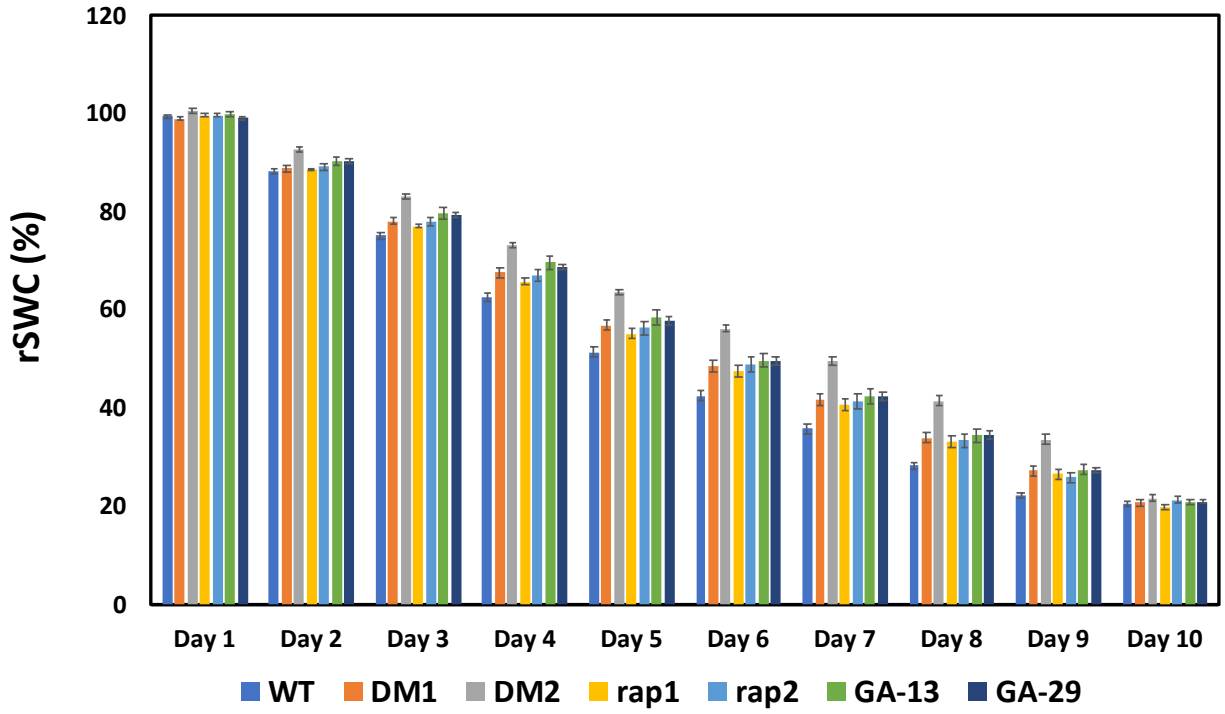

Figure 3.20: Relative soil water content (rSWC) subjected to drought for single and double mutant lines (Table 3.2). Error bars represent SE n=10 replicates one-way ANOVA, post-hoc test).

.

3.2.7 Testing network connections of gene regulatory networks (VBSSM)

Genes from the gene regulatory network were analysed by qPCR to test the hypothesis based on the output of the network modelling. The network suggested that an increase in the level of GAPA-2 gene expression and a decrease in the levels of transcription factor *RAP2.12* may have a positive effect on the expression of Calvin cycle genes under drought conditions. To investigate this hypothesis the expression of 18 Calvin cycle genes were investigated with four replicates per genotype under watered and drought stress condition.

3.2.9.1 GAPDH expression levels

Under drought condition, only the two single mutant lines of *rap2.12 (1-2)* showed significantly increased expression of GAPA-1 compared to WT plants, while the two double mutant lines DM1, and DM2 (Table 3.2) showed no difference in the expression level compared to WT (Figure 3.21). Under well-watered conditions, only *rap1* and *rap2* lines showed increased expression levels compared to WT plants again with both double mutants' lines DM1 and DM2 showing no difference in the expression level compared to WT plants (Figure 3.21).

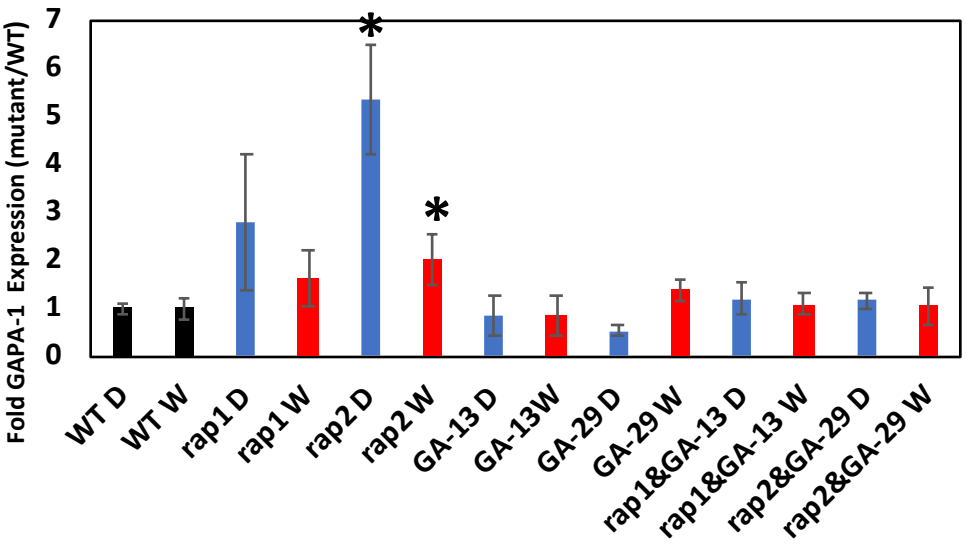

Figure 3.21: Fold expression of Glyceraldehyde- 3-phosphate dehydrogenase A subunit GAPA-1 under drought and watered conditions for two single mutant lines of *rap2.12 (1-2),* two overexpression lines of GAPA-2 (13-29), two double mutant lines of *rap2.12 (1-2)* with overexpression of GAPA-2 (13-29), and WT Columbia (Col-0). Values are mean ± standard error (no. of biological replicates, n=4). Stars showed the significant transgenic lines compare to WT control ($P<0.05$) one-way ANOVA, post-hoc test).

.

Under drought condition line GA-29 showed reduced expression level of GAPA-2 significantly compared to WT plants, however other lines GA-13, *rap1*, *rap2* and both double mutant lines (Table 3.2) revealed no significant difference compared to WT plants (Figure 3.22). Under watered condition line GA-13 showed decreased expression level significantly compared to WT plants, but other lines GA-29, *rap1*, *rap2*, and both double mutant lines (Table 3.2) showed no significant difference compared to WT plants (Figure 3.22).

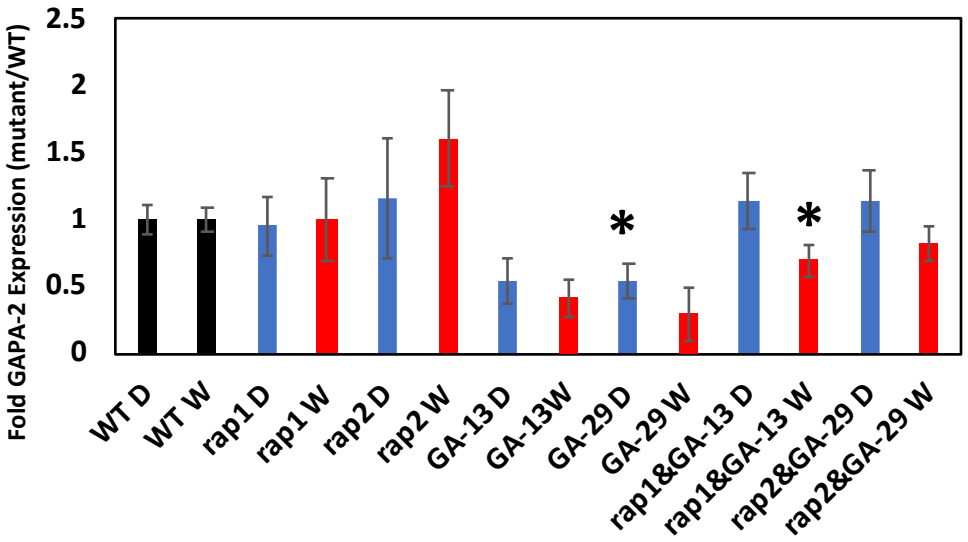

Figure 3.22: Fold expression of Glyceraldehyde- 3-phosphate dehydrogenase A subunit GAPA-2 under drought and watered conditions for two single mutant lines of *rap2.12 (1-2),* two overexpression lines of GAPA-2 (13-29), two double mutant lines of *rap2.12 (1-2)* with overexpression of GAPA-2 (13-29), and WT Columbia (Col-0). Values are mean ± standard error (no. of biological replicates, n=4). Stars showed the significant transgenic lines compare to WT control ($P<0.05$) one-way ANOVA, post-hoc test).

.

Under drought condition, only DM2 (Table 3.2) showed increased the expression level of GAPB compared to WT plants, and line GA-29 showed decreased expression level of GAPB compared to WT plants, however two single mutant line *rap1*, *rap2*, and GA-13 showed no significant difference compared to WT plants (Figure 3.23). Under watered condition single mutant lines *rap1*, *rap2*, and line GA-29 indicated increased expression level of GAPB, but not significant statistically, whereas both double mutant lines (Table

3.2) and line GA-13 presented no significant difference compared to WT plants (Figure 3.23).

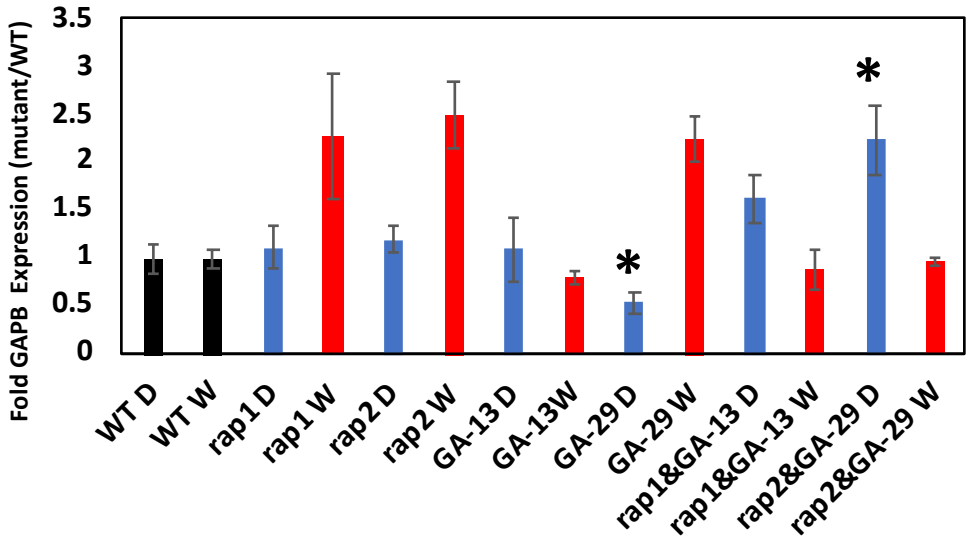

Figure 3.23: Fold expression of Glyceraldehyde- 3-phosphate dehydrogenase A subunit GAPB under drought and watered conditions for two single mutant lines of *rap2.12 (1-2),* two overexpression lines of GAPA-2 (13-29), two double mutant lines of *rap2.12 (1-2)* with overexpression of GAPA-2 (13-29), and WT Columbia (Col-0). Values are mean ± standard error (no. of biological replicates, n=4). Stars showed the significant transgenic lines compare to WT control ($P<0.05$) one-way ANOVA, post-hoc test).

3.2.9.2 RAP2.12 expression level

Under drought condition, both double mutant lines (Table 3.2), and single mutant lines *rap1* and *rap2* indicated reduced expression level significantly of *RAP2.12* compared to WT plants, while lines GA-13 and GA-29 showed no significant difference compared to WT plants (Figure 3.24). Under watered condition again both double mutant lines (Table 3.2) and single mutant lines *rap1*, and *rap2* showed decreased expression level

significantly of *RAP2.12* compared to WT plants, while line GA-29 showed increased the expression level of *RAP2.12* and line GA-13 indicated no significant difference compared to WT plants (Figure 3.24).

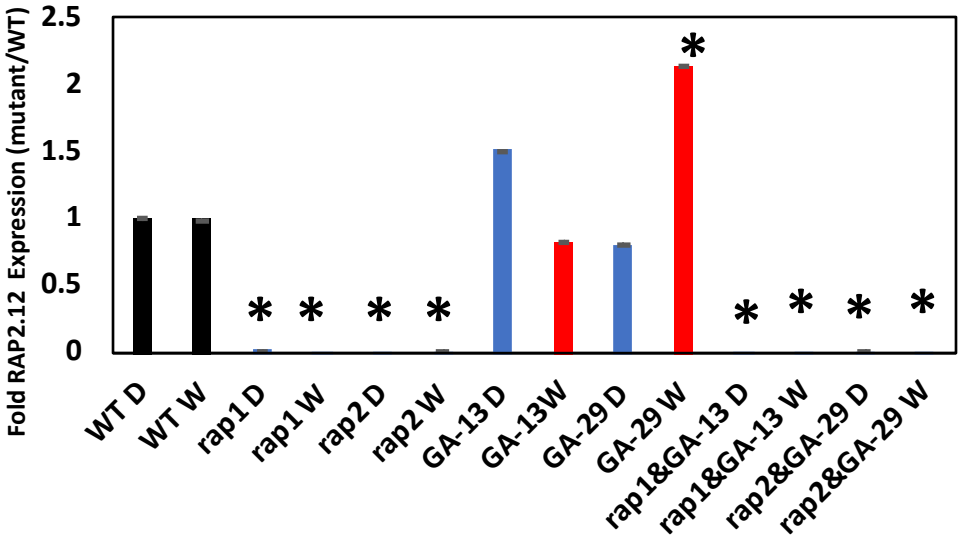

Figure 3.24: Fold expression of a member of the ethylene response factor family *RAP2.12* under drought and watered conditions for two single mutant lines of *rap2.12 (1-2),* two overexpression lines of GAPA-2 (13-29), two double mutant lines of *rap2.12 (1-2)* with overexpression of GAPA-2 (13-29), and WT Columbia (Col-0). Values are mean ± standard error (no. of biological replicates, n=4). Stars showed the significant transgenic lines compare to WT control (P<0.05) one-way ANOVA, post-hoc test).

.

3.2.9.3 Expression of direct and indirect targets of RAP2.12 and GAPA-2

Under drought condition only DM2 and *rap2* lines showed increased expression level of Atg16750 unknow protein, but not significant statistically compared to WT plants, however other lines DM1, *rap1*, GA-13, and GA-29 showed no significant difference compared to

WT plants (Figure 3.25). Under watered condition, only line *rap1* presented reduced expression level of 16750unknow protein significantly compared to WT plants, while other lines *rap2*, both double mutant lines (Table 3.2), GA-13 and GA-29 showed no significant difference compared to WT plants (Figure 3.25).

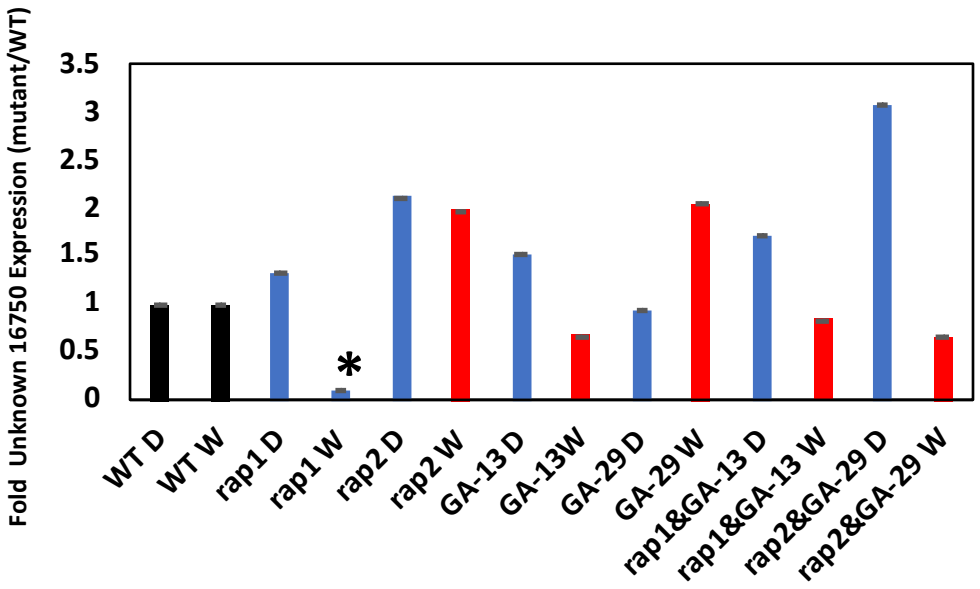

Figure 3.25: Fold expression of At1g16750 Unknown protein under drought and watered conditions for two single mutant lines of *rap1* and *rap2,* two overexpression lines of GAPA-2 (13-29), two double mutant lines of *rap1* and *rap2* with overexpression of GAPA-2 (13-29), and WT Columbia (Col-0). Values are mean ± standard error (no. of biological replicates, n=4). Stars showed the significant transgenic lines compare to WT control ($P<0.05$) one-way ANOVA, post-hoc test).

Under drought condition, the single mutant lines *rap1* and *rap2* increased the expression level of PRK significantly compared to WT plants (Figure 3.26). The remaining genotypes did not show a significant difference in PRK expression under drought (Figure 3.26).

Under watered condition, only the double mutant lines and GA-13 showed decreased expression level of PRK compared to WT plants (Figure 3.26).

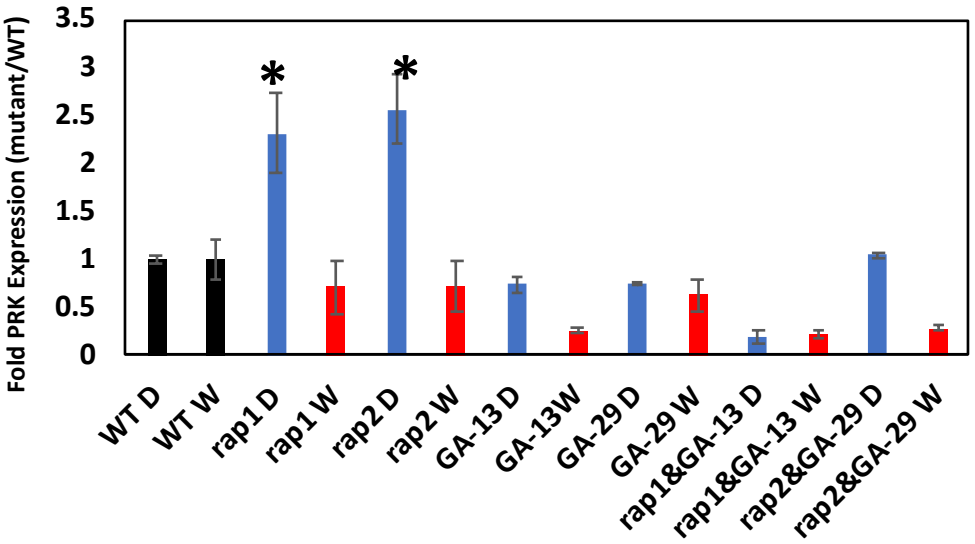

Figure 3.26: Fold expression of Phosphoribulokinase PRK under drought and watered conditions for two single mutant lines of *rap2.12 (1-2),* two overexpression lines of GAPA-2 (13-29), two double mutant lines of *rap2.12 (1-2)* with overexpression of GAPA-2 (13-29), and WT Columbia (Col-0). Values are mean ± standard error (no. of biological replicates, n=4). Stars showed the significant transgenic lines compare to WT control ($P<0.05$) one-way ANOVA, post-hoc test).

Under drought condition only the two single mutant lines *rap1* and *rap2* showed reduced expression level of CP12-1 compared to WT plants. The remaining genotypes showed no significant difference compared to WT plants (Figure 3.27). Under watered condition genotypes indicated no significant difference compared to WT plants (Figure 3.27).

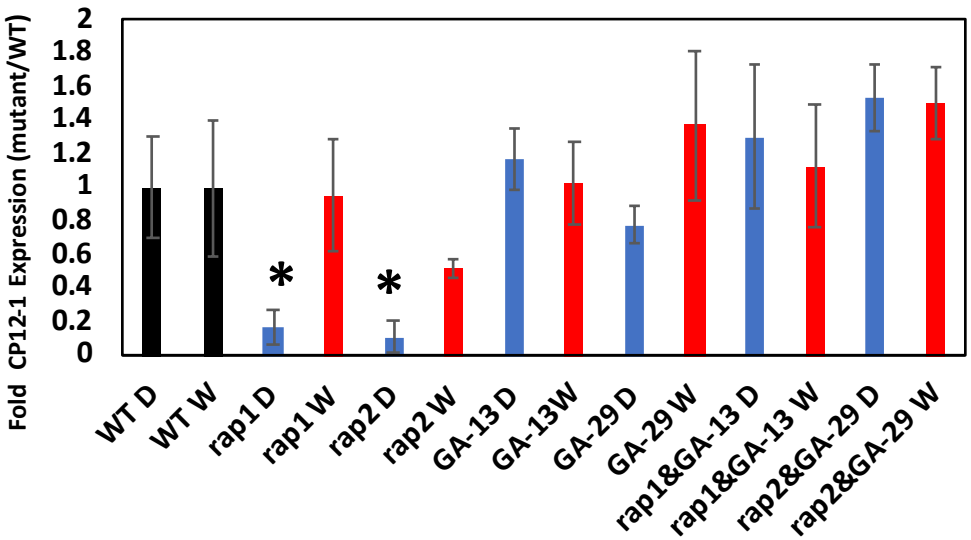

Figure 3.27: Fold expression of CP12-1 under drought and watered conditions for two single mutant lines of *rap2.12 (1-2),* two overexpression lines of GAPA-2 (13-29), two double mutant lines of *rap2.12 (1-2)* with overexpression of GAPA-2 (13-29), and WT Columbia (Col-0). Values are mean ± standard error (no. of biological replicates, n=4). Stars showed the significant transgenic lines compare to WT control ($P<0.05$) one-way ANOVA, post-hoc test).

Under drought condition only line GA-29 showed decreased expression level of CP12-2 significantly compared to WT plants, while other lines DM1, DM2, *rap1*, *rap2* and GA-13 (Table 3.2) indicated no difference compared to WT plants (Figure 3.28). Under watered condition, all single and double mutant lines (Table 3.2) showed no significant difference compared to WT plants (Figure 3.28).

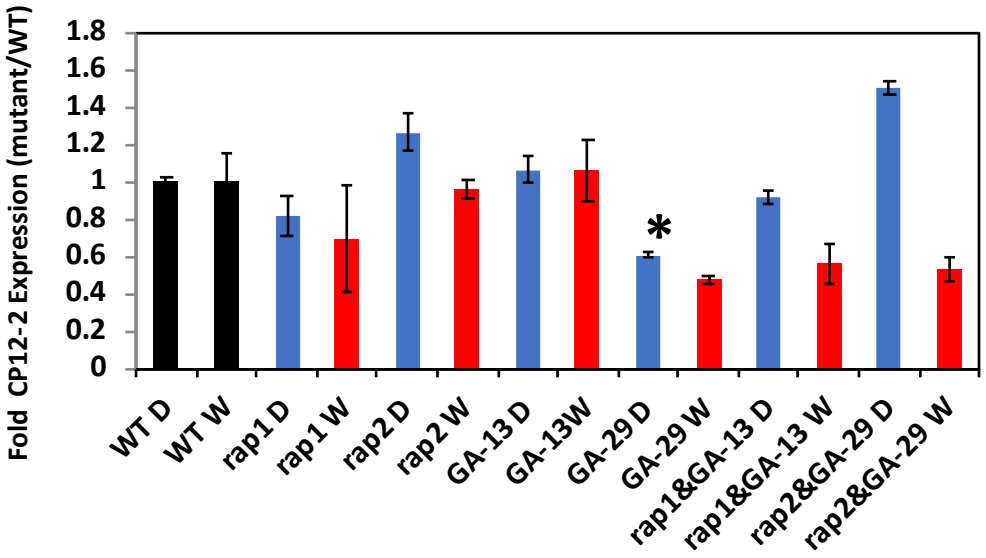

Figure 3.28: Fold expression of CP12-2 under drought and watered conditions for two single mutant lines of *rap2.12 (1-2),* two overexpression lines of GAPA-2 (13-29), two double mutant lines of *rap2.12 (1-2)* with overexpression of GAPA-2 (13-29), and WT Columbia (Col-0). Values are mean ± standard error (no. of biological replicates, n=4). Stars showed the significant transgenic lines compare to WT control ($P<0.05$) one-way ANOVA, post-hoc test).

There was no significant difference in the expression level of CP12-3 under both drought and watered conditions for all single and double mutant lines compared to WT plants (Figure 3.29).

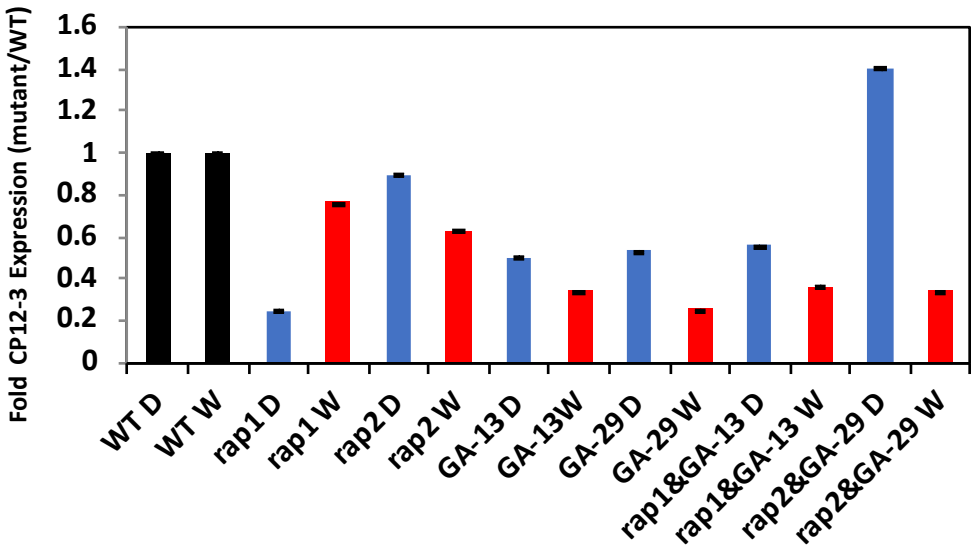

Figure 3.29: Fold expression of CP12-3 under drought and watered conditions for two single mutant lines of *rap2.12 (1-2),* two overexpression lines of GAPA-2 (13-29), two double mutant lines of *rap2.12 (1-2)* with overexpression of GAPA-2 (13-29), and WT Columbia (Col-0). Values are mean ± standard error (no. of biological replicates, n=4). one-way ANOVA, post-hoc test).

Under drought condition, only both double mutant lines DM1 and DM2 (Table 3.2) showed an increased expression level of SBPase compared to WT plants. All other lines showed no significant difference compared to WT plants (Figure 3.30). Under watered condition, all single and double mutant lines (Table 3.2) showed no significant difference in the expression level of SBPase compared to WT plants (Figure 3.30).

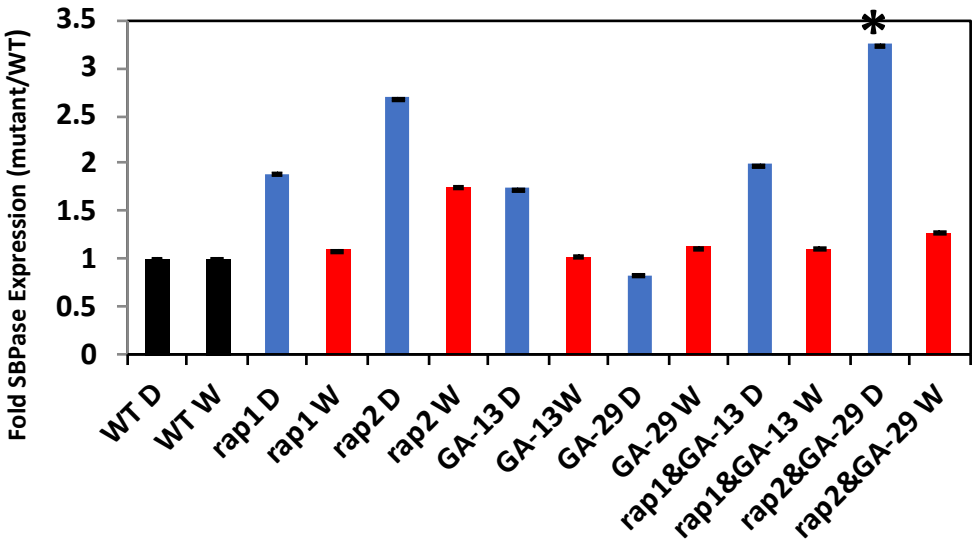

Figure 3.30: Fold expression of Sedoheptulose-1,7-bisphosphatase SBPase under drought and watered conditions for two single mutant lines of *rap2.12 (1-2),* two overexpression lines of GAPA-2 (13-29), two double mutant lines of *rap2.12 (1-2)* with overexpression of GAPA-2 (13-29), and WT Columbia (Col-0). Values are mean ± standard error (no. of biological replicates, n=4). Stars showed the significant transgenic lines compare to WT control ($P<0.05$) one-way ANOVA, post-hoc test).

Under drought condition only the two single mutant lines *rap1* and *rap2* showed an increased expression level of PGK. All other lines showed no significant difference compared to WT plants (Figure 3.31). Under watered condition, all single and double mutant lines (Table 3.2) showed no significant difference in the expression level of SBPase compared to WT plants (Figure 3.31).

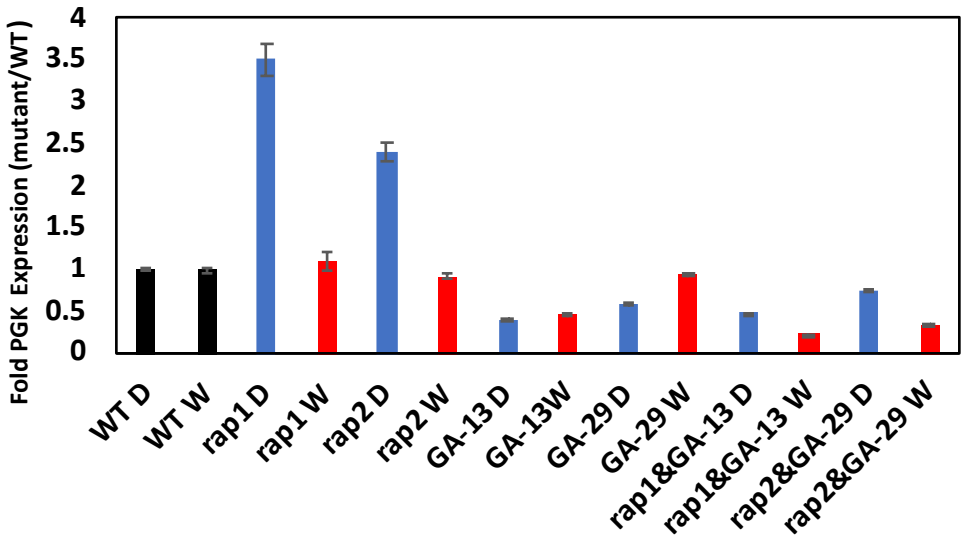

Figure 3.31: Fold expression of Phosphoglycerate kinase PGK under drought and watered conditions for two single mutant lines of *rap2.12 (1-2),* two overexpression lines of GAPA-2 (13-29), two double mutant lines of *rap2.12 (1-2)* with overexpression of GAPA-2 (13-29), and WT Columbia (Col-0). Values are mean ± standard error (no. of biological replicates, n=4) one-way ANOVA, post-hoc test).

Under drought condition, both double mutant lines (Table 3.2) showed a significantly increased expression level of RPE compared to WT plants (Figure 3.32). Under watered condition, all single and double mutant lines (Table 3.2) showed no significant difference in the expression level of RPE compared to WT plants (Figure 3.32).

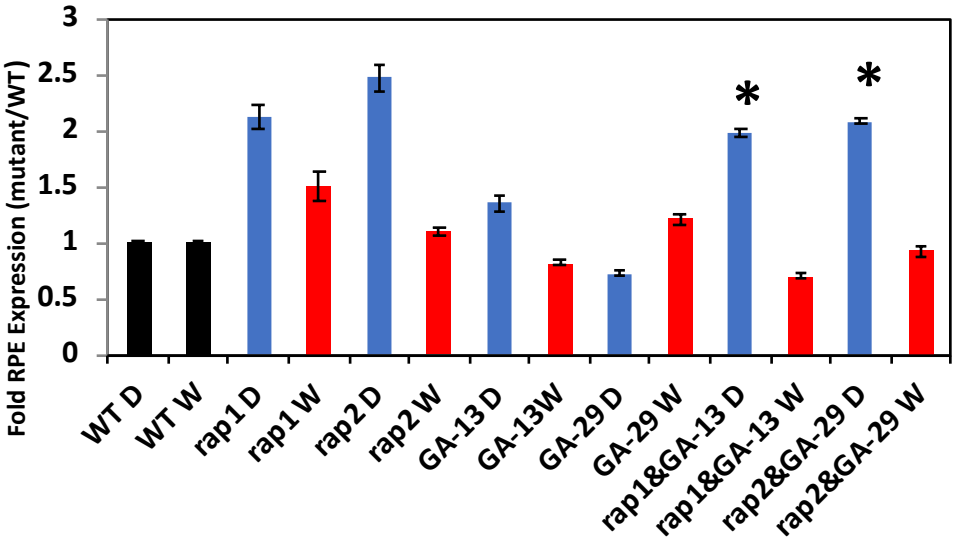

Figure 3.32: Fold expression of Ribulose-5-phosphate-3-epimerase RPE under drought and watered conditions for two single mutant lines of *rap2.12 (1-2),* two overexpression lines of GAPA-2 (13-29), two double mutant lines of *rap2.12 (1-2)* with overexpression of GAPA-2 (13-29), and WT Columbia (Col-0). Values are mean ± standard error (no. of biological replicates, n=4). Stars showed the significant transgenic lines compare to WT control ($P<0.05$) one-way ANOVA, post-hoc test).

Under drought, there was no significant difference in the expression of PDTPI all single and double mutant lines compared to WT plants (Figure 3.33). Under watered conditions double and single mutant lines *rap1*, *rap2*, and GA-13 (Table 3.2) showed decreased expression level of PDTPI compared to WT plants (Figure 3.33).

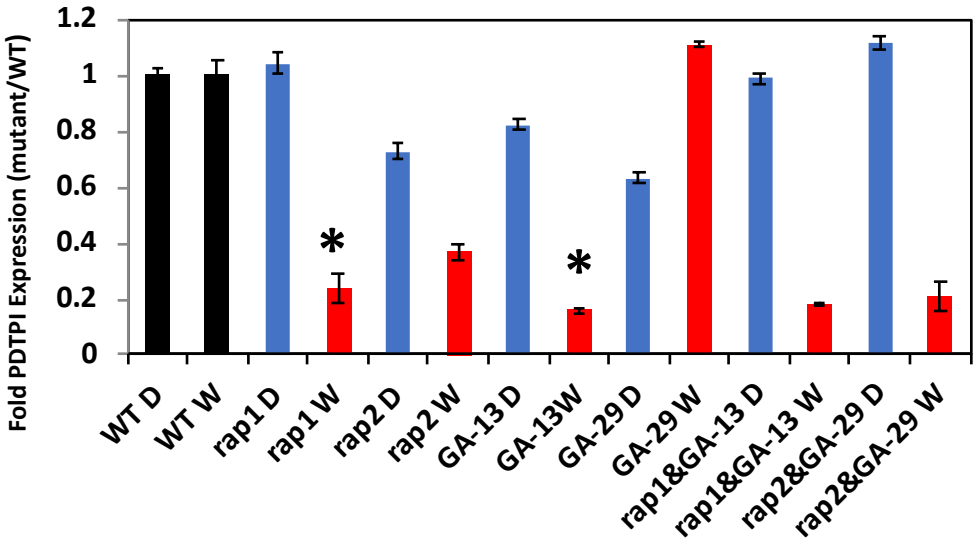

Figure 3.33: Fold expression of Triose phosphate isomerase PDTPI under drought and watered conditions for two single mutant lines of *rap2.12 (1-2),* two overexpression lines of GAPA-2 (13-29), two double mutant lines of *rap2.12 (1-2)* with overexpression of GAPA-2 (13-29), and WT Columbia (Col-0). Values are mean ± standard error (no. of biological replicates, n=4). Stars showed the significant transgenic lines compare to WT control ($P<0.05$) one-way ANOVA, post-hoc test).

Under both drought and watered condition, all single and double mutant lines (Table 3.2) showed no significant difference in the expression level of HCEF1 compared to WT plants (Figure 3.34).

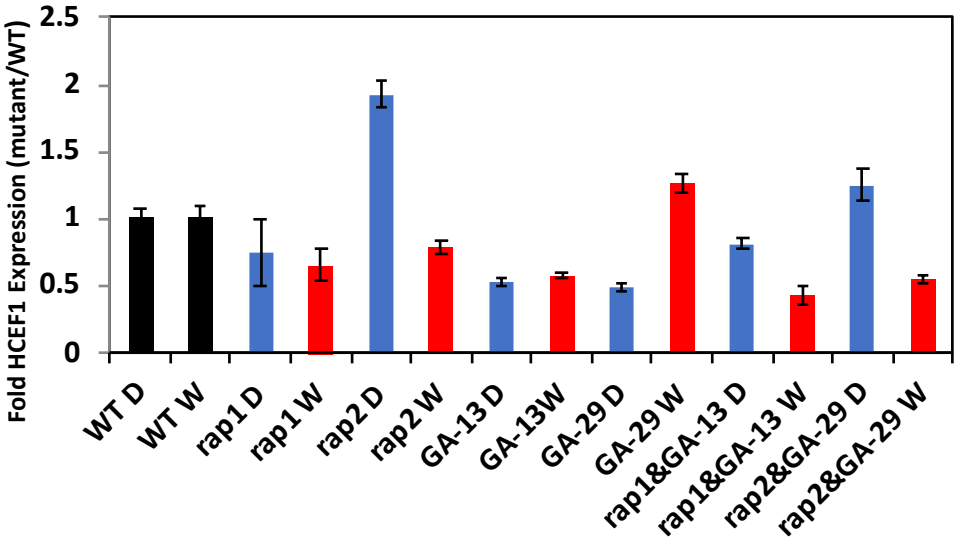

Figure 3.34: Fold expression of High cyclic electron flow 1 HCEF1 under drought and watered conditions for two single mutant lines of *rap2.12 (1-2),* two overexpression lines of GAPA-2 (13-29), two double mutant lines of *rap2.12 (1-2)* with overexpression of GAPA-2 (13-29), and WT Columbia (Col-0). Values are mean ± standard error (no. of biological replicates, n=4) one-way ANOVA, post-hoc test).

Under both drought and watered condition, all single and double mutant lines (Table 3.2) showed no significant difference in the expression level of RBCSA1 compared to WT plants (Figure 3.35).

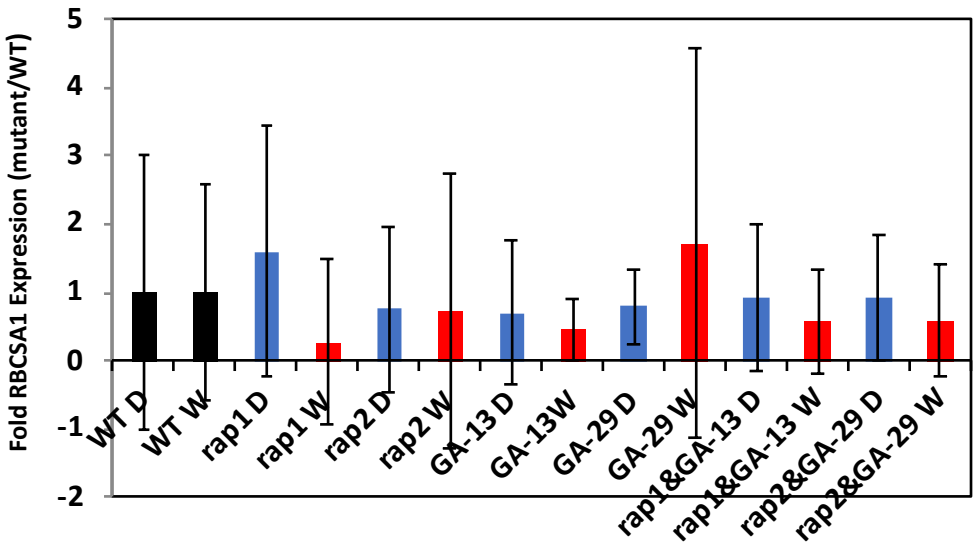

Figure 3.35: Fold expression of Ribulose bisphosphate carboxylase small subunit 1A RBCSA1 under drought and watered conditions for two single mutant lines of *rap2.12 (1-2),* two overexpression lines of GAPA-2 (13-29), two double mutant lines of *rap2.12 (1-2)* with overexpression of GAPA-2 (13-29), and WT Columbia (Col-0). Values are mean ± standard error (no. of biological replicates, n=4) one-way ANOVA, post-hoc test).

Under drought condition only both single mutant lines *rap1* and *rap2* showed an increased expression level of FBA1 compared to WT plants. All other genotypes showed no difference compared to WT plants (Figure 3.36). Under watered condition, both single and double mutant lines (Table 3.2), and GA-13 revealed a significantly decreased expression level of FBA1 compared to WT plants (Figure 3.36).

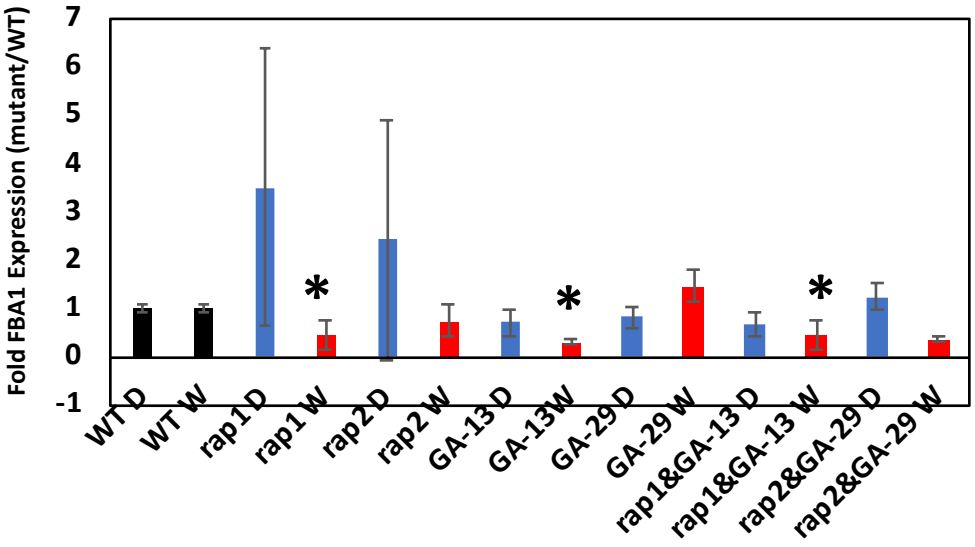

Figure 3.36: Fold expression of Fructose-bisphosphate aldolase 1 FBA1 under drought and watered conditions for two single mutant lines of *rap2.12 (1-2),* two overexpression lines of GAPA-2 (13-29), two double mutant lines of *rap2.12 (1-2)* with overexpression of GAPA-2 (13-29), and WT Columbia (Col-0). Values are mean ± standard error (no. of biological replicates, n=4). Stars showed the significant transgenic lines compare to WT control ($P<0.05$).

Under drought condition, only GA-29 line showed a significantly decreased expression levels of FBA2 compared to WT plants. All other genotypes showed no significant difference compared to WT plants (Figure 3.37). Under watered condition, all single and double mutant lines (Table 3.2) indicated no significant difference in the expression level of FBA2 compared to WT plants (Figure 3.37).

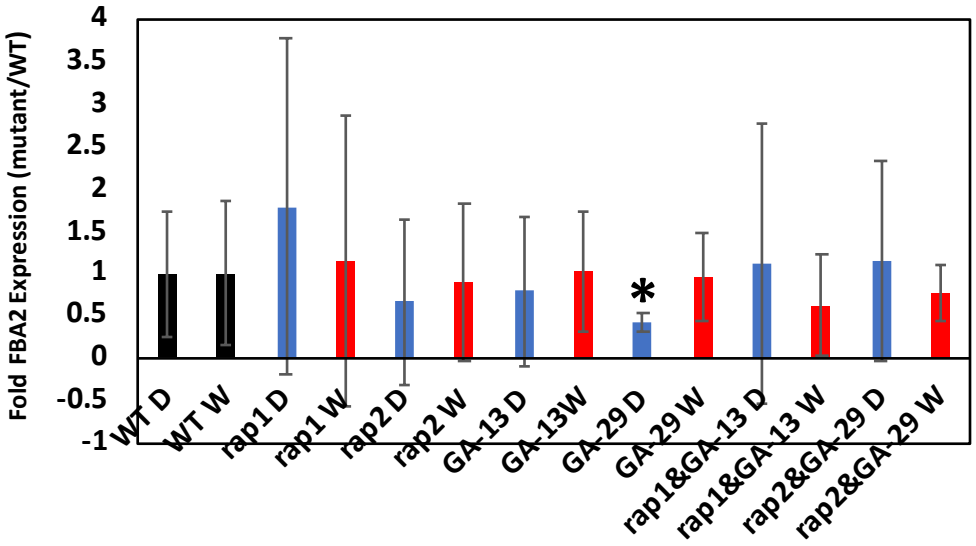

Figure 3.37: Fold expression of Fructose-bisphosphate aldolase 2 FBA2 under drought and watered conditions for two single mutant lines of *rap2.12 (1-2),* two overexpression lines of GAPA-2 (13-29), two double mutant lines of *rap2.12 (1-2)* with overexpression of GAPA-2 (13-29), and WT Columbia (Col-0). Values are mean ± standard error (no. of biological replicates, n=4). Stars showed the significant transgenic lines compare to WT control ($P<0.05$) one-way ANOVA, post-hoc test).

Under both drought and watered condition, all single and double mutant lines (Table 3.2) showed no significant difference in the expression level of TK2 compared to WT plants (Figure 3.38).

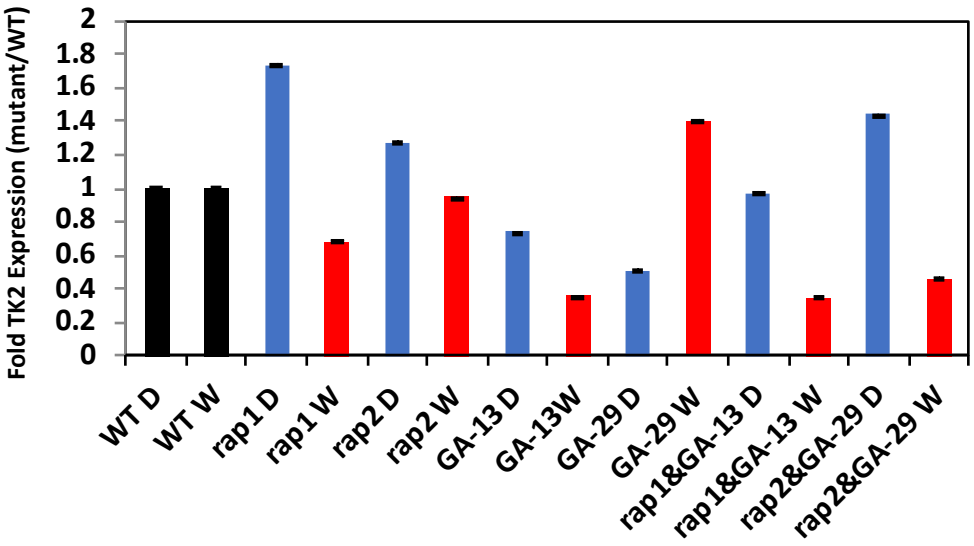

Figure 3.38: Fold expression of FBA2 under drought and watered conditions for two single mutant lines of *rap2.12 (1-2),* two overexpression lines of GAPA-2 (13-29), two double mutant lines of *rap2.12 (1-2)* with overexpression of GAPA-2 (13-29), and WT Columbia (Col-0). Values are mean ± standard error (no. of biological replicates, n=4) one-way ANOVA, post-hoc test).

The conclusion from qPCR and Protein analysis

The qPCR analysis showed that only *RAP2.12* is regulating Calvin cycle gene expression during drought, as there was differential expression compared to the WT. However, this may not always be as predicted in the network. Moreover, western blot indicated that both single mutant lines of *RAP2.12* had slightly increased the GAPA and B protein levels under drought condition.

3.3 Discussion

Gene regulatory networks for *RAP2.12* and GAPA-2 were tested in this chapter. This was done to determine the accuracy of the VBSSM modelling and also to test the regulation of the expression of Calvin cycle genes involved that are not known to be regulated by the above two genes, and thus establish new targets of these genes and understand the role they may play maintaining photosynthesis during drought. Growth analyses clearly showed highly variable and inconsistent results between the single and double mutants under well-watered conditions, which suggests that changing *RAP2.12* and GAPA-2 levels did not affect rosette growth or development. The main findings from qPCR direct and indirect targets of *RAP2.12* and GAPA-2 in relation to the predicted network .

It is evident that *RAP2.12* clearly impacted Calvin cycle gene expression predominately under drought stress conditions, even though it may not be exactly as predicted by the modelling. Network inference linked *RAP2.12* to the transcriptional regulation of Calvin cycle enzymes under drought stress conditions, which was confirmed to be the case. Importantly, this regulation was not as prevalent under well-watered conditions, and therefore this seems to be drought specific. On the other hand, the presumed GAPA-2 OE lines (13,29) showed no significant increase in GAPA expression levels and had no impact on most Calvin cycle gene expression, suggesting that the GAPA-2 OE lines (13,29) could have been silenced in plants, or were still segregating.

Chapter 4: Effect of decreased GAPA and GAPB using T-DNA insertion and antisense technology on Arabidopsis photosynthesis and growth

4.1 Introduction

The photosynthetic glyceraldehyde-3-phosphate dehydrogenase (GAPDH) is a target of thioredoxins in plant chloroplasts (Wolosiuk and Buchanan, 1978; Sparla et al., 2002). The GAPA and GAPB formed the chloroplast of GAPDH. The subunit synthesis of these enzymes is subject on the sort of organism. These subunits are nearby 36 and 39 kDa correspondingly, and their expression is encouraged by light (Sparla et al., 2002). The key difference between the GAPA and GAPB proteins is a C-terminal extension on the GAPB protein which confers thioredoxin- mediated redox regulatory capacity onto the GAPDH enzyme and plays a fundamental role in GAPDH protein to protein communications (Baalmann et al., 1996; Fermani et al., 2007). Evidence has gathered suggesting that the major active form of GAPDH in higher plants is a heterotetramer containing two subunits of GAPA and two subunits of GAPB (A2B2).

Additionally, an A4 tetramer has been found in spinach chloroplast organisations contributing roughly 20% of the entire GAPDH activity (Scagliarini et al., 1998). This form of GAPDH has been entitled non-regulatory because of the lack of a C-terminal extension. The relative importance of these different forms of plastid GAPDH has not been studied. In a study by Howard et al. (2011b) stromal extracts from dark-adapted leaves of species from Leguminosae (pea, Medicago, broad bean, French bean), the Solanaceae (potato, tomato, and tobacco), the Amaranthaceae (spinach), and the Brassicaceae (Arabidopsis) were examined. Native proteins were separated using BN-PAGE. The study showed that all species identified with A2B2 heterotetramer, however, some plants recognised without A4 (Howard et al., 2011b). This raises the hypothesis in this project to investigate the role for GAPB protein to determine the rate of photosynthesis.

In this chapter to study the important of GAPDH (A2B2) in determine the rate of photosynthesis. In addition, evaluate the GAPDH (A2B2) influence and effect on Arabidopsis photosynthesis, and growth under well-water condition. Plants with reduced the GAPA and GAPB protein were produced using two different molecular approach. Firstly, T-DNA insertion lines of GAPA and GAPB, and double mutant lines between GAPA and GAPB, and co-suppressed lines of GAPA in Arabidopsis plants were identified and analysis by Dr Andrew Simkin in our lab these lines are GAPA-1 (164), GAPB (308), GAPA-1 and GAPA-2 (B11-1), GAPA-1 and GAPA-2 (B114-1), and double mutant lines between GAPA-1 (164) & GAPB (308) table (Table 4.1) indicated the lines feature with location of T-DNA insertion. Secondly, antisense construct with decreased the GAPA and GAPB protein in Arabidopsis plants were produced by me these T2 lines three lines of GAPA (GA-7, GA-13, and GA-15) and four GAPB lines (GB-9, GB-10, GB-12, and GB-13) were identified by three different molecular approach plates with kanamycin, qPCR expression analysis and western blot and (Table 4.1).

The aim of this chapter was to

1. Identify the second homozygous T-DNA insertion line of GAPB, as previously in our lab only one T-DNA insertion line of GAPB was identified.

2. To carry out preliminary physiology and growth analyses on T-DNA insertion mutant lines of GAPA, and GAPB to evaluate the photosynthetic capacity and growth

3. Identify transgenic antisense lines with a reduction in GAPA, and GAPB through different generations (T1 and T2)

4. To carry out preliminary physiology and growth analyses on T2 lines were identified from transgenic T1 lines with reduction of GAPA, and GAPB to evaluate the photosynthetic capacity and growth.

4.1 Summary of transgenic lines used in this study

Line	Gene	Short name	Insertion Site	Notes
SAIL_164_D01	GAPA-1	164	in 5'UTR, 1st exon, 1st intron, or 2nd exon	No GAPA
SAIL_308_A06	GAPB	308	5'UTR	No GAPB
B11-1	GAPA	B11-1		co-suppressed GAPB No GAPA
B114-1	GAPA	B114-1		co-suppressed GAPB No GAPA
Cross 164/308-1	GAPA & GAPB			No GAPB + half of GAPA
Cross 164/308-4	GAPA & GAPB			NO GAPB + half GAPA
Antisense T2 GAPA L 13	GAPA	13		Knockdown qPCR + protein
Antisense T2 GAPA L 15	GAPA	15		Knockdown qPCR + protein
Antisense T2 GAPA L 7	GAPA	7		Knockdown qPCR + protein
Antisense T2 GAPB L10	GAPB	10		Knockdown qPCR + protein
Antisense T2 GAPB L12	GAPB	12		Knockdown qPCR + protein
Antisense T2 GAPB L13	GAPB	13		Knockdown qPCR + protein
Antisense T2 GAPB L9	GAPB	9		Knockdown qPCR + protein

4.2 Result

4.2.1 T-DNA insertion mutant GAPB (Sail_267)

This study aimed to determine the relative roles of the GAPA and GAPB forms of the plastid GAPDH enzyme in determining the rate of photosynthetic carbon assimilation using Arabidopsis knock out mutants. One T-DNA insertion line for GAPB (Sail_308) was identified by Dr Simkin in our lab group. An attempt was also made to identify a second insertion mutant of GAPB. The identification and location of the T-DNA insertion line for GAPB Sail_267 was chosen from the TAIR website. Seeds were sown in soil and were germinated in a long day growth room with (photoperiod: 16 h light / 8 h dark). Plants tissues were harvested at the seedling stage four weeks following germination. PCR analysis was conducted using specific primers of this T-DNA insertion, plus the left border primer for the Sail mutant (primer sequences can be found in Chapter 2). Twenty plants were screened by PCR for the GAPB insertion (sail_267), and wild-type (Col-0) was used as a positive control. The DNA extracted from these plants was amplified, and a band at 968bp was identified using gene-specific primers, forward and reverse of GAPB (sail_267), except plants 2 and 7 (Figure 4.1A). Also, using forward gene-specific primers of GAPB (sail_267) and left border of sail; all plants presented no band (Figure 4.1B). Furthermore, using reverse gene-specific primers of GAPB (sail_267) and left border of sail; all plants showed no band (Figure 4.1C). Overall, analysis of this T-DNA insertion mutant showed that they were WT, despite this being repeated again no positive results were obtained, and it was decided that the next step needed to produce an independent GAPB mutant be to build antisense construct of GAPB by gateway technology and create transgenic plants.

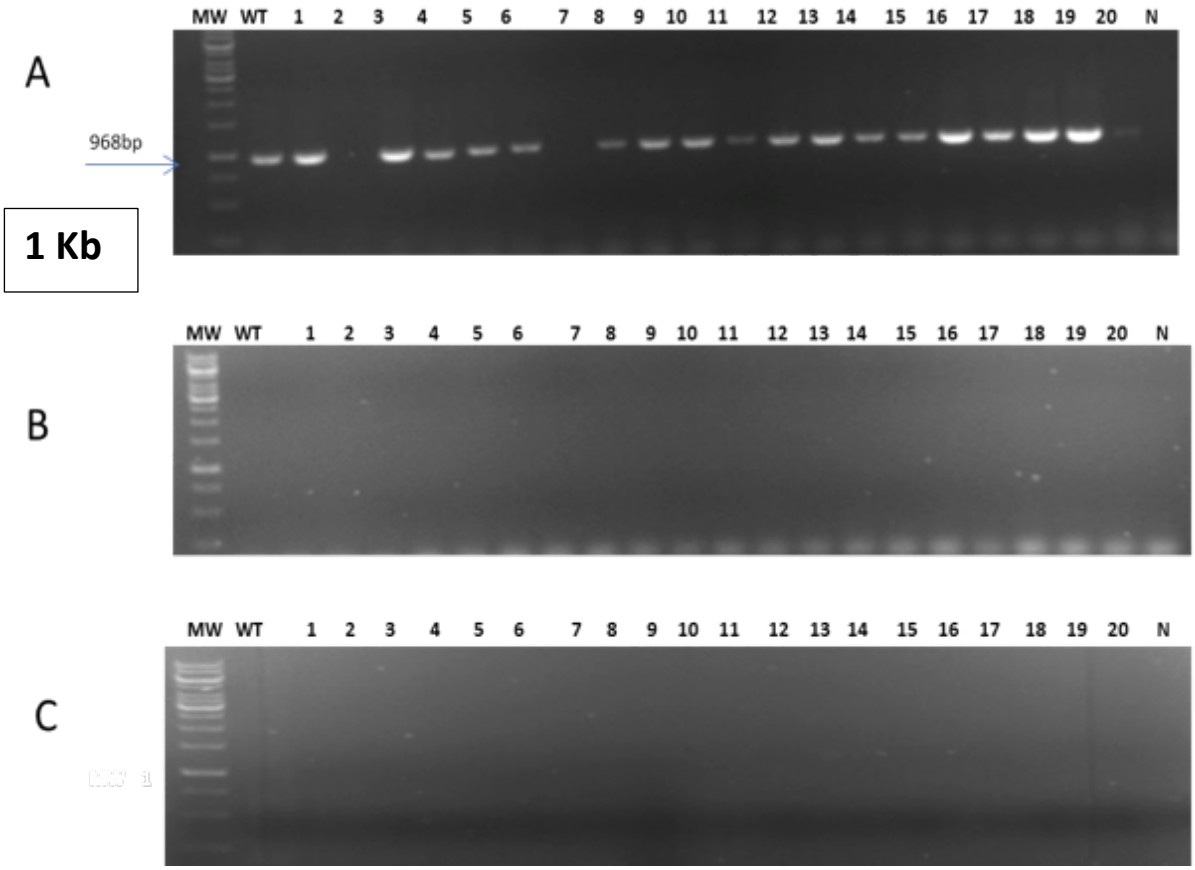

Figure 4.1: Analysis of GAPB insertion mutants (SAIL_267)

(A) PCR analysis by gene-specific primers of GAPB mutant (SAIL_267) were used for detection WT allele.

(B) PCR analysis by using forward gene-specific primer of GAPB mutant (SAIL_267) with LB insertion primer of SAIL was used for detection the T-DNA insert.

(C) PCR analysis by using reverse gene-specific primer of GAPB mutant (SAIL_267) with LB insertion primer of SAIL were used for detection the T-DNA insert. PCR analysis of GAPB (SAIL_267) and WT plants, after 35 cycles most of GAPB (SAIL_267) plants showed a signal for with gene-specific primers, (no insert plants for GAPB (SAIL_267). PCR products run alongside molecular weight markers (1kb DNA ladder from Invitrogen). The marker was used in this PCR 1 Kb.

4.2.2 Cloning GAPA, and GAPB Using Gateway Technology

The small region of the coding sequence of the Arabidopsis GAPA-1 (AT3G26650), GAPA-2 (AT1G12900) together, and GAPB (AT1G42970) cDNA were used to generate two down-expression constructs GAPA and GAPB in the vector PGWB2 (Nakagawa et al., 2007). These constructs were transformed into Arabidopsis using the floral dip method (Clough and Bent, 1998), and the resulting transgenic plants were selected on kanamycin 50 µg/mL containing a medium. Positive transformed colonies were identified by colony PCR with M13 forward and reverse primers (Figure 4.2). Then plasmids for each two constructs were isolated by using GeneJET Plasmid Miniprep Kit as described by the supply company (Thermo Fisher Scientific). Afterwards, the entry construct was confirmed by sequencing before proceeding to the LR cloning reaction (Figure 4.3 and 4.4). The gene of interest was cloned into the destination vector PGWB2 (Nakagawa et al., 2007). Next, the construct was transformed by heat shock into E. coli OmniMAXTM cells, plated on LB Agar plates containing 50 µg/ml of Kanamycin and incubated overnight at 37 °C. Positive transformed colonies were identified by colony PCR with forward of PGWB2 primer and reverse primers for the gene of interest GAPA, and GAPB (Figure 4.5).

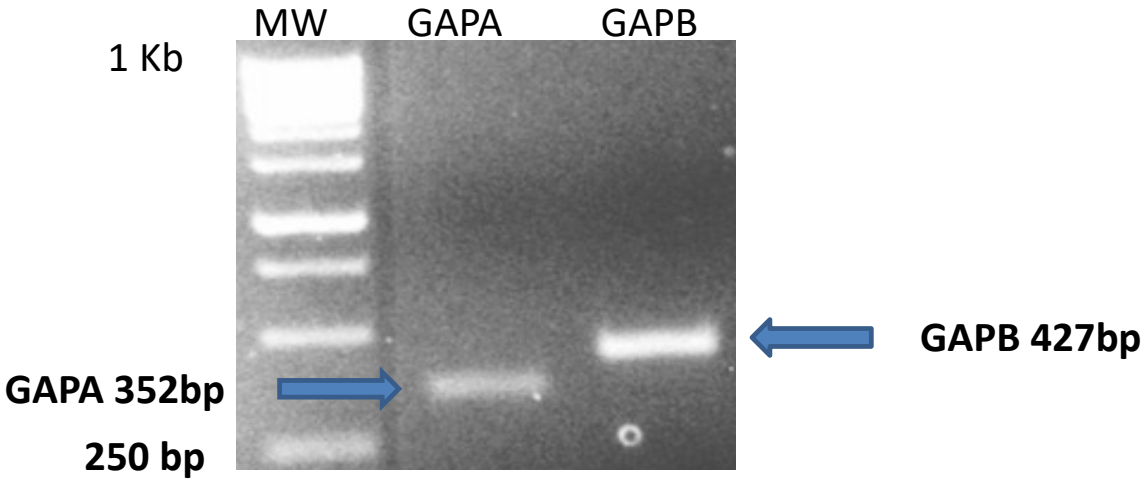

(A) Figure 4.2: PCR analyses to an amplified small region of cDNA sequence to clone GAPA and GAPB by gateway technology (Antisense construct). The size of cDNA region for cloned of GAPA antisense was 352bp, and the size of cDNA region for cloned of GAPB antisense was 427bp. The PCR reaction was 20 µl, and the PCR products were run on 0.5% agarose gel for 30 min at 110 v. PCR products run alongside molecular weight markers (1kb DNA ladder from Invitrogen). The marker was used in this PCR 1 Kb.

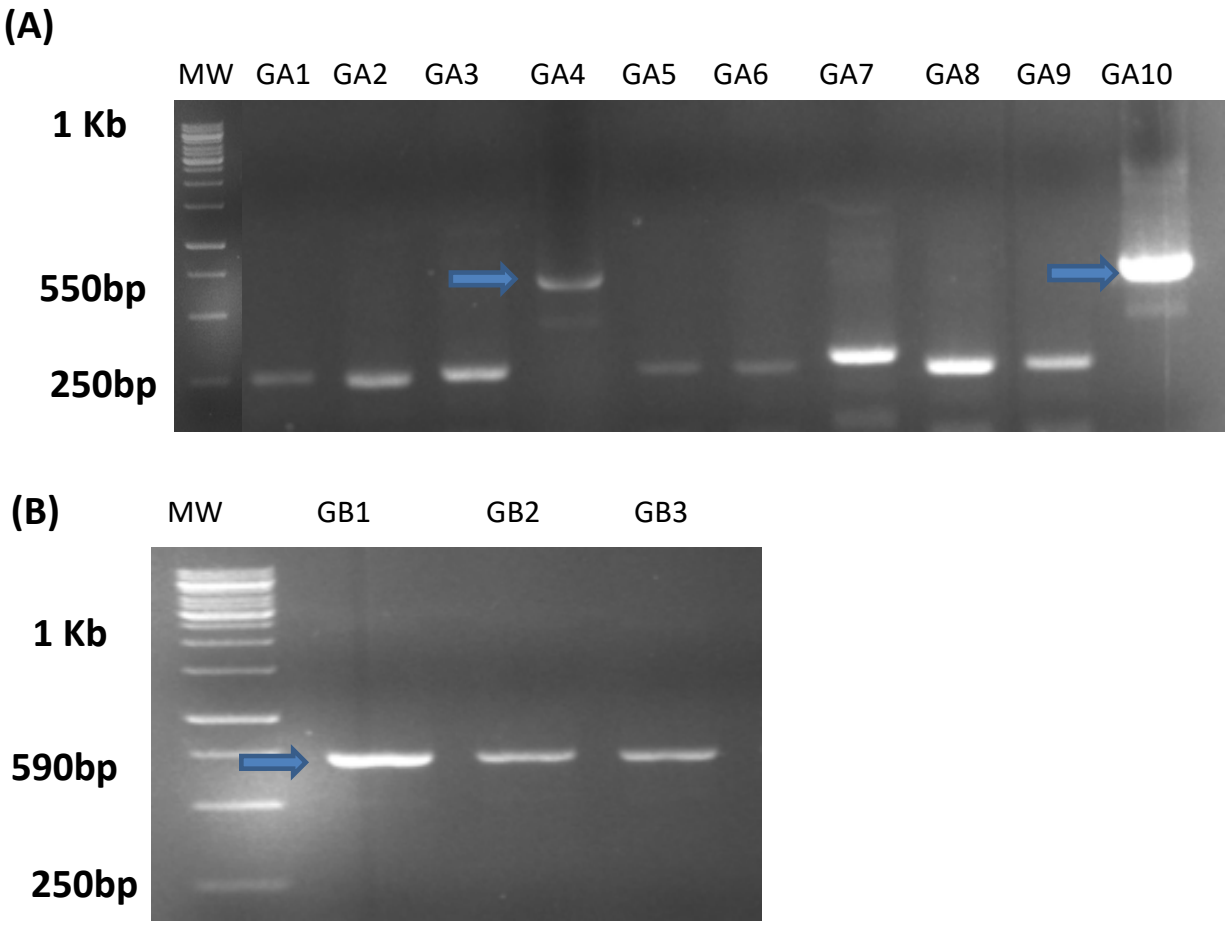

Figure 4.3: Colony PCR of the pENTR™/D-TOPO® vector to identify positive clones using M13 Forward + Reverse primers of the (GAPA and GAPB). (A) Colony PCR for GAPA using M13 F + R primers of the gene of interest lane 4, and 10 were identified as positive colony with expected size the bands indicated with 250 bp unnecessary bands **(B)** Colony PCR for GAPB by using M13 F + R primers of the gene of interest lane 1, 2, and 3 were identified as positive colony with expected size. The PCR reaction was 20 µl, and the PCR products were run on 0.5% agarose gel for 30 min at 110 v. PCR products run alongside molecular weight markers (1kb DNA ladder from Invitrogen). The marker was used in this PCR 1 Kb.

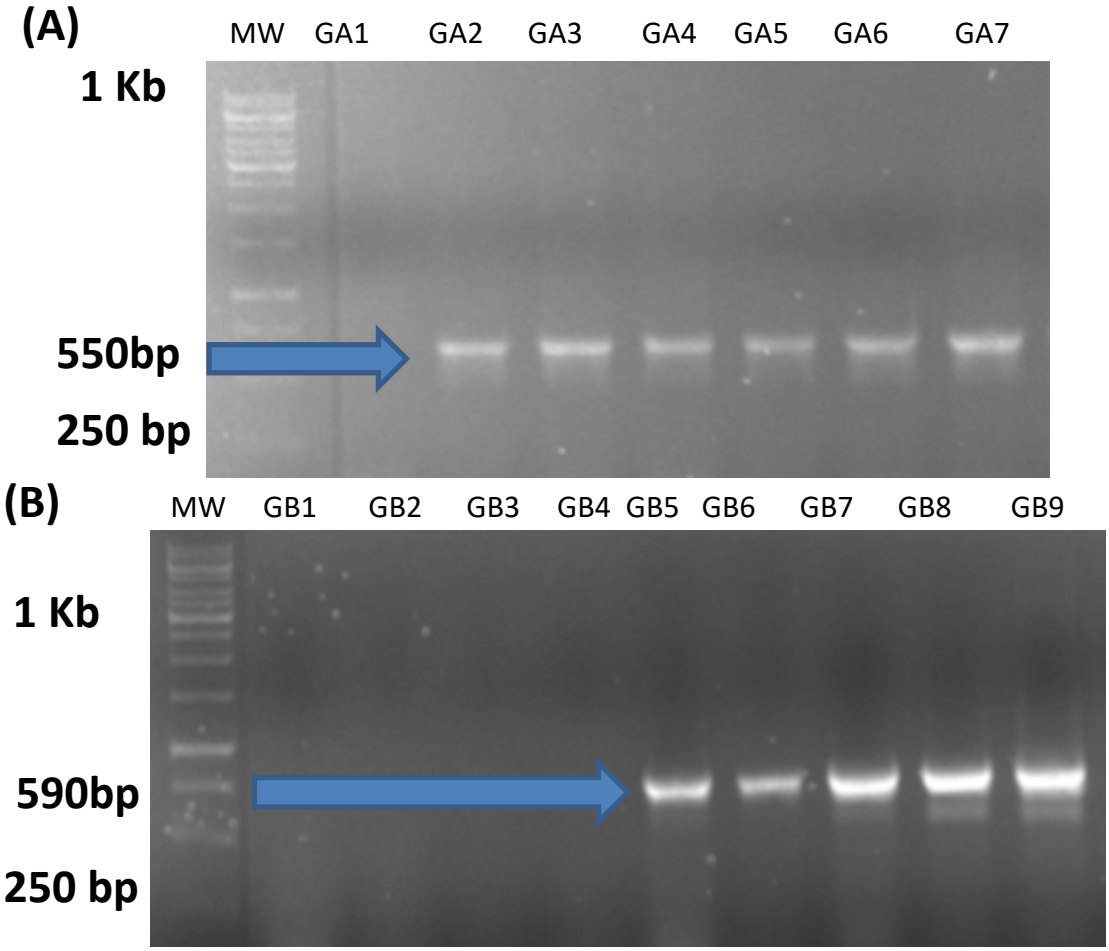

Figure 4.4: Colony PCR after LR reaction to identify positive colony ligated to destination vector (PGWB2) this PCR analysis has been done by using Forward primer of PGWB2 and Reverse primer of the gene of interest (GAPA and GAPB). **(A)** Colony PCR for GAPA gene after LR reaction by using the Forward primer of PGWB2, and Reverse primer of the gene of interest (GAPA). **(B)** Colony PCR for GAPB gene after LR reaction by using the Forward primer of PGWB2, and Reverse primer of the gene of interest (GAPB). The PCR reaction was 20 µl, and the PCR products were run on 0.5% agarose gel for 30 min at 110 v. PCR products run alongside molecular weight markers (1kb DNA ladder from Invitrogen). The marker was used in this PCR 1 Kb.

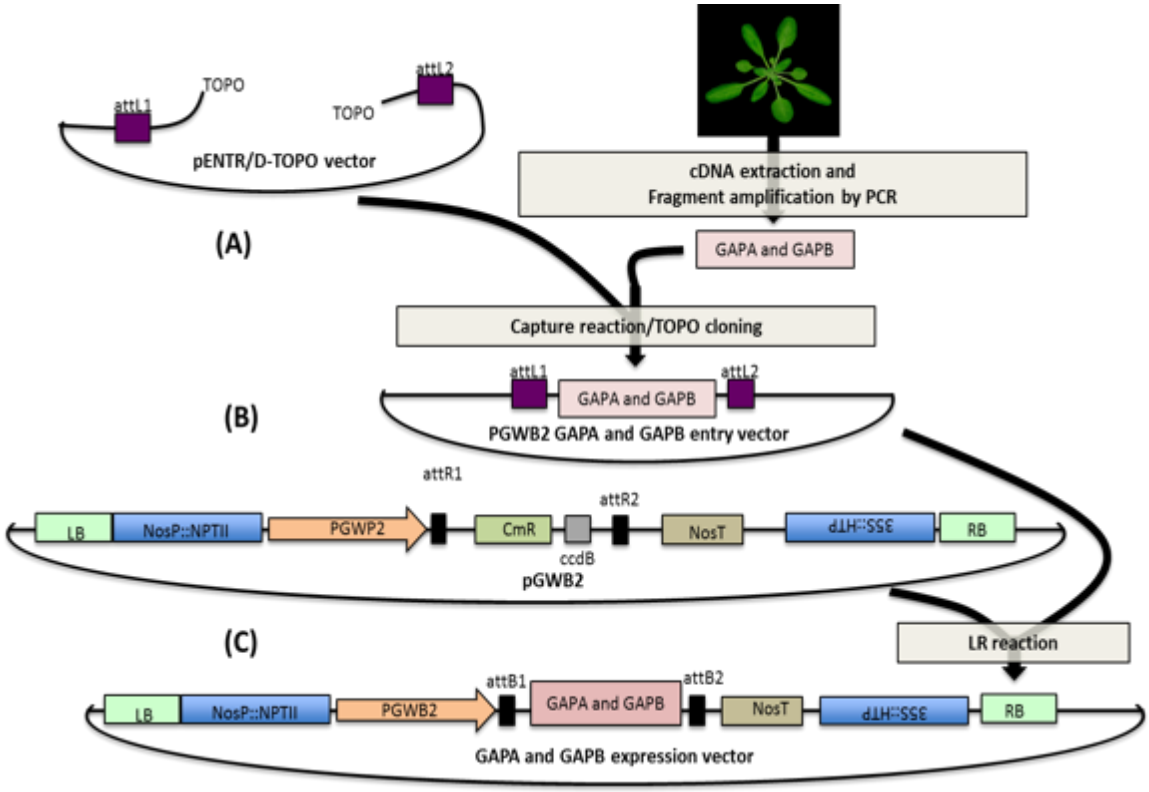

Figure 4.5: Building GAPA (PGWB2) vector for plant down expression. **(a)** Genomic DNA from Arabidopsis thaliana was used to amplify part of the cDNA sequence of gene GAPA and GAPB. **(b)** These fragments were then cloned into pENTR/D TOPO cloning vector to generate pENTR-GAPA and GAPB. **(c)** This plasmid was later used in a recombination reaction with destination vector PGWB2 to generate GAPA and GAPB (PGWB2) expression vector. The expression vector produced also carries the NosP:: NPTII and the 35:: HTP genes which confer resistance to the Kanamycin and Hygromycin antibiotics respectively and allow for selection in both bacteria and plants.

4.2.3 Preliminary screening of T1 progeny of GAPA and GAPB Antisense lines

The preliminary analyses of the T1 transgenic plants of GAPA and GAPB antisense comprised of two different processes: molecular and physiological analyses. The molecular screenings were done in three different approaches: Screening plants in MS Media containing antibiotic resistance to transgenic plants, gene expression analysis using qPCR and protein expression analysis using the Western blot. Plants confirmed to have a decreased GAPA, and GAPB protein levels were subject to physiological analyses to study whether the reductions had an impact on photosynthesis or growth.

4.2.4 Screening GAPA T1 plants on Ms Media containing Kanamycin antibiotics

Transformed plants were selected by using antibiotics, 50µg/mL kanamycin, containing a medium. Plants (13) of GAPA were resistant to Kanamycin, and these plants were subjected to molecular analysis to study the gene expression by qPCR and examine the protein level by immunoblot analysis. An example of positively transformed plants of GAPA T1 after resistance on Kanamycin plates (Figure 4.6).

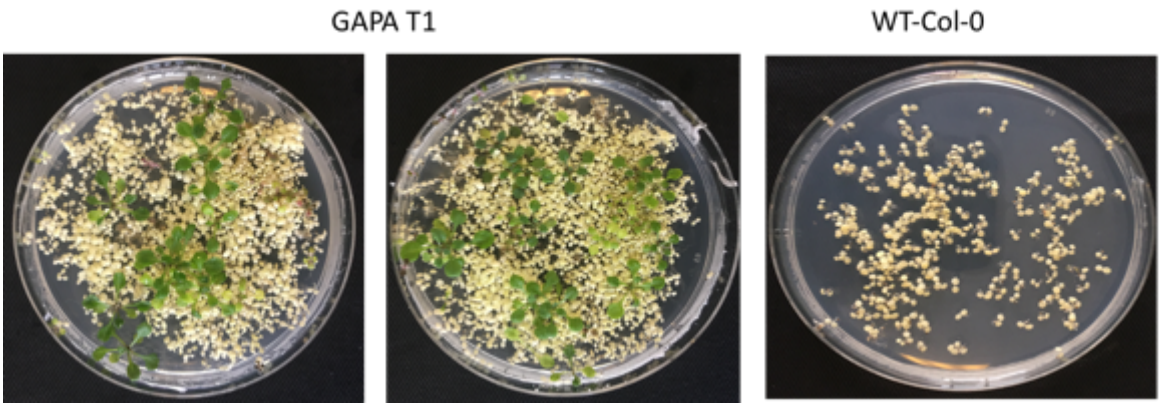

Figure 4.6: Identification of positive T1 progeny of putative GAPA transformants by kanamycin screening following Agrobacterium transformation. Seeds from T0 plants were germinated on MS medium containing and seedlings with green cotyledons identified after 14 days of germination.

4.2.5 Gene expression analysis of GAPA T1 Antisense plants using qPCR

To determine the transcript level (gene expression) in the transgenic GAPA T1 antisense plants, tissues were harvested in liquid N2 from the transgenic plants. The result of transgenic plants was selected on kanamycin-containing medium, and positive resistance plants were moved to soil with independent pots. RNA was isolated, and cDNA was synthesised. Afterwards, GAPA T1 cDNAs were amplified using qPCR specific designed primers for GAPA-1 and GAPA-2 (Primers sequences showed in Chapter 2). The qPCR analysis using GAPA-1 primers showed only plant A-7, A-13 showed reduced the expression level of GAPA-1 compared to WT plants (Figure 4.7A). The qPCR analysis using GAPA-2 primer indicated only plants A-7, A-12, A13, A-14 and A-15 showed reduced the expression level of GAPA-2 compared to WT Plants (Figure 4.7B).

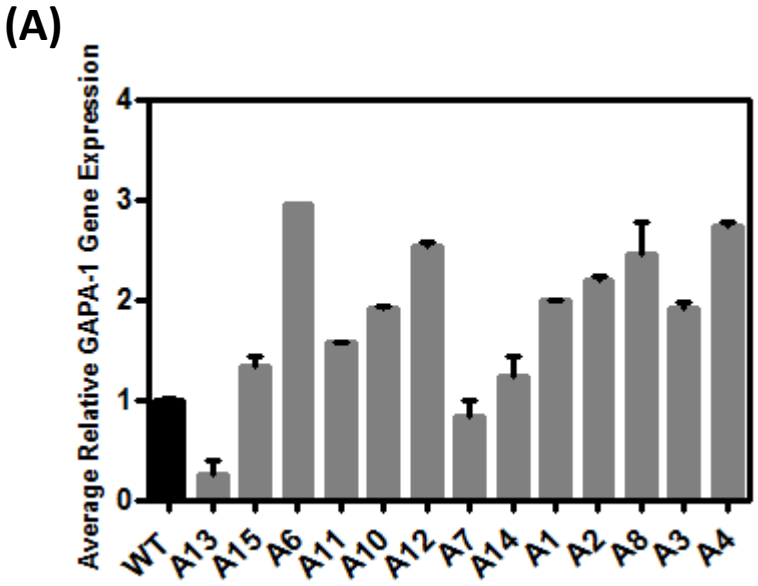

Figure 4.7A: Determination of the transcript levels of the GAPA transcript in T1 transgenic Arabidopsis plants by using the GAPA-1 primer. RNA was extracted from the leaf tissue in the seedling stage 4 weeks after potting. The expression was relative to the gene expression of a stable actin reference gene. Plants A-7 and A13 showed reduced the expression level of GAPA-1 compared to WT plants.

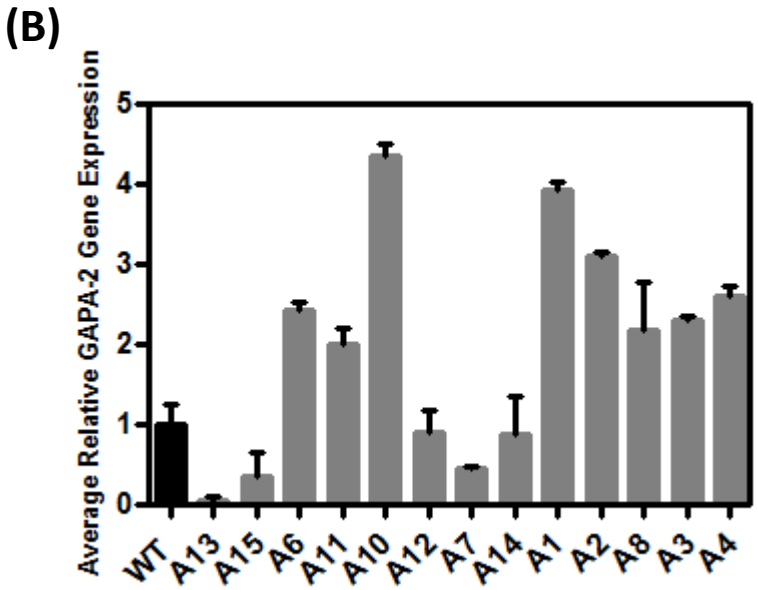

Figure 4.7B: Determination of the transcript levels of the GAPA transcript in T1 transgenic Arabidopsis plants by using the GAPA-2 primer. RNA was extracted from the leaf tissue in the seedling stage 4 weeks after potting. The expression was relative to the gene expression of a stable actin reference gene. Plants A-13, A-15, A-12, A-7 and A-14 showed reduced the expression level of GAPA-2 compared to WT plants.

4.2.6 Protein analysis (Western Blot) of GAPA of transgenic T1 Arabidopsis plants.

To investigate whether protein level is decreased, the protein was extracted from the leaves of the transgenic plants and was analysed using immunoblot. Samples were loaded on an equal protein basis, into 12% SDS-polyacrylamide gels. The proteins were run and separated by electrophoresis, transferred onto PVDF membranes, probed and rinsed with GAPDH antibody. A band was predictable at about 37.6 kDa indicating the GAPA gene. Plants 7, 13, and 15 were shown clearly decreased the protein level of GAPA compared to WT plants (Figure 4.8). This reduction in protein levels correlated with the gene expression (qPCR) result.

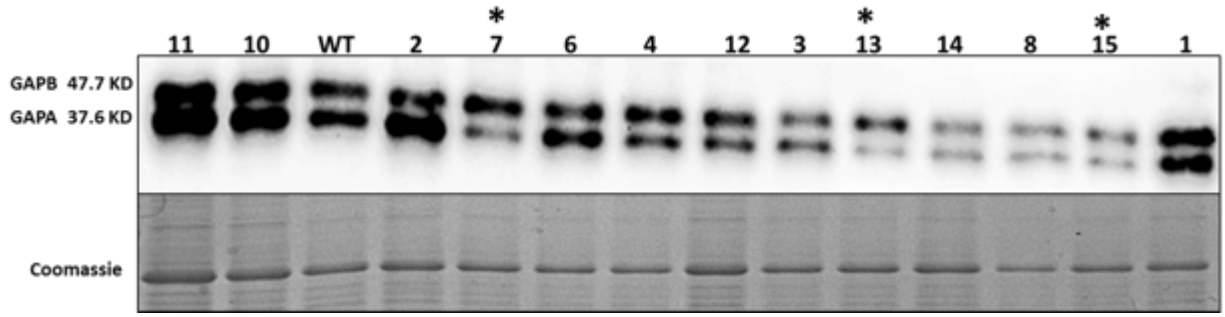

Figure 4.8: Immunoblot analysis of transgenic GAPA antisense T1 plants. A total extractable leaf tissue protein were loaded on an equal protein basis, into 12% SDS-polyacrylamide gels and blotted to PVDF membrane for individual transgenic plants and WT (col-0). Antibody raised against GAPDH protein was used to identify GAPA. Coomassie which showed the loading of protein. Stars indicate clear differences for transgenic plants compared to WT plant.

4.2.7 Screening GAPB T1 plants on Ms Media containing Kanamycin antibiotics

Transformed plants were selected by using antibiotics 50 µg/mL kanamycin containing a medium. Twelve plants of GAPB were resistance on Kanamycin plates. Then these plants were transferred to molecular analysis to study the gene expression by qPCR and examine the protein level by Western blot. An example of positively transformed plants of GAPB T1 after resistance on Kanamycin plates (Figure 4.9).

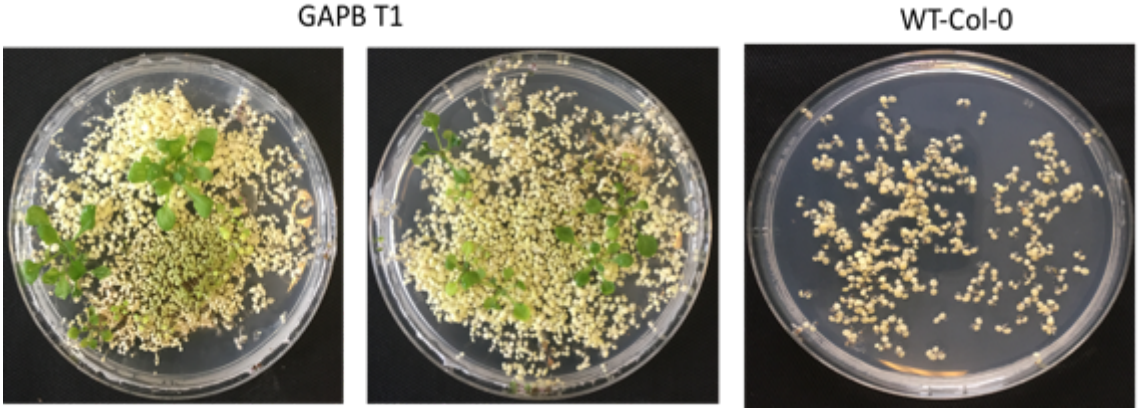

Figure 4.9: Screening T1 progeny positive transgenic plants of GAPB by kanamycin antibiotic after transformed by Agrobacterium. Seeds from T0 plants were germinated on MS medium containing and seedlings with green cotyledons identified after 14 days of germination.

4.2.8 Gene expression analysis of GAPB T1 Antisense plants using qPCR

To study the transcript level (gene expression) in transgenic GAPB T1 antisense plants, tissues were harvested in liquid nitrogen from the transgenic plants. The result of transgenic plants was selected on kanamycin-containing medium, and positive resistance plants were moved to soil with independent pots. RNA was isolated, and cDNA was synthesised. Afterwards, GAPB T1 cDNAs were amplified using qPCR specific designed primers (sequences showed in Chapter 2). Plants B-12, B-5, B-6, B-8, B-9, B-10, and B-13 indicated reduced the expression level of GAPB compared to WT plants (Figure 4.10).

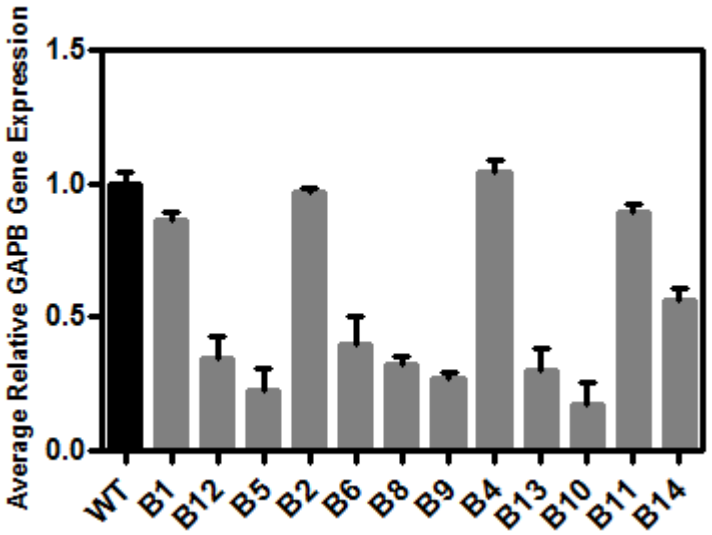

Figure 4.10: Determination of the transcript levels of the GAPB transcript in T1antisense transgenic Arabidopsis plants. RNA was extracted from the leaf tissue in the seedling stage 4 weeks after potting. The expression was relative to the gene expression of a stable actin reference gene. Plants B12, B5, B6, B8, B9, B10 and B13 showed reduced the expression level of GAPB compared to WT plants.

4.2.9 Protein analysis (Western Blot) of GAPB in transgenic T1 Arabidopsis plants.

To investigate whether protein expression is decreased, a protein was extracted from the leaves of the transgenic plants and was analysed using immunoblot. Samples were loaded on an equal protein basis, into 12% SDS-polyacrylamide gels. The proteins were run and separated by electrophoresis, transferred onto PVDF membranes, probed and rinsed with GAPDH antibody. A band was predictable at about 47.7 kDa indicating the GAPB gene. Plants 12, 5, 8, 9, 10, and 13 were shown clearly decreased the protein level of GAPB compared to WT plants (Figure 4.11). This reduction in protein levels correlated with the gene expression (qPCR) result.

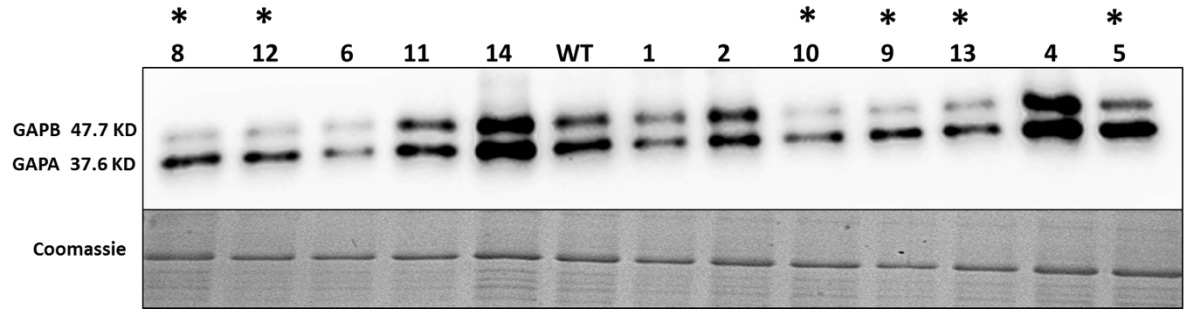

Figure 4.11: immunoblot analysis of transgenic GAPB antisense T1 plants. A total extractable leaf tissue protein was loaded on an equal protein basis, into 12% SDS-polyacrylamide gels and blotted to PVDF membrane for individual transgenic plants and WT (col-0). Antibody raised against GAPDH protein was used to identify GAPB. Coomassie which showed the loading of protein. Stars indicated clear differences for transgenic plants compared to WT plant.

4.2.10 Growth Analysis of GAPA and GAPB Antisense T2 lines

4.2.10.1 Rosette area

WT Columbia (Col-0), azygous, three independent antisense lines of GAPA (7,13, and 15) and four independent antisense lines of GAPB (9,10,12, and 13) were grown in growth chambers at 22 °C under short day (Photoperiod: 8 hours' light / 16 hours' dark), and relative humidity (RD) 50%. Photographs of the plants were taken three times each week starting after 15 days of germination. Rosette area of plants was measured by using the ImageJ program. The rosette area after 15 days of germination showed GAPA line (7,13, and 15) significantly larger compared to WT plants. On the other hand, the GAPB line (10, 12, and 13) were significantly larger compared to WT plants; however GAPB line 9 showed no significant difference compared to WT plants (Figure 4.12A). The rosette area after 20 days of germination indicated GAPA line 13 significantly larger compared to WT plants; however, GAPA line (7 and 15) and GAPB line (9, 10, 12, and 13) showed no significant difference compared to WT plants (Figure 4.12B). The rosette area after 25 days of germination presented only GAPB line 13 significantly larger compared to WT plants. Nevertheless, GAPA line (7, 13 and 15) and GAPB line (9, 10 and 12) indicated no significant difference compared to WT plants (Figure 4.12C). The rosette area after 30 days of germination showed GAPB line 10 significantly larger compared to WT plants; however, GAPA line (7, 13, and 15) and GAPB line (9, 12, and 13) showed no significant difference compared to WT plants (Figure 4.12D). The rosette area after 40 days of germination showed no significant differences either GAPA line (7, 13, and15) and GAPB line (9, 10, 12 and 13) compared to WT plants (Figure 4.12E). The rosette area after 53 days of germination indicated no significant differences either GAPA line (7, 13 and15) and GAPB line (9, 10, 12 and 13) compared to WT plants (Figure 4.12F).

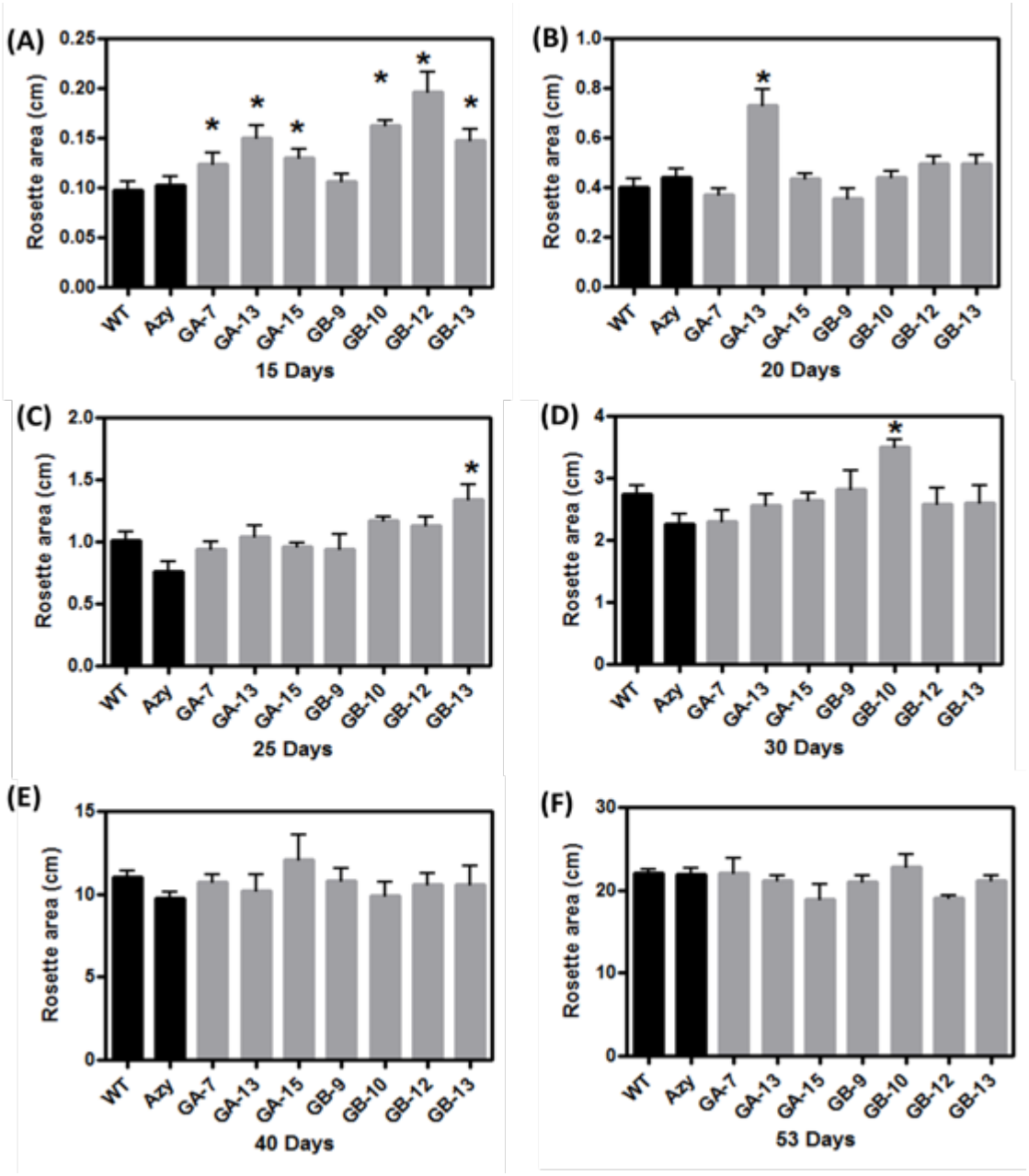

Figure 4.12: Comparison of the average rosette area of WT Columbia (Col-0) and three independent antisense lines of GAPA (7, 13, and 15) and four independent antisense lines of GAPB (9, 10, 12, and 13). Plants were grown in short day room (photoperiod: 8 hours' light / 16 hours dark). **(A)** Rosette area after 15 days of germination. **(B)** Rosette area after 20 days of germination. **(C)** Rosette area after 25 days of germination. **(D)** Rosette area after 30 days of germination. **(E)** Rosette area after 40 days of germination. **(F)** Rosette area after 53 days of germination. Error bars represent SE, n=8 replicates. Stars showed the significant transgenic lines compare to WT control ($P<0.05$) one-way ANOVA, post-hoc test).

4.2.10.2 Number of leaves

The count leaves numbers of WT Columbia (Col-0), azygous, three independent antisense lines of GAPA (7, 13 and 15), and four independent antisense lines of GAPB (9,10,12, and 13) were counted at 38 days after potting 53 days after sowing the seeds. The average leaves number of GAPA line (7, 13 and 15) had a smaller number of leaves significantly compared to WT plants. It was 28.5, 28.75 and 29 respectively, whereas WT had 34 leaves. On the other hand, the GAPB line (9, 10, 12, and 13) had a smaller number of leaves significantly compared to WT plants. It was 29.62, 29, 30.25 and 30.25 respectively, while WT had 34 leaves (Figure 4.13).

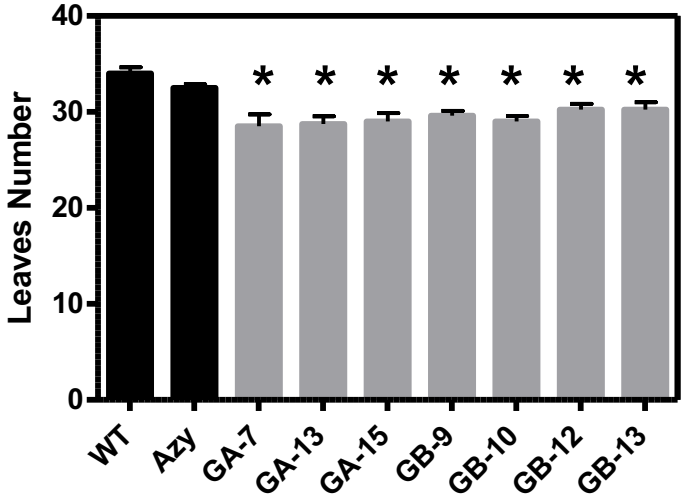

Figure 4.13: Comparison the average of a count, leaves a number of WT Columbia (Col-0) and three independent antisense lines of GAPA (7, 13 and 15) and four independent antisense lines of GAPB (9, 10, 12 and 13). Plants were grown in short day room (photoperiod: 8 hours' light / 16 hours dark). Count leaves numbers were taken at 53 days of germination (38 days after potting). Error bars represent SE n=8 replicates. Stars showed the significant transgenic lines compare to WT control ($P<0.05$) one-way ANOVA, post-hoc test).

4.2.10.3 Rosette Dry weight

The rosette dry weight of WT Columbia (Col-0), azygous, three independent antisense lines of GAPA (7, 13, and 15), and four independent antisense lines of GAPB (9, 10, 12, and 13) were weighted at 38 days after potting 53 days after sowing. The average rosette dry weights of GAPA (7, 13 and 15) were significantly smaller compared to WT plants. On the other hand, the average rosette dry weights of GAPB (9, 10, 12 and 13) were significantly smaller compared to WT plants (Figure 4.14).

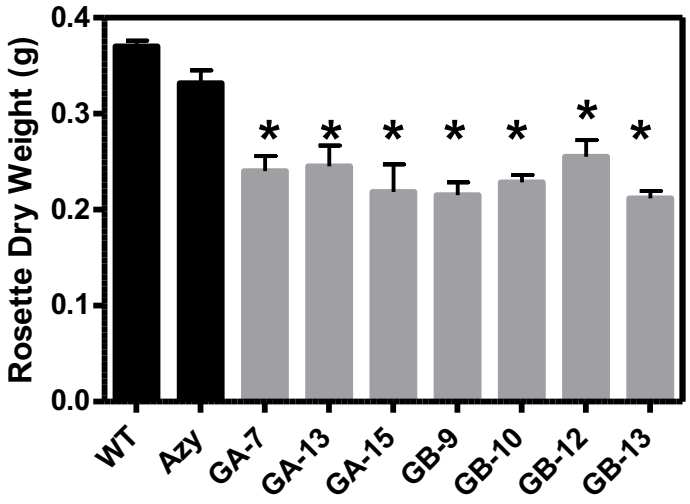

Figure 4.14: Comparison the average of dry rosette weight of WT Columbia (Col-0) and three independent antisense lines of GAPA (7,13 and 15) and four independent antisense lines of GAPB (9,10,12, and 13). Plants were grown in short day room (photoperiod: 8 hours' light / 16 hours dark). Rosette dry weights were taken at 53 days of germination (38 days after potting). Error bars represent SE n=8 replicates. Stars showed the significant transgenic lines compare to WT control ($P<0.05$) one-way ANOVA, post-hoc test).

4.2.10.4 The phenotype of GAPA and GAPB Antisense T2 lines

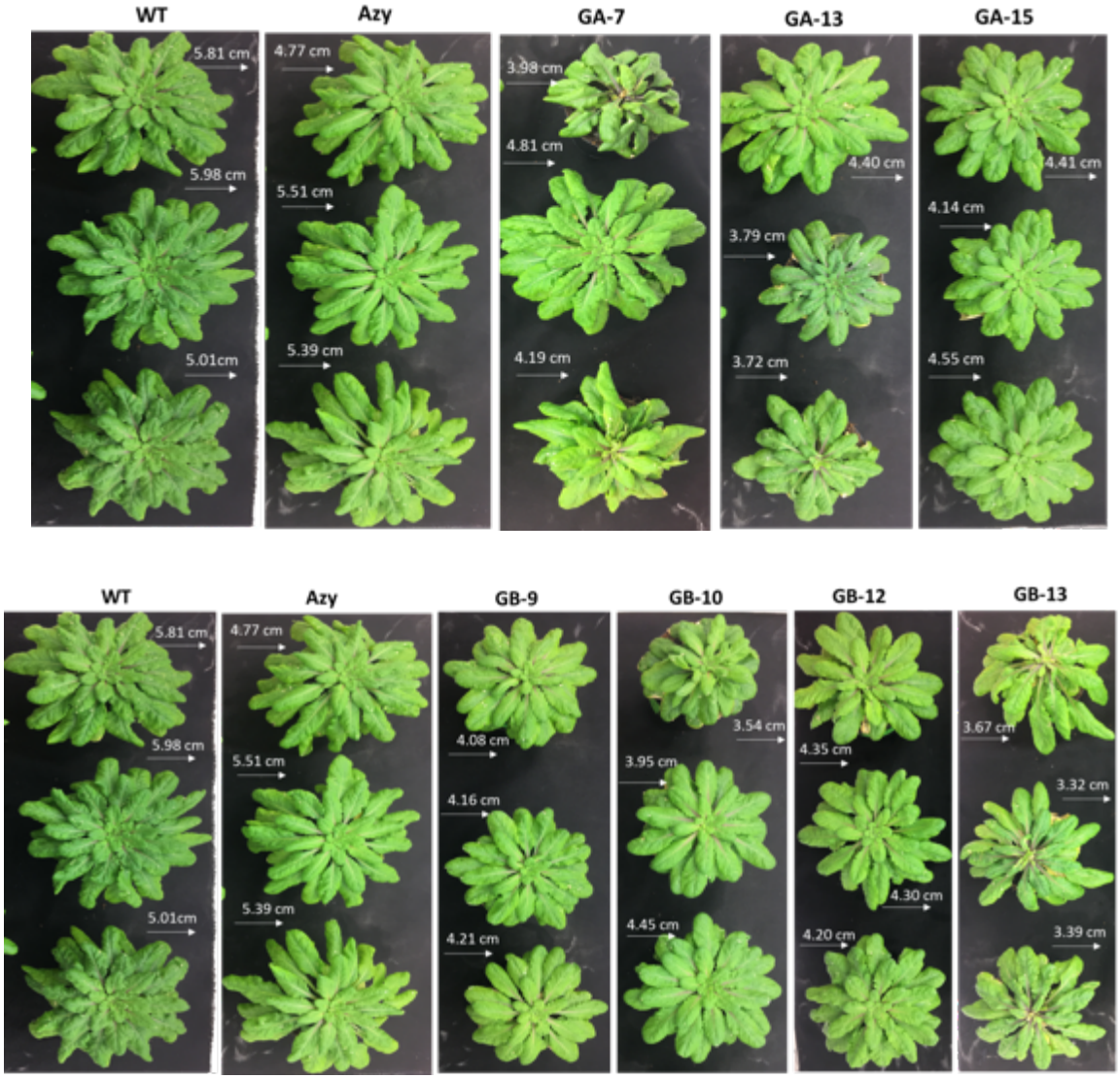

Figure 4.15: Photo of GAPA and GAPB antisense lines compared to WT and azygous plants and harvested at 38 days after potting. Plants were grown in growth chambers at 22 °C under short day (Photoperiod: 8 hours' light / 16 hours' dark) and relative humidity (RD) 50%. (The Scale bar represents in each individual plant by cm from Image J program).

4.2.11 Growth Analysis of GAPA and GAPB T-DNA and co-suppressed lines

4.2.11.1 Rosette area

WT Columbia (Col-0), azygous, GAPA-1 line (164), GAPB line (308), two co-suppressed lines of GAPA (B11-1 and B114-1) and the two crossed lines (GA-164/GB-308-1 and GA-164/GB-308-4) were grown in growth chambers at 22 °C under short day (Photoperiod: 8 hours' light / 16 hours' dark), and relative humidity (RD) 50%. Photographs of the plants were taken three times each week starting after 18 days of germination. The rosette area after 18 days of germination showed GAPA-1 (164) and GAPB (308) were significantly larger compared to WT plants, while the co-suppressed line of GAPA (B114-1) and two crossed lines (GA-164/GB-308-1 and GA-164/GB-308-4) were significantly smaller compared to WT plants (Figure 4.16A). The rosette area after 25 days of germination indicated GAPA-1 line (164), two co-suppressed lines of GAPA (B11-1 and B114-1) and two crossed lines (GA-164/GB-308-1 and GA-164/GB-308-4) were significantly smaller compared to WT plants; however, GAPB (308) showed no significant difference compared WT plants (Figure 4.16B). The rosette area after 30 days of germination indicated GAPA-1 line (164), two co-suppressed lines of GAPA (B11-1 and B114-1) and two crossed lines (GA-164/GB-308-1 and GA-164/GB-308-4) were significantly smaller compared to WT plants; however, GAPB (308) showed no significant difference compared WT plants (Figure 4.16C). The rosette area after 35 days of germination showed co-suppressed line of GAPA (B11-1), and two crossed lines (GA-164/GB-308-1 and GA-164/GB-308-4) were significantly smaller compared to WT plants, nevertheless GAPA-1 (164), GAPB (308) and co-suppressed line of GAPA (B114-1) showed no significant difference compared WT plants (Figure 4.16D). The rosette area after 42 days of germination indicated GAPA-1 line (164), two co-suppressed lines of GAPA (B11-1

and B114-1) and two crossed lines (GA-164/GB-308-1 and GA-164/GB-308-4) were significantly smaller compared to WT plants; however, GAPB (308) showed no significant difference compared WT plants (Figure 4.16E). The rosette area after 46 days of germination showed two co-suppressed lines of GAPA (B11-1 and B114-1) and two crossed lines (GA-164/GB-308-1 and GA-164/GB-308-4) were significantly smaller compared to WT plants; however, GAPA-1 (164), and GAPB (308) showed no significant difference compared to WT plants (Figure 4.16F).

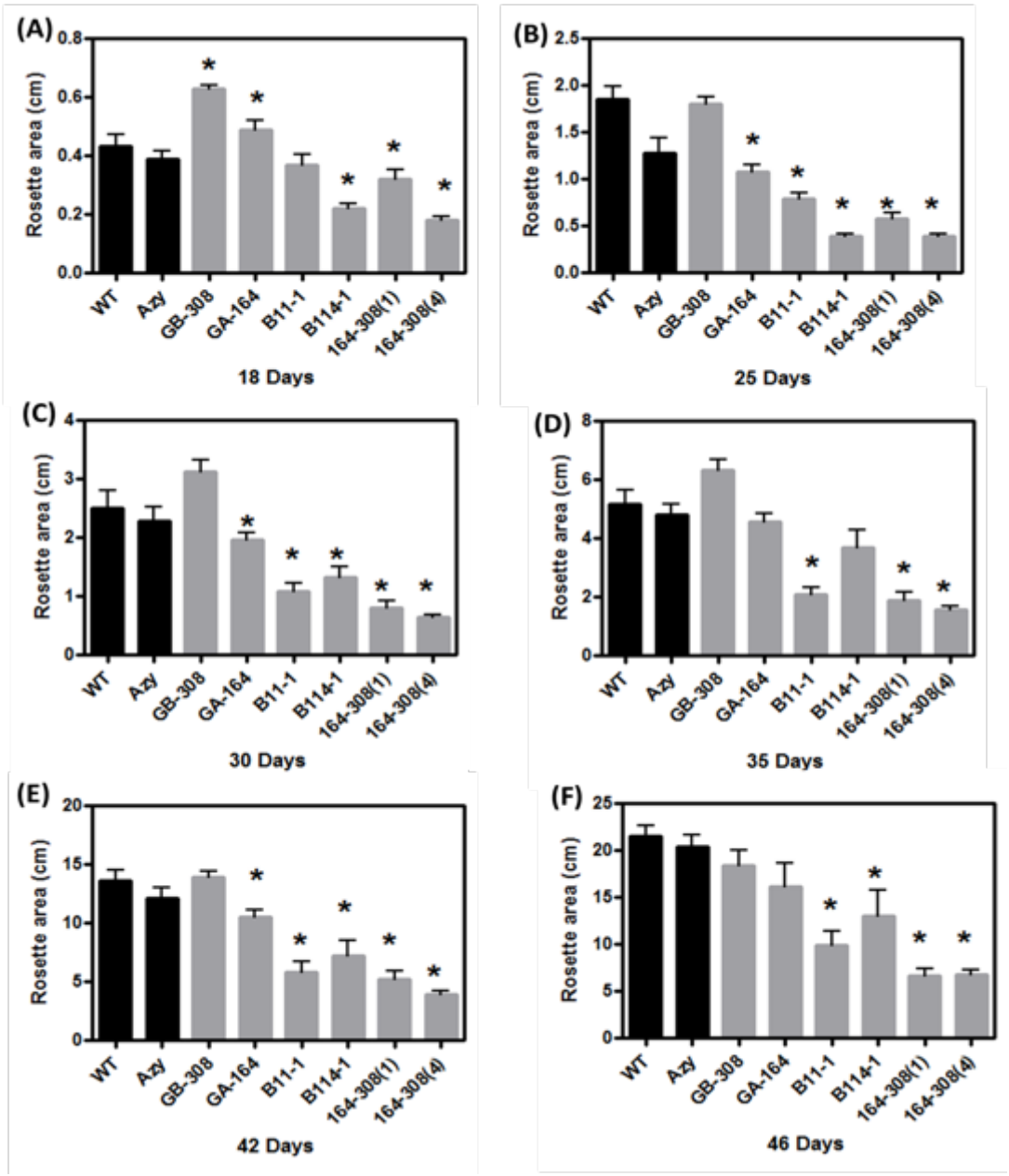

Figure 4.16: Comparison of the average rosette area of WT Columbia (Col-0) and GAPA-1 line (164), GAPB line (308), two co-suppression lines of GAPA (B11-1 and B114-1), and two crossed line (GA-164/GB-308-1 and GA-164/GB-308-4). Plants were grown in short day room (photoperiod: 8 hours' light / 16 hours dark). **(A)** Rosette area after 18 days of germination. **(B)** Rosette area after 25 days of germination. **(C)** Rosette area after 30 days of germination. **(D)** Rosette area after 35 days of germination **(E)** Rosette area after 42 days of germination. **(F)** Rosette area after 46 days of germination. Error bars represent SE, n=8 replicates. Stars showed the significant transgenic lines compare to WT control ($P<0.05$) one-way ANOVA, post-hoc test).

4.2.11.2 Numbers of leaves

The count leaves numbers of WT Columbia (Col-0), azygous, GAPA-1 line (164), GAPB line (308), two co-suppressed lines of GAPA (B11-1 and B114-1), and two crossed line (GA-164/GB-308-1 and GA-164/GB-308-4) were counted at 38 days after potting 53 days after sowing seeds. The average of leaves number of GAPA-1 line (164), GAPB line (308), two co-suppressed lines of GAPA (B11-1 and B114-1), and two crossed lines (GA-164/GB-308-1 and GA-164/GB-308-4) had a smaller number of leaves significantly compared to WT plants (Figure 4.17).

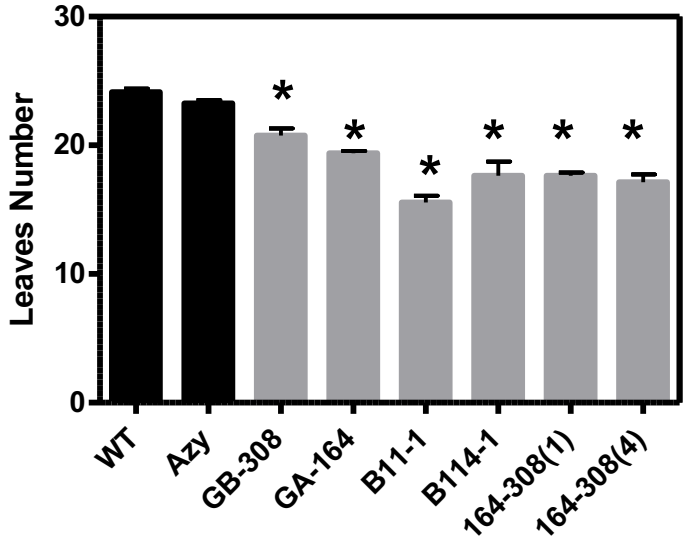

Figure 4.17: Comparison of the average number of leaves of WT Columbia (Col-0) and GAPA-1 line (164), GAPB line (308), two co-suppressed lines of GAPA (B11-1 and B114-1), and two crossed line (GA-164/GB-308-1 and GA-164/GB-308-4). Plants were grown in short day room (photoperiod: 8 hours' light / 16 hours dark). Leaf numbers were determined at 53 days of germination (38 days after potting). Error bars represent SE n=8 replicates. Stars showed the significant transgenic lines compare to WT control ($P<0.05$) one-way ANOVA, post-hoc test).

4.2.11.3 Rosette Dry weight

The rosette dry weight of WT Columbia (Col-0), azygous, GAPA-1 line (164), GAPB line (308), two co-suppressed lines of GAPA (B11-1 and B114-1) and two crossed line (GA-164/GB-308-1 and GA-164/GB-308-4) were weighted at 38 days after potting 53 days after sowing seeds. The average of dry rosette weight of GAPA-1 line (164), GAPB line (308), two co-suppressed lines of GAPA (B11-1 and B114-1) and two crossed line (GA-164/GB-308-1 and GA-164/GB-308-4) showed significantly smaller weight compared to WT plants (Figure 4.18).

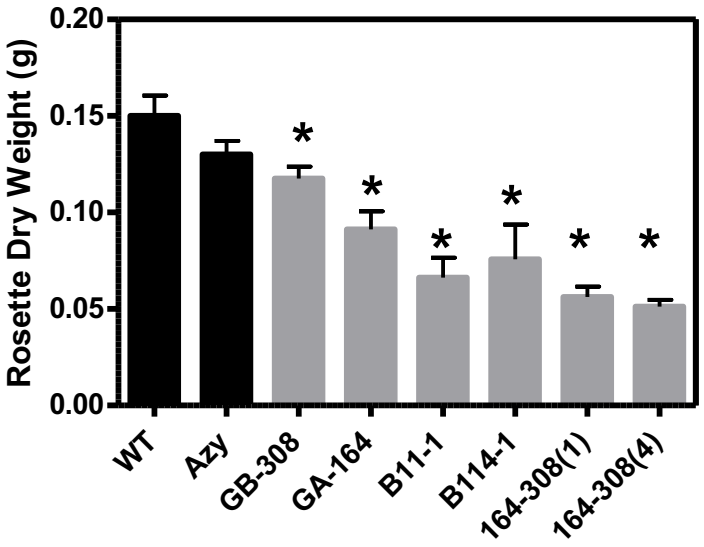

Figure 4.18: Comparison the average of dry rosette weight of WT Columbia (Col-0) and GAPA-1 line (164), GAPB line (308), two co-suppressed lines of GAPA (B11-1 and B114-1), and two crossed line (GA-164/GB-308-1 and GA-164/GB-308-4). Plants were grown in short day room (photoperiod: 8 hours' light / 16 hours dark). Rosette dry weights were taken at 53 days of germination (38 days after potting). Error bars represent SE n=8

replicates. Stars showed the significant transgenic lines compare to WT control (P<0.05) one-way ANOVA, post-hoc test).

4.2.11.4 The phenotype of T-DNA insertion lines of GAPA-1 line (164), GAPB line (308), two co-suppressed lines of GAPA (B11-1 and B114-1), and two crossed line (GA-164/GB-308-1 and GA-164/GB-308-4)

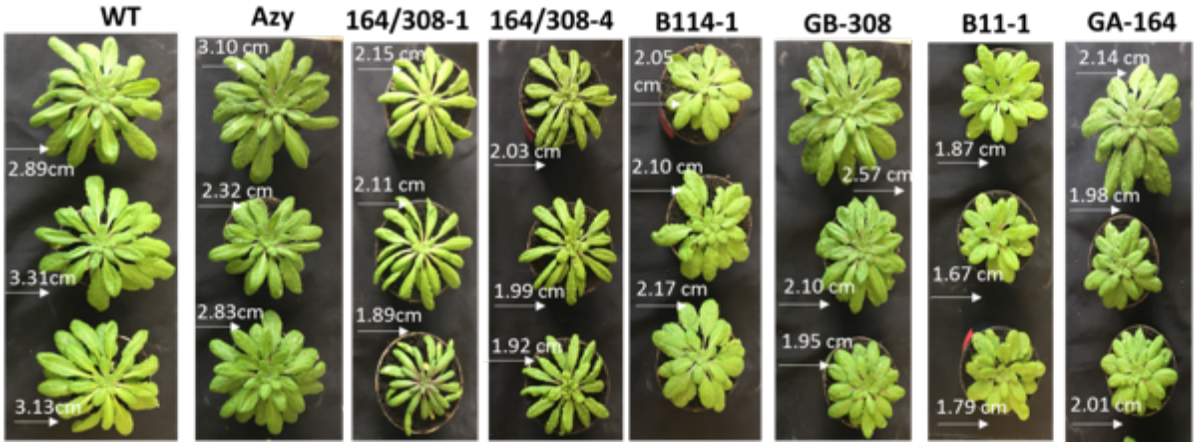

Figure 4.19: Photo of T-DNA insertion lines of GAPA-1 line (164), GAPB line (308), two co-suppressed lines of GAPA (B11-1 & B114-1), and two crossed line (GA-164/GB-308-1 & GA-164/GB-308-4) compared to WT and azygous plants and harvested at 38 days after potting. Plants were grown in growth chambers at 22 °C under short day (Photoperiod: 8 hours' light / 16 hours' dark), and relative humidity (RD) 50%. (The Scale bar represents in each individual plant by cm from Image J program).

4.2.12 Chlorophyll fluorescence imaging of antisense T2 lines GAPA and GAPB

To explore the impact of decreased levels of antisense lines GAPA and GAPB protein on photosynthesis, plants were grown at in growth chambers at 22 °C under short day (Photoperiod: 8 hours' light / 16 hours' dark), and relative humidity (RD) 50% and the quantum efficiency of PSII photochemistry (*Fq'/Fm'*) examined using chlorophyll a fluorescence imaging (Baker, 2008; Murchie and Lawson, 2013). At the low level of light GAPA antisense lines (GA-7, GA-13, and GA-15), and GAPB antisense lines (GB-9, GB-10, GB-12 and GB-13) revealed no significant difference *Fq'/Fm'* at an irradiance of 200 μmol m^{-2} s^{-1} compared to WT plants (Figure 4.20A). Also, at a high level of light GAPA antisense lines (GA-7, GA-13, and GA-15), and GAPB antisense lines (GB-9, GB-10, GB-12 and GB-13) showed no significant difference *Fq'/Fm'* at an irradiance of 600 μmol m^{-2} s^{-1} compared to WT plants (Figure 4.20B).

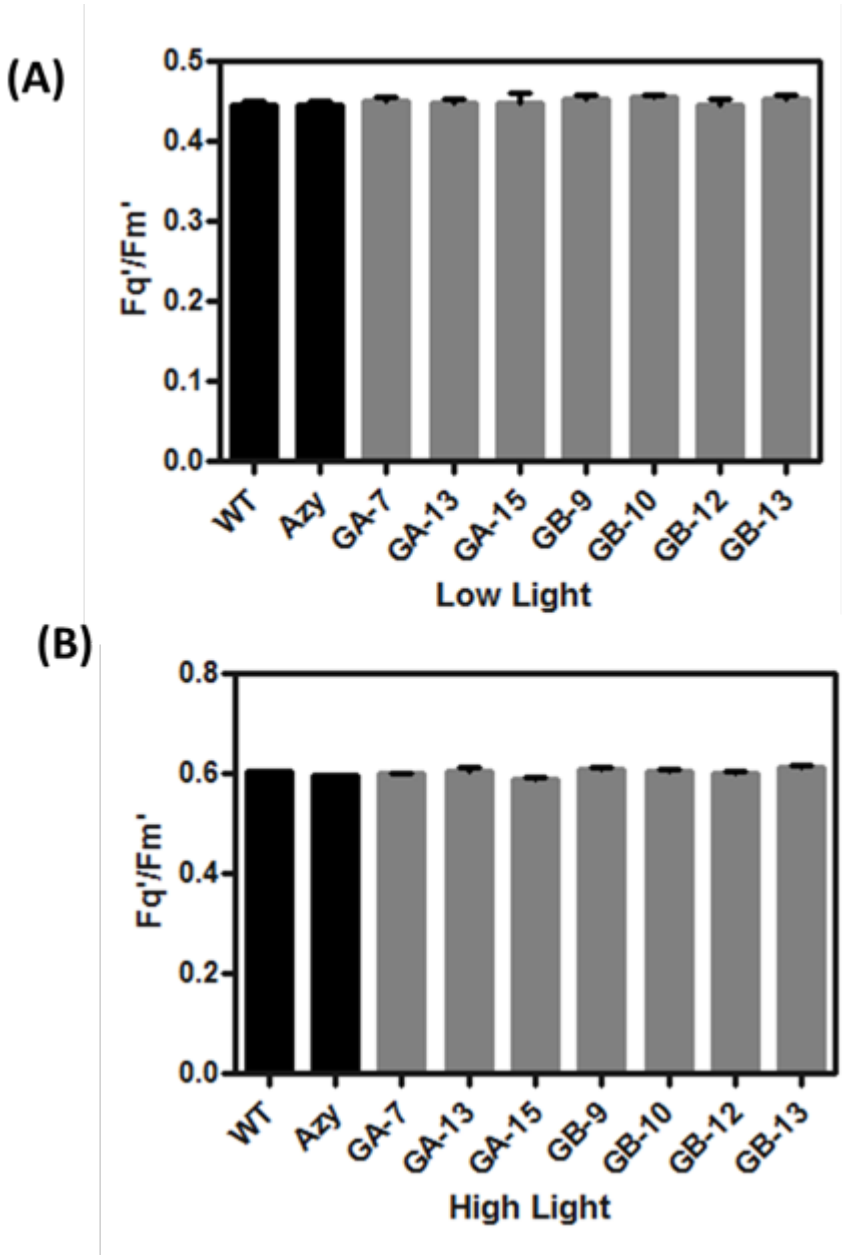

Figure 4.20: Photosynthetic capacity in transgenic seedlings determined using chlorophyll fluorescence imaging. WT plants and transgenic plants of GAPA and GAPB antisense lines were grown in controlled environment conditions with a light intensity 130 µmol m^{-2} s^{-1} , 8-h light/16-h dark cycle for 15 days. **(A)** Chlorophyll fluorescence imaging used to determine *Fq'/Fm'* (maximum PSII operating efficiency) at the low level of light at an irradiance of 200 µmol m^{-2} s^{-1} . **(B)** Chlorophyll fluorescence imaging used to determine *Fq'/Fm'* (maximum PSII operating efficiency) at the high level of light at an irradiance of 600 µmol m^{-2} s^{-1} . Error bars represent SE n=8 replicates. Stars showed

the significant transgenic lines compare to WT control (P<0.05) one-way ANOVA, post-hoc test).

4.2.13 Chlorophyll fluorescence imaging of T-DNA insertion and co-suppressed lines of GAPA and GAPB

To investigate the impact of knockout T-DNA insertion mutant of GAPA and GAPB individually and crossed on photosynthesis, plants were grown at in growth chambers at 22 °C under short day (Photoperiod: 8 hours' light / 16 hours' dark), and relative humidity (RD) 50% and the quantum efficiency of PSII photochemistry (*Fq'/Fm'*) investigated using chlorophyll a fluorescence imaging (Baker, 2008; Murchie and Lawson, 2013) to determine for GAPA-1 line (164), GAPB line (308), two co-suppressed lines of GAPA (B11-1 & B114-1) and two crossed line (GA-164/GB-308-1 and GA-164/GB-308-4) compared WT plants. At the low level of light two co-suppressed lines of GAPA (B11-1 and B114-1) and crossed line (GA-164/GB-308-4) showed decreased in the average levels of *Fq'/Fm'* at an irradiance of 200 µmol m^{-2} s^{-1} compared to WT plants. However, GAPA-1 line (164), GAPB line (308) and crossed line (GA-164/GB-308-1) presented no significant difference compared to WT plants (Figure 4.21A). Furthermore, at the high level of light GAPA-1 line (164), GAPB line (308), two co-suppressed lines of GAPA (B11-1 and B114-1) and two crossed line (GA-164/GB-308-1 and GA-164/GB-308-4) indicated no significant difference *Fq'/Fm'* at an irradiance of 600 µmol m^{-2} s^{-1} compared to WT plants (Figure 4.21B).

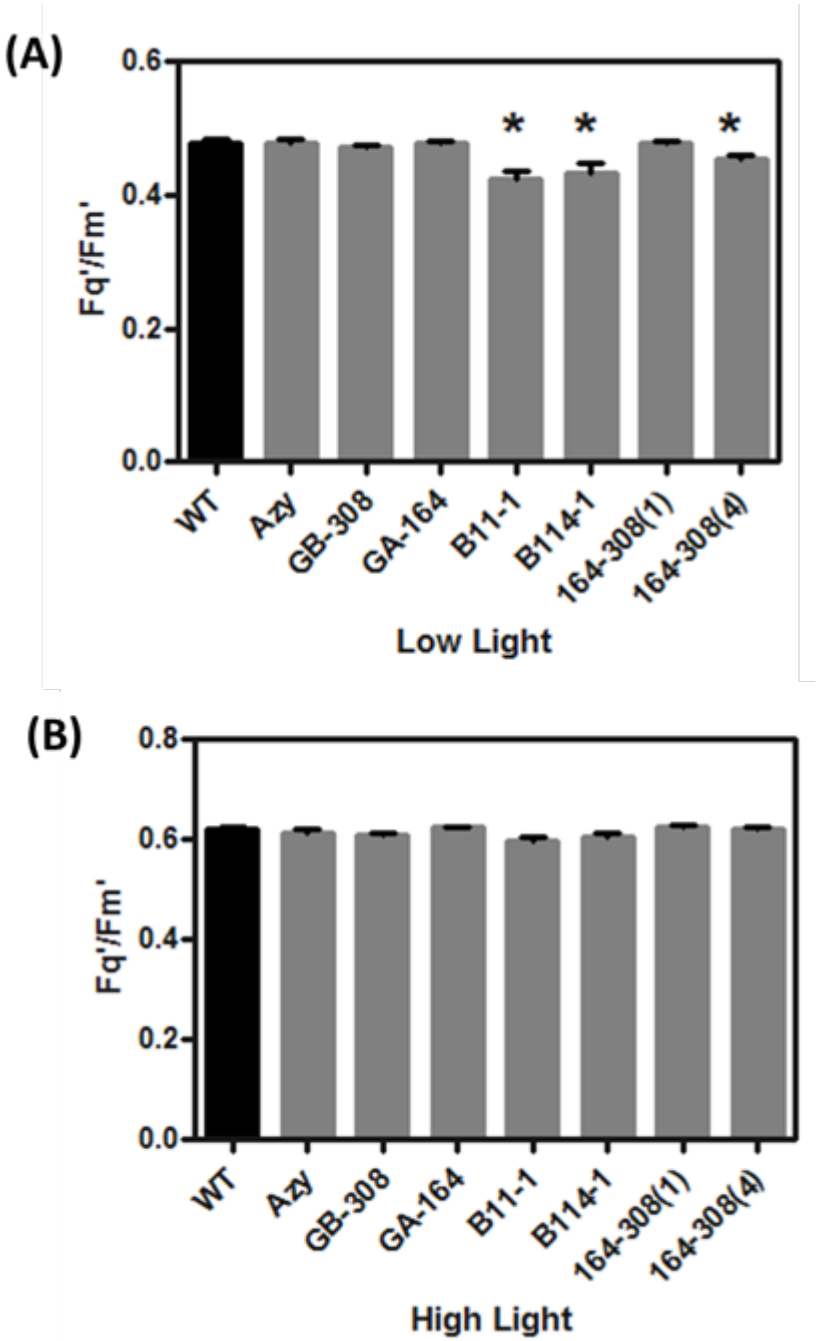

Figure 4.21: Photosynthetic capacity in transgenic seedlings determined using chlorophyll fluorescence imaging. WT plants and transgenic plants of GAPA and GAPB T-DNA insertion lines independent and crossed were grown in controlled environment conditions with a light intensity 130 µmol m^{-2} s^{-1} , 8-h light/16-h dark cycle for 15 days. **(A)** Chlorophyll fluorescence imaging used to determine *Fq'/Fm'* (maximum PSII operating efficiency) at the low level of light at an irradiance of 200 µmol m^{-2} s^{-1} . **(B)** Chlorophyll

fluorescence imaging used to determine *Fq'/Fm'* (maximum PSII operating efficiency) at the high level of light at an irradiance of 600 μmol m^{-2} s^{-1} . Error bars represent SE n=8 replicates. Stars showed the significant transgenic lines compare to WT control (P<0.05) one-way ANOVA, post-hoc test).

4.2.14 *A/Ci* photosynthetic gas exchange measurement of antisense lines GAPA and GAPB T2 lines

To investigate the effect of the reduced level of GAPA and GAPB protein on leaf photosynthetic rate, the response of light-saturated photosynthesis to increasing CO_2 concentrations (*A/Ci* curve) was determined for the three T2 lines of transgenic GAPA and four T2 antisense lines of transgenic GAPB compared to the WT plants. Plants were grown in growth chambers at 22 °C under short day (Photoperiod: 8 hours' light / 16 hours' dark), and relative humidity (RD) 50%. The gas exchange measurements were done on fully mature leaves after six weeks of germination. The results presented that a clear decreased on photosynthetic CO_2 assimilation was observed in three antisense lines of GAPA (GA-7, GA-13 and GA-15) (Figure 4.22). On the other hand, GAPB antisense line GB-13 indicated a significant decrease in photosynthesis compared to WT plants, however (GB-9, GB-10 and GB-12) were showed a reduced on photosynthetic CO_2 assimilation, but not significant (Figure 4.22). The maximum carboxylation rate (Vc_{max}) and maximum electron transport flow (J_{max}), and the C3 photosynthesis model (Farquhar et al., 1980) were fitted to the *A/Ci* data using a spreadsheet provided by (Sharkey et al., 2007). The result for GAPA antisense lines showed a significant decreased for line GA-13, however, line GA-7, and GA-15 indicated slightly reduction in Vc_{max}, but not significant compared to WT plants. Moreover, the result for GAPB antisense lines showed an only significant reduction in Vc_{max} for line GB-13, but line GB-9, GB-10 and GB-12 indicated

slightly decreased, but not significant compared to WT (Figure 4.23).Furthermore, the result of J_{max} indicated line GA-7 and GA-13 decreased slightly, the level of J_{max} compared to WT, however not significant (Figure 4.24). Additionally, the result of J_{max} showed line GB-13 decreased significantly compared to WT, however, line GB-10, and GB-12 indicated small reduction but not significant compared to WT. Also, GB-9 showed no difference compared to WT (Figure 4.24).

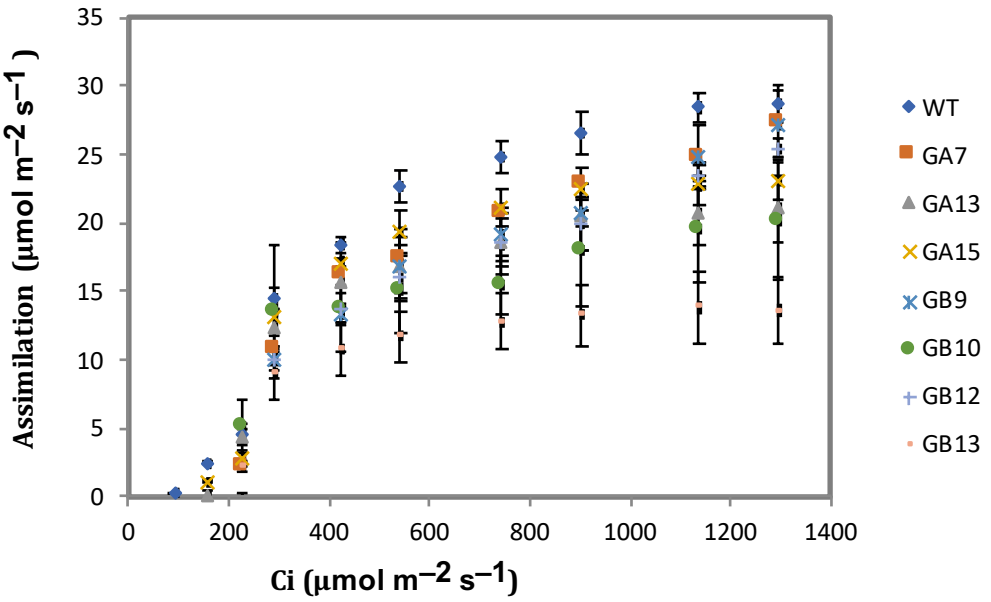

Figure 4.22: Photosynthetic CO_2 assimilation response to different internal concentrations of CO_2 (Ci) (A/Ci curve) of three antisense lines of GAPA (GA-7, GA-13 and GA-15) and four lines of GAPB (GB-9, GB-10, GB-12 and GB-13) compared to the WT plants. Plants were grown in growth chambers at 22°C under short day (Photoperiod: 8 hours' light / 16 hours' dark), and relative humidity (RD) 50%, saturating photosynthetic photon flux density (PPFD) of 1000 µmol m^{-2} s^{-1} for the duration of the *A/C*i response curve using a CIRAS-1 portable gas exchange system. Values represent three plants from three independent lines compared to the WT line.

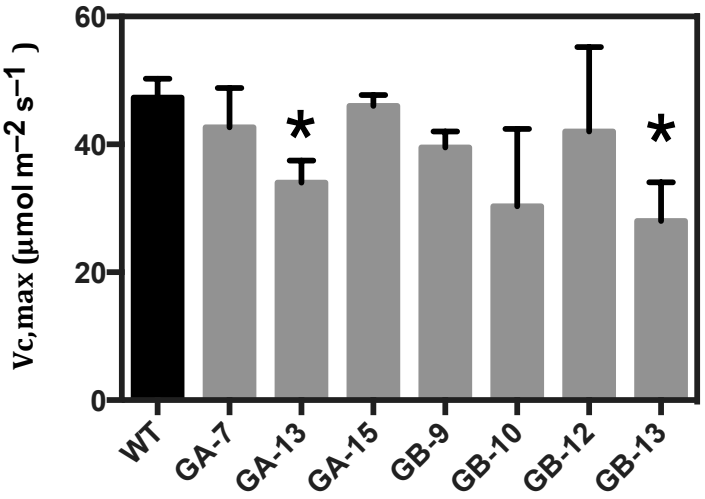

Figure 4.23: The maximum carboxylation rate (Vc_{max}) from (A/Ci curve) for the line (GA-7, GA-13, and GA-15) and GAPB antisense lines (GB-9, GB-10, GB-12 and GB-13) compared to WT. Values represent the average of three plants from each individual transgenic line compared to WT line. Stars showed the significant transgenic lines compare to WT control ($P<0.05$) one-way ANOVA, post-hoc test).

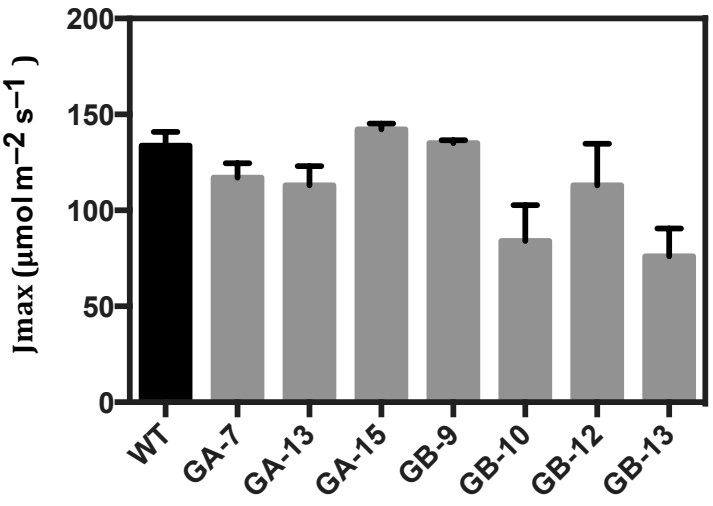

Figure 4.24: The maximum electron transport flow (J_{max}) from (*A/Ci* curve) for GAPA antisense lines (GA-7, GA-13, and GA-15) four independents of GAPB antisense lines (GB-9, GB-10, GB-12 and GB-13) compared to WT. Values represent the average of three plants from each individual transgenic line compared to WT line. Stars showed the significant transgenic lines compare to WT control ($P<0.05$) one-way ANOVA, post-hoc test).

4.2.15 *A/Ci* photosynthetic gas exchange measurement of T-DNA insertion and co-suppressed lines of GAPA and GAPB

To investigate the effect of the knockout T-DNA insertion mutant of GAPA and GAPB individually and crossed, on leaf photosynthetic rate, the response of light-saturated photosynthesis to increasing CO_2 concentrations (*A/Ci* curve) was determined for GAPA-1 line (164), GAPB line (308), two co-suppressed lines of GAPA (B11-1 and B114-1) and two crossed line (GA-164/GB-308-1 and GA-164/GB-308-4) compared to the WT plants. Plants were grown in growth chambers at 22 °C under short day (Photoperiod: 8 hours' light / 16 hours' dark), and relative humidity (RD) 50%. The gas exchange measurements were done on fully mature leaves after six weeks of germination. The results clearly showed that a significant decreased photosynthetic CO_2 assimilation was observed in two co-suppressed lines of GAPA (B11-1 and B114-1), however GAPA-1 line (164), GAPB line (308) and two crossed line (GA-164/GB-308-1 and GA-164/GB-308-4) presented a decreased on photosynthetic CO_2 assimilation, but not a significant compared WT plant. (Figure 4.25). The maximum carboxylation rate (Vc_{max}) and maximum electron transport flow (J_{max}), and the C3 photosynthesis model (Farquhar et al., 1980) were fitted to the *A/Ci* data using a spreadsheet provided by (Sharkey et al., 2007). The results of Vc_{max} showed two co-suppressed lines of GAPA (B11-1 and B114-1) a decreased significantly compared to WT, however GAPA-1 line (164), GAPB line (308) and two crossed line (GA-164/GB-308-1 and GA-164/GB-308-4) indicated a decreased in Vc_{max}, but not significant compared to WT (Figure 4.26). Furthermore, the result of J_{max} showed again only two co-suppressed lines of GAPA (B11-1 and B114-1) decreased significantly compared to WT, but GAPA-1 line (164), GAPB line (308), and two crossed line (GA-164/GB-308-1 and GA-164/GB-308-4) indicated a reduction, however not significant compared to WT (Figure 4.27).

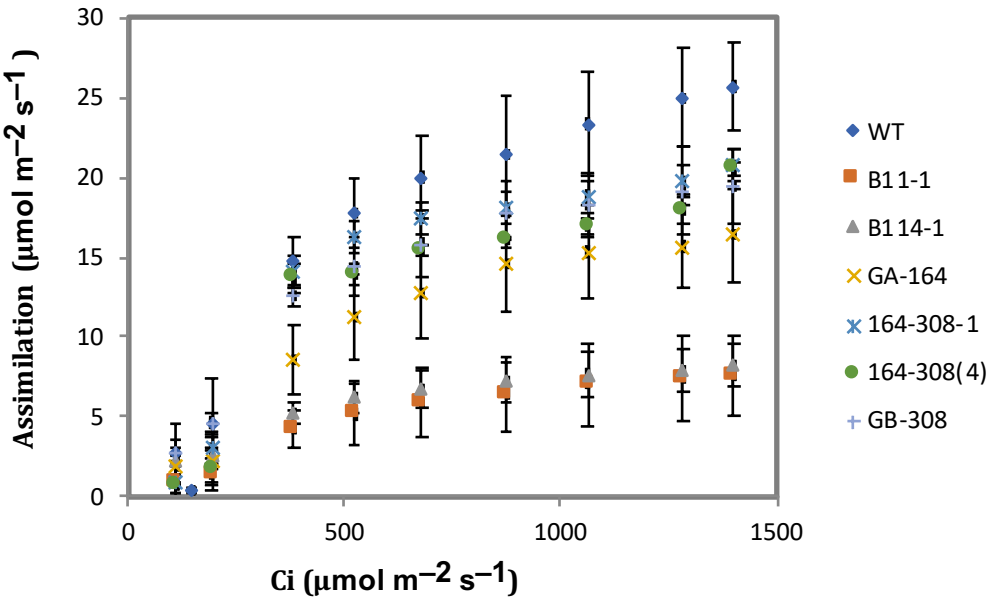

Figure 4.25: Photosynthetic CO_2 assimilation response to different internal concentrations of **CO_2** (Ci) (*A/Ci* curve) for GAPA-1 line (164), GAPB line (308), two co-suppressed lines of GAPA (B11-1 and B114-1) and two crossed line (GA-164/GB-308-1 and GA-164/GB-308-4) compared to the WT plants. Plants were grown in growth chambers at 22°C under short day (Photoperiod: 8 hours' light / 16 hours' dark), and relative humidity (RD) 50%, saturating photosynthetic photon flux density (PPFD) of 1000 µmol m^{-2} s^{-1} for the duration of the *A/C*i response curve using a CIRAS-1 portable gas exchange system. Values represent three plants from two independent lines compared to the WT line.

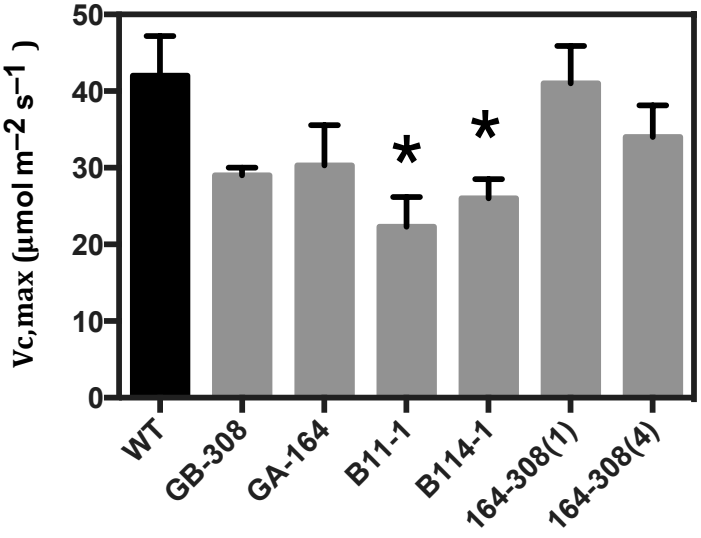

Figure 4.26: The maximum carboxylation rate (Vc_{max}) from (*A/Ci* curve) for line GAPA-1 line (164), GAPB line (308), two co-suppressed lines of GAPA (B11-1 and B114-1), and two crossed line (GA-164/GB-308-1 and GA-164/GB-308-4) compared to WT. Values represent the average of three plants from six individual transgenic lines. Stars showed the significant transgenic lines compare to WT control ($P<0.05$) one-way ANOVA, post-hoc test).

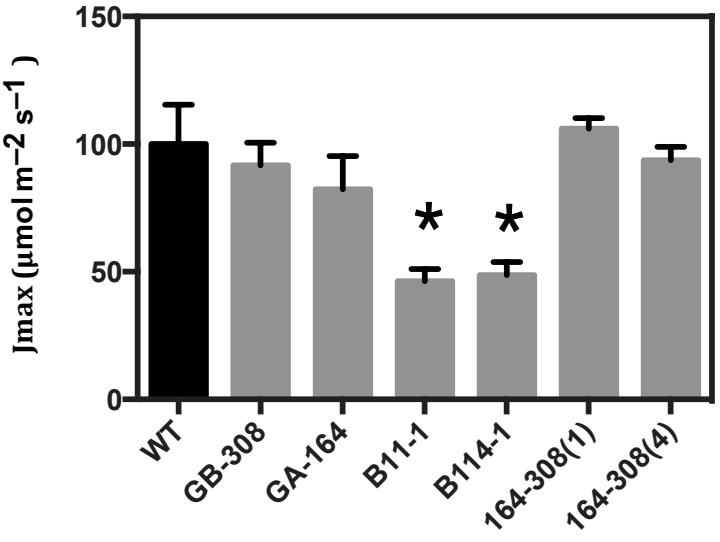

Figure 4.27: The maximum electron transport flow (J_{max}) from (*A/Ci* curve) for line GAPA-1 line (164), GAPB line (308), two co-suppressed lines of GAPA (B11-1 and B114-1), and two crossed line (GA-164/GB-308-1 and GA-164/GB-308-4) compared to WT. Values represent the average of three plants from six individual transgenic lines. Stars showed the significant transgenic lines compare to WT control (P<0.05) one-way ANOVA, post-hoc test).

4.3 Discussion

A multiprotein complex among two of the thioredoxin-regulated enzymes, phosphoribulokinase (PRK) and glyceraldehyde-3-phosphate dehydrogenase (GAPDH), mediated by the small chloroplast protein CP12 (Wedel et al., 1997; Wedel and Soll, 1998; Graciet et al., 2003). This complex has been revealed to be present in several higher plant species (Wedel et al., 1997; Wedel and Soll, 1998; Scheibe et al., 2002; Howard et al., 2011a) and existent in algal type (Avilan et al., 1997; Boggetto et al., 2007; Oesterhelt et al., 2007) and present in a cyanobacterium (Tamoi et al., 2005). Previously studies showed a large amount of reductions in the levels of (GAPDH), (FBPase) and (PRKase) is not restrictive photosynthetic capacity through the Calvin cycle (Price et al., 1995; Paul et al., 1995; Raines, 2006; Stitt and Schulze, 1994; Koßmann et al., 1994). Moreover, antisense study in tobacco plants of PRK and GAPDH have indicated that these enzymes did not have significant impact on growth until the level of PRK gene reduced 15% compared to WT (Paul et al., 1995; Banks et al., 1999) and decreased the level of GAPDH gene 35% compared to WT (Price et al., 1995b). To address the second objective of this thesis and find out why the A2B2 form is found as predominant form in most species of plants studied to date. Some plants have no evident levels of A4, but no plants have yet been found without the A2B2 form (Howard et al., 2011b). The relative importance of these different forms of plastid GAPDH has not been studied and the role of the GAPD (B) subunit in determining photosynthetic capacity in higher plants. As no study antisense plants or overexpression work has been done on GAPDH (B) subunit. Several of transgenic T-DNA insertion single and double mutant of GAPA and GAPB plus two co-suppressed lines of GAPA has been identified by (Dr Simkin) in our lab. Moreover, antisense plants with decreased GAPA and GAPB protein expression gene were produced, by transformation with an Arabidopsis antisense construct using PGWB2

vector. The main findings in this chapter showed the growth analysis of T2 antisense lines for both GAPA and GAPB were variable and had some inconsistencies and no significant difference compared to WT plants. By contrast, the rosette growth analysis for GAPB (308) and GAPA (164) were showed variable and inconsistent and no significant difference compared to WT plants. However, two co-suppressed lines of GAPA and two crossed lines of GAPA with GAPB were affected significantly compared to WT. Furthermore, the number of leaves and rosette dry weight (biomass) in all transgenic single and crossed lines were impacted significantly compared to WT therefore, suggesting that these genes possible play vital roles in growth and development stage for Arabidopsis plants. Moreover, all transgenic lines for both genes GAPA and GAPB indicated a clear reduction in the photosynthetic **CO_2** assimilation compared to WT plants. Although additional work is needed as these results were only significant statistically for one antisense line of GAPB antisense line (13) and two co-suppressed lines of GAPA, however, this result has revealed the potential importance of the GAPB subunit in determining the photosynthetic capcity in higher plants.

Chapter 5: Effect of decreased GAPB using Antisense technology on Tobacco photosynthesis

5.1 Introduction

The Calvin–Benson cycle is the key pathway of carbon fixation it is located in the chloroplast stroma. Furthermore, this cycle plays a vital role in the metabolism of plants, as well as in carbon flux (Geiger and Servaites, 1994). The GAPDH holoenzyme is homotetramer produce of A form subunits, and it has been indicated that CP12 binding to this form of GAPDH confers redox regulation, facilitated directly by thioredoxins (Graciet et al., 2003c). There is a B form of the GAPDH subunit which forms a functional heterotetramer (A2B2) with the A subunit in higher plants. The B subunit of GAPDH found in higher plants is supposed to have due to a gene duplication of the GAPA gene and subsequent fusion with the C-terminus of CP12 (Pohlmeyer et al., 1996; Petersen et al., 2006). This C-terminal extension includes two cysteine residues and has been existing to confer Trx-mediated redox regulation on the GAPDH A2B2 enzyme (Sparla et al., 2002). The CP12 has been recognised as an element of a complex having the A2B2 heterotetramer (Carmo-Silva et al., 2011). Moreover higher plants species with no evident A4 homotetramer have been presented to form a PRK/GAPDH/CP12 complex *in vivo* (Wedel et al., 1997; Scheibe et al., 2002; Howard et al., 2008; Carmo-Silva et al., 2011).

Previously indicated a high quantity of decrease of GAPA was essential to impact growth in GAPDH antisense plants (Price et al., 1995b). The recent study by Howard et al. (2011b) showed that the relative amount for A4 and A2B2 varies among species; however, A2B2 form is almost always predominant. Some plants identified previously without A4, but no plants recognised without A2B2. Up to date, no study showed the role of GAPB to determine the photosynthesis capacity in higher plants.

In this study, GAPB tobacco antisense lines were produced previously in our lab to study the vital role of GAPB subunit (GAPDH) enzyme in determining the rate of photosynthetic carbon assimilation. Furthermore, Evaluate the GAPB in determine the rate of photosynthesis in antisense lines of GAPB tobacco plants.

The aim of this chapter was to

1. Undertake molecular analysis using qPCR and immunoblot analysis to identify the tobacco antisense lines with reduced GAPB protein levels compared to WT plants.

2. Undertake a preliminary physiological study of the transgenic GAPB antisense plants to evaluate the photosynthetic capacity by used chlorophyll fluorescence imaging, and the gas exchange analysis.

5.2 Results

5.2.1 Gene expression analysis of GAPB Tobacco Antisense plants using qPCR

To examine the transcript level (gene expression) in the transgenic T2 GAPB antisense plants of tobacco, the GAPB cDNA of the different plants within three independent lines (GB-6, GB-7 and GB-9) were amplified using qPCR. The results showed that the average relative expression levels were decreased the expression level of GAPB significantly in line GB-6 and line GB-9 compared to WT line. By contrast, GB-7 indicated no significant difference compared to the WT line. The average plants in this qPCR were six plants per line (Figure 5.1) and gene expression in individual GAPB plants (Figure 5.2A, 5.2B and 5.2C).

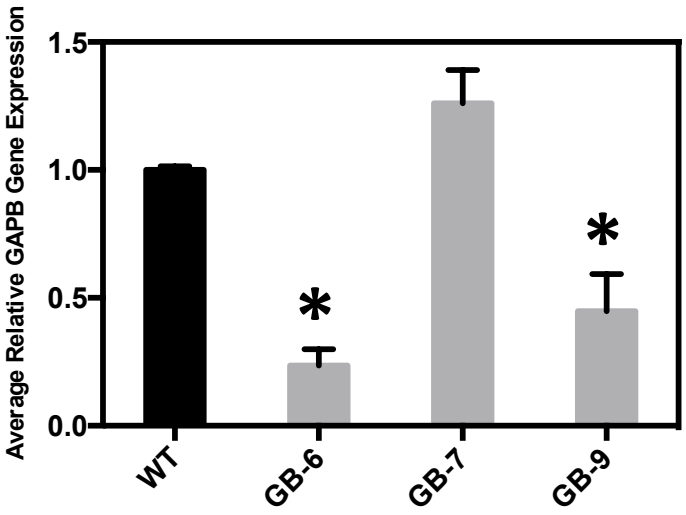

Figure 5.1: Determination the level of GAPB gene expression in transgenic T2 Tobacco plants

The RNA was extracted from the mature seedling stage (4 weeks) from T2 plants. GAPB antisense construct was amplified using specific primers (chapter 2). The expression was normalised against actin reference gene. GAPB gene expression in individual GAPB antisense plants into three independent lines (GB-6, GB-7 and GB-9) compared to WT line. Values represent the average of six plants from three different transgenic lines compared to WT line. Stars indicated significant differences from WT ($P<0.05$) one-way ANOVA, post-hoc test).

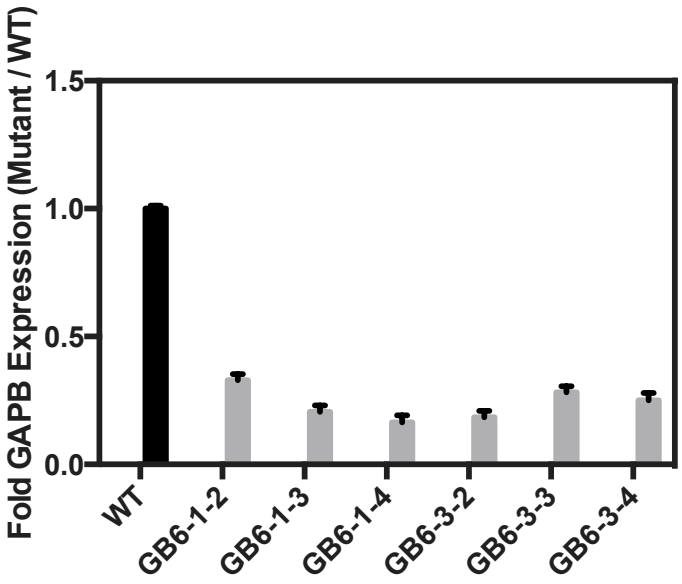

Figure 5.2A: Determination the level of GAPB gene expression in transgenic T2 Tobacco individual plants line GB-6. The RNA was extracted from the mature seedling stage (4 weeks) from T2 plants. GAPB antisense construct was amplified using specific primers (chapter 2). The expression was normalised against actin reference gene.

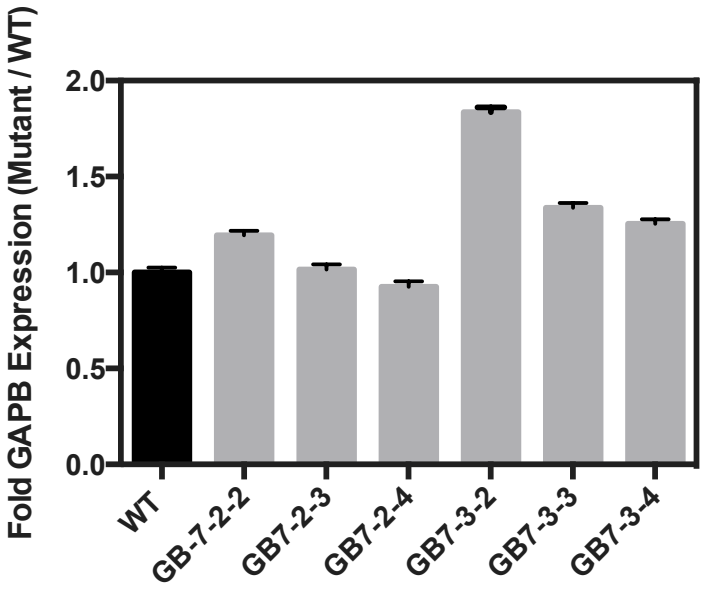

Figure 5.2B: Determination the level of GAPB gene expression in transgenic T2 Tobacco individual plants line GB-7. The RNA was extracted from the mature seedling stage (4 weeks) from T2 plants. GAPB antisense construct was amplified using specific primers (chapter 2). The expression was normalised against actin reference gene.

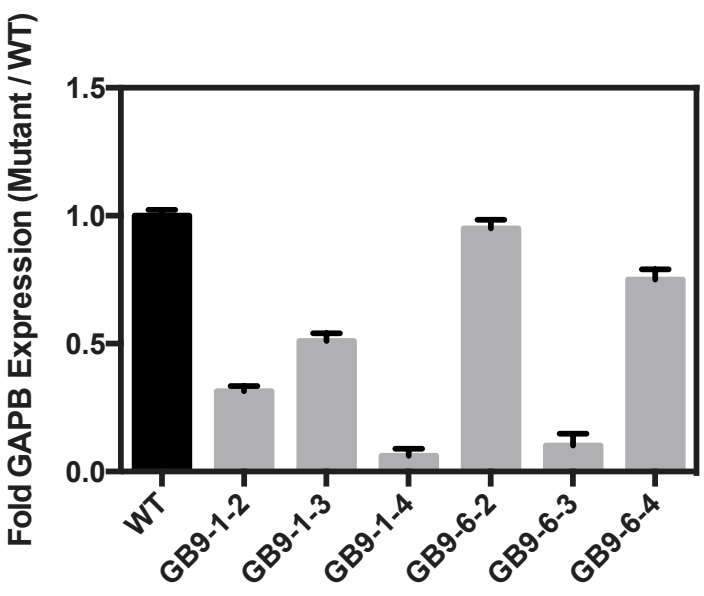

Figure 5.2C: Determination the level of GAPB gene expression in transgenic T2 Tobacco individual plants line GB-9 The RNA was extracted from the mature seedling stage (4 weeks) from T2 plants. GAPB antisense construct was amplified using specific primers (chapter 2). The expression was normalised against actin reference gene.

5.2.2 Protein expression analysis (Western Blot) of GAPB in transgenic Antisense tobacco plants

To investigate whether protein expression is decreased on the tobacco GAPB antisense lines, the protein was extracted from leaf discs was harvested from six plants of three independent lines of GAPB (GB-6, GB-7 and GB-9) and the WT control. Western blot analyses clearly showed that the six plants of line GB-6 (GB-6-1-2, GB-6-1-3, GB-6-1-4, GB-6-3-2, GB-6-3-3, and GB-6-4) were decreased the protein level of GAPB protein compared to WT plants (Figure 5.3). Moreover, four plants for line GB-9 (GB-9-1-2, GB-9-1-4, GB-9-6-2, and GB-9-6-4) were revealed that reduced the protein level of GAPB protein compared to WT plants (Figure 5.3). On the other hand, line, GB-7 indicated a reduction in both genes of GAPA and GAPB protein for some plants (GB-7-2-2, GB-7-2-4, GB-7-3-2 and GB-7-3-3) compared to WT plants.

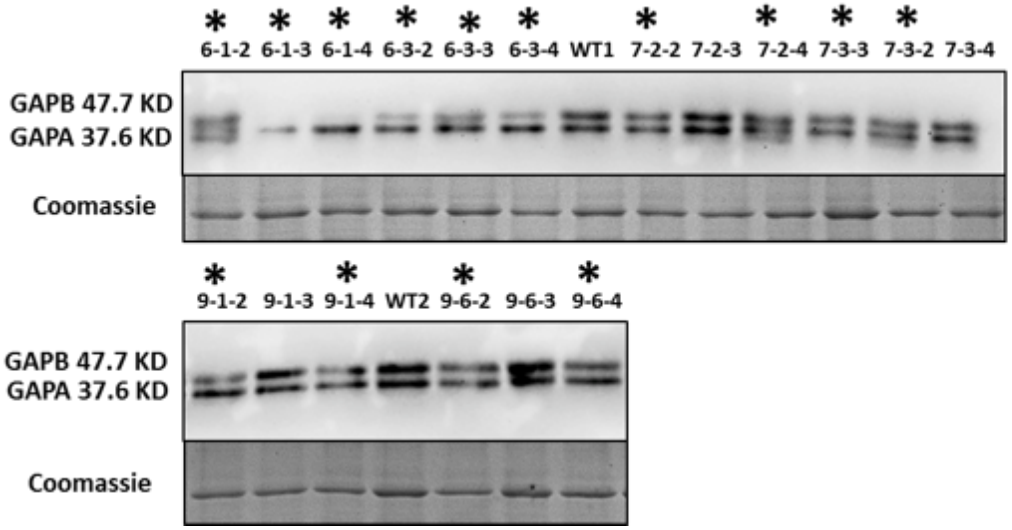

Figure 5.3: Immunoblot analyses of transgenic GAPB antisense tobacco plants. **(A)** A total extractable leaf tissue protein of individual transgenic plants six plants per three independent lines of GAPB (GB-6, GB-7 and GB-9) and WT plants were loaded onto 12% polyacrylamide gels and blotted to PVDF membrane. Antibody raised against GAPDH protein was used to identify GAPB. **(B)** Coomassie stain which showed the loading of protein. Values represent the average of six plants from three individual transgenic lines compared to WT line. Stars indicated clear differences from WT plants.

5.2.4 Chlorophyll fluorescence imaging

Tobacco antisense seeds were grown on soil in controlled environment chambers at an irradiance of 130 µmol photons m^{-2} s^{-1}, 22 °C, relative humidity of 60%, in a 12 hours photoperiod. Then, plants were transferred to individual 8 cm pots and grown for two weeks at 130 µmol photons m^{-2} s^{-1}, 22 °C, relative humidity of 60%, in a 12 hours photoperiod. Plants were transferred to larger pots (17cm across and 23cm deep). Three days earlier to chlorophyll fluorescence imaging, plants were transferred to the greenhouse and grown in natural irradiance with supplementary light to maintain the levels between 400–600 µmol m^{-2} s^{-1} PPFD at bench level. To screen for potential changes in photosynthesis in 14-d-old seedlings of GAPB antisense lines, chlorophyll *a* fluorescence imaging was used to investigate the quantum efficiency of PSII photochemistry (*F*q′/*F*m′) (Baker, 2008; Murchie and Lawson, 2013). Either at low light level with *F*q′/*F*m′ at an irradiance of 400 µmol m^{-2} s^{-1} and high light level with *F*q′/*F*m′ at an irradiance of 800 µmol m^{-2} s^{-1} eight replicates plants from three independent lines of GAPB antisense lines (GB-6, GB-7 and GB-9) showed no significant reduction in photosynthesis compared (Figure 5.4A and 5.4B).

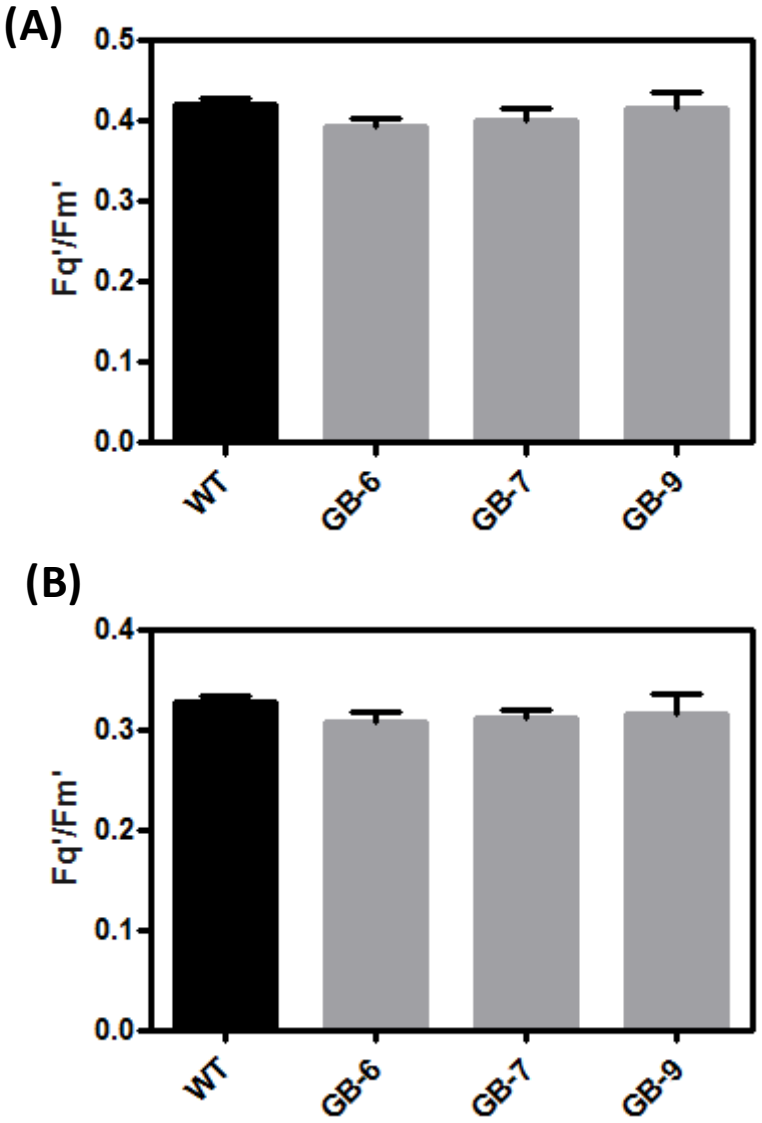

Figure 5.4: photosynthetic efficiency in young seedlings. Determination of photosynthetic efficiency in wild-type (WT), GB-6, GB-7 and GB-9 seedlings using chlorophyll fluorescence imaging. WT and mutant plants were grown in controlled environment conditions with a light intensity of 130 µmol m^{-2} s^{-1} ; *Fq′ /Fm'* (maximum PSII operating efficiency). **(A)** Chlorophyll fluorescence imaging used to determine Fq'/Fm' (maximum PSII operating efficiency) at the high level of light at an irradiance of 800 µmol m^{-2} s^{-1} . **(B)** Chlorophyll fluorescence imaging used to determine *Fq'/Fm'* (maximum PSII

operating efficiency) at the low level of light at an irradiance of 400 μmol m^{-2} s^{-1} . Values represent the average of eight plants from three individual transgenic lines compared to WT line. Stars showed significant differences from WT ($P<0.05$) one-way ANOVA, post-hoc test).

5.2.5 *A/Ci* photosynthetic gas exchange measurement of GAPB antisense lines

To investigate the effect of the reduced level of GAPB protein on leaf photosynthetic rate, the response of light-saturated photosynthesis to increasing **CO_2** concentrations (*A/Ci* curve) was determined for the six plants from three independent lines of GAPB antisense lines (GB-6, GB-7 and GB-9). Six plants per lines were transferred into large pots and grown for a further four weeks in the greenhouse, in natural light with supplementation providing light levels changing between 600–1400 μmol m^{-2} s^{-1} . The rate of **CO_2** assimilation (*A*) was determined as a function of internal **CO_2** concentration (*C*i) in newest fully expanded leaf. The results presented that a lower photosynthetic **CO_2** assimilation was observed in three independent lines of GAPB (GB-6, GB-7 and GB-9) but not significant statistically compared to WT plants (Figure 5.4). The maximum carboxylation rate (V_{cmax}) and maximum electron transport flow (J_{max}), and the C3 photosynthesis model (Farquhar et al., 1980) were fitted to the *A/Ci* data using a spreadsheet provided by (Sharkey et al., 2007). The result of V_{cmax} for line GB-6 and GB-7 showed significant reduction statistically compared to WT plants. However, line GB-9 indicated reduction, but not significant statistically by ANOVA compared to WT plants (Figure 5.5). The result of J_{max} for line GB-6, GB-7 and GB-9 showed decreased in J_{max}, but not significant statistically compared to WT plants (Figure and Table 5.6).

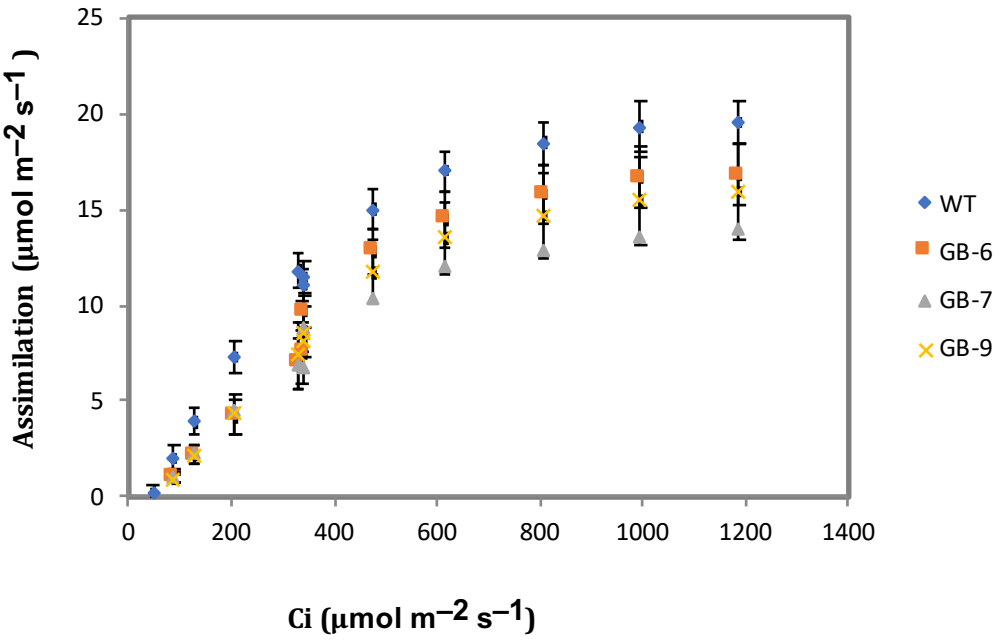

Figure 5.4: Photosynthetic CO_2 assimilation (A) response to different internal Concentrations of CO_2 (Ci) (*A/Ci* curve) of two independents of GAPB antisense lines GB-6, GB-7 and GB-9 compared to the WT line.

Plants were transferred into large pots and grown for a further four weeks in the greenhouse, in natural light with supplementation providing light levels changing between 600–1400 µmol m^{-2} s^{-1} . Gas exchange measurements were performed on young fully expanded leaves with a light-saturated level of 1500 µmol m^{-2} s^{-1} using an open infrared gas exchange system. Values represent six plants compared to the WT line.

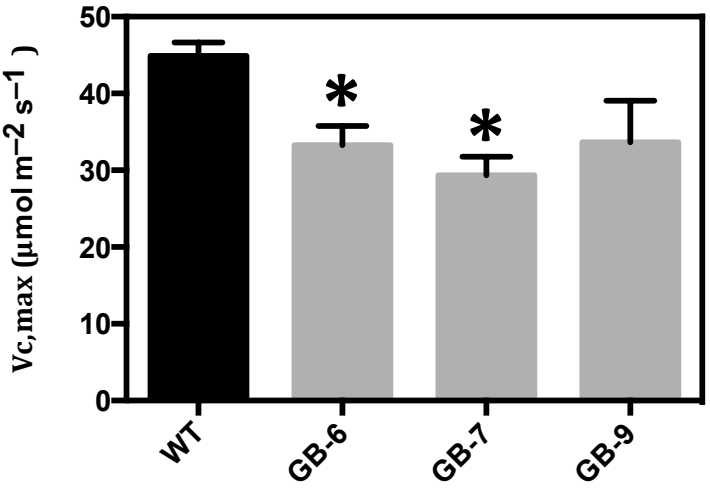

Figure 5.5: The maximum carboxylation rate (Vc_{max}) of three independents of GAPB antisense lines (GB-6, GB-7 and GB-9) compared to the WT line. Values represent the average of six plants from three individual transgenic lines compared to WT line. Stars showed significant differences from WT ($P<0.05$) one-way ANOVA, post-hoc test).

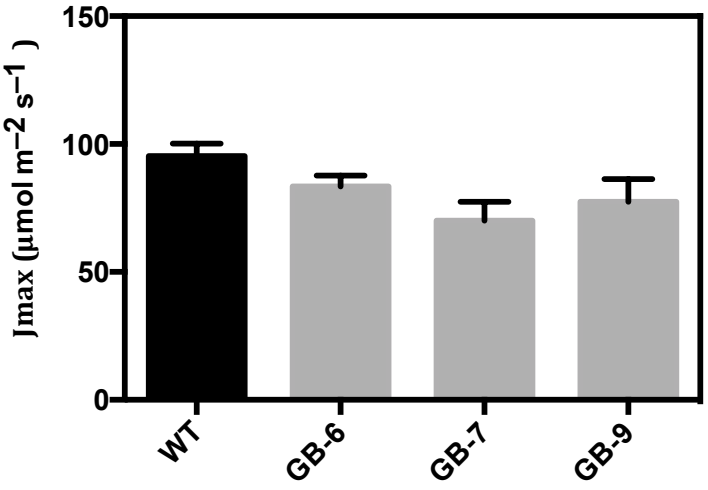

Figure 5.6: The maximum electron transport flow (J_{max}) from (*A/Ci* curve) of three independents of GAPB antisense lines (GB-6, GB-7 and GB-9) compared to the WT line. Values represent the average of six plants from three individual transgenic lines compared to WT line. one-way ANOVA, post-hoc test).

5.3 Discussion

There is evidence a role for CP12 in the formation of a multiprotein complex including the enzymes PRK and GAPDH (Wedel et al., 1997; Wedel and Soll, 1998; Scheibe et al., 2002; Graciet et al., 2003; Marri et al., 2008). The complex association and dissociation are fast and is mediated by alterations in the redox state of thioredoxin f (Howard et al., 2008; Marri et al., 2009). Manipulations with an antisense gene can help as a tool to study the influence of a particular plant gene inactivation. Transgenic plants with an antisense gene already establish a new characteristic, indicating that the technique has a great scientific and business value (Ecker and Davis, 1986).

The previous researches on transgenic tobacco antisense plants for PRK and GAPDH have indicated that small reduction on these enzymes have no severe effect on photosynthesis and growth (Paul et al., 1995; Banks et al., 1999; Price et al., 1995). Recently, a transgenic study in tobacco despite decrease the level of CP12 protein above than 90%, the photosynthetic, PRK and GAPDH activities did not impact. This suggestion is non-existent of the PRK/GAPDH/ CP12 complex in darkened tobacco leaves (Howard et al., 2011b; Howard et al., 2011a). Furthermore, antisense CP12 plants tobacco plants showed a variety of abnormal phenotypes, comprising changed leaf morphology, reduced apical dominance, and slow development (Howard et al., 2011a).

Up to date, no study showed the role for GAPB subunit of GAPDH enzyme in determining the rate of photosynthesis. In this chapter, transgenic tobacco plants with reduced GAPB gene and protein expressions were identified and confirmed in the T2 generation. The GAPB genes expression was analysed using qPCR to verify whether the gene was still

expressed at the transcript level and using immunoblot (western blot) to determine the protein level of GAPB in the T2 generation. Consequently, the Molecular analysis showed a significant decrease in all transgenic lines of GAPB except line GB-7 showed no significant differences compared to WT. However, line GB-7 showed some plants were reduced the protein level of both GAPA and GAPB which suggestion could be this line decreased the protein level of both GAPA and GAPB in plants. Although, all transgenic tobacco lines showed a clear decreased in the photosynthetic CO_2 assimilation compared to WT plants. The main funding in this chapter has indicated the potential importance of the GAPB subunit in determining photosynthetic capacity in higher plants.

Chapter 6: General Discussion

6.1 Exploitation of transcriptional network modelling (VBSSM) for *RAP2.12* and GAPA-2 under drought

The initial determinant of crop yield is the increasing rate of photosynthesis over the growing season which is the result of the crop's ability to capture light, the efficiency by which this light is transformed to biomass and how much biomass is converted into the usable product, e.g. grain in the case of wheat and rice. Old-style breeding and agronomic approaches have maximised light capture and conversion of biomass to end products, and consequently, to increase yield, the efficiency of energy conversion will have to be improved. In plants that fix atmospheric CO_2 using the Calvin cycle enzyme ribulose-1,5-bisphosphate carboxylase (C3 plants) the theoretical maximum energy conversion efficiency attainable is 4.6%, but in the field efficiencies of less than 50% of this are normal. There is fascinating sign from research using transgenic plants that manipulation of the Calvin cycle can support to closing this gap in efficiency and that this might increase yield in the absence of significant stress (Zhu et al., 2010; Raines, 2011). However, to fully maximise any efficiency gains through the manipulation of this pathway, it will also be essential to develop strategies that will minimise the negative impact of stress responses, such as drought.

Drought stress has a strict effect on plants and affects growth and development. Many studies have concentrated on the impact of drought on plant transcriptomes, predominantly in Arabidopsis (Kreps, 2002; Seki et al., 2002; Kilian et al., 2007; Harb et al., 2010). It is clear that in order design plants with improved photosynthetic performance in drought stress will require sufficient data about the interactions between genes and,

thereby, more complex manipulations of metabolic enzymes within the associated networks of the Calvin cycle. It is not possible to empirically test all of the potential objectives in the various combinations that together may have positive and synergistic effects, as the number of potential mixtures of manipulations that would need to be tested far exceeds the availability of resources and time.

To discover potential targets for manipulation to improve photosynthesis, reverse engineering carried out based on a transcriptional network of the Calvin cycle generated from a microarray time series data was performed (Bechtold et al., 2016). The practical output of this approach is that it can be used to identify highly connected genes (hubs) that are influential in regulating the expression of other genes in the network. VBSSM has been used to identify that effect in phenotypes in knockout insertion mutants exposed to environmental stresses such as drought (Bechtold et al. 2016). In that work, a soil-based gradual drought was applied to Col-0 plants until the relative soil water content (rSWC) reached 20%, and a time-series transcriptomics analysis was performed as explained in chapter 1. VBSSM has also been used to identify novel highly connected genes in Arabidopsis that result in phenotypes in knockout insertion mutants subjected to environmental stresses (Bechtold et al., 2016) (As explained in Chapter 1 with more details of VBSSM Modelling). The outputs from the model suggest that increasing the levels of expression of the GAPA-2 (At1g12900) gene and decreasing the levels of both transcription factors *RAP2.12* (At1g53910) and (At1g16750), will have a positive effect on the expression of a number of Calvin cycle genes in plants grown under drought (orange and yellow circles, Figure 2.1). As described in Chapter 3 single and double mutant lines of RAP.12 and GAPA-2 (Table 3.2) did not show altered growth and development. Previously, inducible expression of *RAP2.12* or *RAP2.3* resulted in plants

with tolerance to osmotic stress, whereas only the double knockout mutant of these genes was delicate to osmotic stress (Papdi et al., 2015). It is consequently possible that *RAP2.12* is functionally dismissed with *RAP2.3*, and maybe *RAP2.2* (Gibbs et al., 2014; Papdi et al., 2015) and could explain why the single knockout of *rap2.12-1* and *rap2.12-2* did not show a drought phenotype.

Furthermore, GAPA-2 OE lines (13, 29) used in this study could have been silenced in plants or were still segregating. Subsequent analysis of expression levels of Calvin cycles genes presents in the network by altering *RAP2.12,* and GAPA-2 indicated the whole drought gene expression and difficult to determine the main result, but we can conclude that the single mutants of *RAP2.12* (*rap2.12-1* and *rap2.12-2*) effect on Calvin cycle gene expression mostly under drought stress conditions, but not necessarily as predicted by the modelling. The drought experiment in this project was a mild drought treatment. It is essential to make the difference between mild drought stress and intense drought stress, because it has been shown that plants respond differently to different stages of drought stress (Skirycz et al., 2011), where the response of a plant to drought depends on the intense and period of the drought and the developmental step of the plants at the time of the drought (Claeys and Inze, 2013). In Chapter 3 it was shown that CP12-1 expression substantially decreased in both single mutant lines of *rap2.12* under drought conditions, and therefore this indicated that *RAP2.12*, might regulate the expression of CP12-1, which plays an essential role in regulating Calvin cycle enzymes.

Moreover, to better understand the role of *RAP2.12* during drought stress the mutant's performance over the whole period of the stress including relative leaf water content (RWC) and water potential rather than relative soil water content (rSWC) should be measured, as plants of different genotype consume soil water at different amounts

(Lawlor 2013; Claeys et al. 2014). This would allow a well comparison of the effect of *RAP2.12* on the drought response. Moreover, operating physiological measurements over the entire dehydration period would be much more useful than single-time point measurements as it would reveal the point during the drought when the gene of interest has an impact on the plant's stress response (Claeys et al., 2014). Using these approaches and changes to phenotyping mutant lines would help to amount possible target genes accurately and be more informative to understanding their role in drought stress response.

6.2 The relative importance of chloroplast GAPDH A and B subunits in determining the rate of photosynthesis

Research using antisense technology has permitted us to investigate the implications that changing the levels of one enzyme can have on complex metabolic pathways such as the Calvin cycle. This part of this thesis has examined the consequences of the reduction in the levels of the GAPA and GAPB proteins on the growth and photosynthesis capacity in Arabidopsis and tobacco plants. The activity of the GAPDH enzyme is regulated by the formation of a multiprotein complex involving PRK, mediated by the chloroplast protein, CP12 (Pohlmeyer et al., 1996; Wedel et al., 1997; Scheibe et al., 2002; Graciet et al., 2004; Marri et al., 2005, 2009; Maberly et al., 2010; Howard et al., 2011a). The formation and breakdown of the PRK/GAPDH/CP12 complex in vivo have been revealed to occur in response to alterations in light availability, modulating the quick deactivation and activation of PRK and GAPDH activity (Howard et al., 2008). CP12 protein shares sequence similarity to the N- terminus of the GAPB (B) subunit of the Calvin Benson cycle protein GAPDH, and it was presented that it was involved in the formation of the multiprotein complex made up of GAPDH, PRK, and CP12 (Pohlmeyer et al., 1996; Wedel et al., 1997; Wedel and Soll, 1998). In addition, the mechanism by which the CP12

protein facilitates the formation and breakdown of the PRK/GAPDH/CP12 complex in vitro both chloroplastic Trx f and m have been revealed to mediate the inactivate of the PRK/GAPDH/CP12 complex, through lowering of the two cysteine pairs on the CP12 protein (Marri et al., 2009). These findings provide proof of a link between the redox state of Trx and that of CP12 in the construction and breakdown of the PRK/GAPDH/CP12 complex. When high levels of reduced Trx are accessible, CP12 will be continued in a reduced state, and slight or no formation of the PRK/GAPDH/CP12 complex will arise. On the contrary when levels of reduced Trx decreases, levels of oxidized CP12 will rise resulting in the creation of the PRK/GAPDH/CP12 (Graciet et al., 2003; Trost et al., 2006; Marri et al., 2008 , 2009 , 2010; Erales et al., 2009 , 2011; Carmo-Silva et al., 2011; Moparthi et al., 2014, 2015).

Transcript analysis of CP12 in Arabidopsis has revealed that expression is not limited to photosynthetic tissue, showing that the role for these proteins is not restricted to the PRK/GAPDH complex (Singh et al., 2008). The study by Howard et al. (2011) used a transgenic method to explore the importance of CP12 in the control of PRK and GAPDH activities and carbon assimilation in vivo. The findings of this study showed that CP12 antisense tobacco plants presented a series of abnormal growth phenotypes, including changed leaf morphology, decreased apical dominance, and slow development. The extent of the alterations experimental in these plants was unexpected given what was known about the role of CP12; however, they show that CP12 is vital for normal plant development. Furthermore, the antisense lines, decreases in CP12 protein content of more than 90% did not influence dark or light activities of PRK and GAPDH.

The recent study by López-Calcagno et al. (2017) indicated that CP12-1 and 12-1/3 show small decreases in PRK protein amount in the order of 50–60% and showed a mild growth phenotype. The CP12-1/2 and CP12-1/2/3 mutants have an additional severe reduction in PRK protein (>75% less than the wild-type) and, though plants have a significant slow growth phenotype, no observable decrease in CO_2 assimilation was sign in the mature leaves. Furthermore, *RNAi* lines, with affected reductions of >80% less that of wild-type levels of PRK, not only develop a severe growth phenotype but also have significant decreases in photosynthetic CO_2 assimilation.

It has been shown that decreases in PRK activity can lead to reductions in photosynthesis and that decreases of >85% of wild-type PRK activity levels lead to significant reductions in photosynthetic amounts, however slighter reductions in PRK do not impact CO_2 assimilation (Paul et al., 1995; Habash et al., 1996). The previous research showed a higher degree of reduction was needed to affect growth and development in plants antisense GAPDH (Price et al., 1995b) plastidic aldolase (Haake et al., 1998) FBPase (Koßmann et al., 1994) PRKase (Paul et al., 1995). Furthermore, Studies on transgenic tobacco antisense with respect to PRK and GAPDH have showed that these enzymes have no severe impact on photosynthesis and growth until levels are reduced 15% of wild-type for PRKase (Paul et al., 1995; Banks et al., 1999) and less 35% in GAPDH antisense plants (Price et al., 1995b). The relative importance of different forms of plastid GAPDH A2B2 has not been studied for GAPB subunit in determining photosynthetic capacity in higher plants. The second objective in this project was to gain a better understanding of the relative importance of GAPDH in regulating photosynthetic carbon assimilation in higher plants a range of transgenic Arabidopsis and Tobacco lines with reduction of GAPB and GAPA were analysed as described in chapter 4 and chapter 5.

In chapter 4 the results presented in this thesis clearly showed a slow growth phenotype in *A. thaliana* under normal growth conditions in transgenic Arabidopsis plants. Double mutant lines GAPA with GAPB and two co-suppressed lines indicated significant impact; however other lines especially GAPB showed inconsistency and no significant effect was observed. Furthermore, all transgenic Arabidopsis plants had a small number of leaves and less weight dry rosette significantly compared to the WT line. Our preliminary results suggest that both GAPA and GAPB are essential for normal growth and development in Arabidopsis plants. In addition, the result of gas exchange photosynthesis carried out in this study has shown a clear reduction in the photosynthetic CO_2 assimilation for all transgenic lines of Arabidopsis which has revealed the potential importance of the GAPB subunit in determining photosynthetic capacity, although further work is needed as these results were only significant statistically for one antisense line of GAPB antisense line (13) and two co-suppressed lines of GAPA.

Previously taking an antisense approach in tobacco, it was shown that although decreases of over 90% in CP12 protein levels, photosynthetic carbon fixation and PRK and GAPDH activities were mainly unaffected. This was steady with the apparent absence of the PRK/GAPDH/ CP12 complex in darkened tobacco leaves (Howard et al., 2011b; Howard et al., 2011a) and indicated that CP12 does not have a principal role in controlling PRK and GAPDH activity in tobacco (Howard et al., 2011a). In chapter 5 the result of gas exchange photosynthesis carried out in this study has revealed that clear reductions in the photosynthetic CO_2 assimilation for all transgenic lines of GAPB antisense tobacco plants which shows may the importance of the GAPB subunit in determining photosynthetic capacity.

Moreover, some studies indicated that CP12 could act as a companion for GAPDH inhibiting heat-induced aggregation and deactivation in vitro and protect from oxidative stress in vivo to both GAPDH and PRK (Erales et al., 2009; Marri et al., 2014). Transgenic plants in this study were grown growth under normal condition; it would be great opportunity to expose these plants under stress condition for further analysis for the role of GAPB subunit under stress condition for example under drought. Recently the study by Zeng et al. (2016) showed the expression pattern profiles of GAPDH family Arabidopsis and was produced with microarray data and exposed to a range of stress treatment. Under cold treatments in Arabidopsis GAPAs indicated slightly increased expression at an early stage in the shoot but were strongly rise in roots. GAPB were very transcribed in both shoots and roots. Exposed to heat stress, transcriptions of GAPAs were reduced in both shoots and roots with an exception for GAPB was slightly increase in shoots. Throughout drought treatment, GAPAs showed down-regulated expression in shoots and unstable expression in roots, while GAPB was increase at first and decrease regulated later in shoots. At root, GAPB was irregularly rise and down-regulated. Finally, under salt stress, both GAPAs and GAPB were up-regulated over the exposure period as the processing time rising. Furthermore, Arabidopsis GAPDHs (GAPAs, and GAPB) expression profiles under osmotic stress similar to that under salt treatment (Zeng et al., 2016).

6.3 Summary

- Single and double mutant lines of *RAP2.12* with GAPA-2 did not affect the growth and phenotype of plants.
- *RAP2.12* impacted most Calvin cycle gene expression predominately under drought stress condition.
- Reduced the protein level of GAPA and GAPB in Arabidopsis plants affected the rosette area for co-suppressed lines of GAPA and crossed lines between GA-164/GB-308, but other transgenic lines did not show impact. Furthermore, all transgenic lines of GAPA and GAPB had a small number of leaf and affected the dry rosette weight which has revealed the potential importance of the GAPA and GAPB proteins for normal growth in higher plants.
- Reduced the protein level of GAPA and GAPB in Arabidopsis plant showed a decrease in the photosynthetic CO_2 assimilation, which has shown the potential importance of the GAPB subunit in determining the photosynthetic rate.
- Decreased the protein level of GAPB in tobacco plant showed a clear reduction in the photosynthetic CO_2 assimilation, which has shown the potential importance of the GAPB subunit in determining the photosynthetic rate.

Reference List

Abdeen, A., Schnell, J. and Miki, B. (2010) Transcriptome analysis reveals absence of unintended effects in drought-tolerant transgenic plants overexpressing the transcription factor ABF3. *BMC Genomics*. doi:10.1186/1471-2164-11-69.

Aguirrezabal, L., Bouchier-Combaud, S., Radziejwoski, A., et al. (2006) Plasticity to soil water deficit in Arabidopsis thaliana: Dissection of leaf development into underlying growth dynamic and cellular variables reveals invisible phenotypes. *Plant, Cell and Environment*. doi:10.1111/j.1365-3040.2006.01595.x.

Anderson, L.E., Ringenberg, M.R. and Carol, A.A. (2004) Cytosolic glyceraldehyde-3-P dehydrogenase and the B subunit of the chloroplast enzyme are present in the pea leaf nucleus. *Protoplasma*. doi:10.1007/s00709-003-0030-6.

Andre, C., Froehlich, J.E., Moll, M.R., et al. (2007) A Heteromeric Plastidic Pyruvate Kinase Complex Involved in Seed Oil Biosynthesis in *Arabidopsis. The Plant Cell*. doi:10.1105/tpc.106.048629.

Aronsson, H. and Jarvis, P. (2002) A simple method for isolating import-competent Arabidopsis chloroplasts. *FEBS Letters*. doi:10.1016/S0014-5793(02)03342-2.

Avilan, L., Gontero, B., Lebreton, S., et al. (1997) Memory and imprinting effects in multienzyme complexes I. Isolation, dissociation, and reassociation of a phosphoribulokinase-glyceraldehyde-3-phosphate dehydrogenase complex from Chlamydomonas reinhardtii chloroplasts. *European Journal of Biochemistry*. doi:10.1111/j.1432-1033.1997.00078.x.

Baalmann, E., Scheibe, R., Cerff, R., et al. (1996a) Functional studies of chloroplast glyceraldehyde-3-phosphate dehydrogenase subunits A and B expressed in Escherichia coli: formation of highly active A4 and B4 homotetramers and evidence that aggregation of the B4 complex is mediated by the B subunit

carb. *Plant molecular biology*, 32 (3): 505–13. Available at: http://www.ncbi.nlm.nih.gov/pubmed/8980499.

Baalmann, E., Scheibe, R., Cerff, R., et al. (1996b) Functional studies of chloroplast glyceraldehyde-3-phosphate dehydrogenase subunits A and B expressed in Escherichia coli: Formation of highly active A4and B4homotetramers and evidence that aggregation of the B4complex is mediated by the B subunit carboxy. *Plant Molecular Biology*. doi:10.1007/BF00019102.

Baerenfaller, K., Massonnet, C., Walsh, S., et al. (2012) Systems-based analysis of Arabidopsis leaf growth reveals adaptation to water deficit. *Molecular Systems Biology*. doi:10.1038/msb.2012.39.

Baker, N.R. (2008) Chlorophyll Fluorescence: A Probe of Photosynthesis In Vivo. *Annual Review of Plant Biology*. doi:10.1146/annurev.arplant.59.032607.092759.

Baker, N.R. and Rosenqvist, E. (2004) Applications of chlorophyll fluorescence can improve crop production strategies: An examination of future possibilities. *Journal of Experimental Botany*. doi:10.1093/jxb/erh196.

Banks, F.M., Driscoll, S.P., Parry, M.A., et al. (1999) Decrease in phosphoribulokinase activity by antisense RNA in transgenic tobacco. Relationship between photosynthesis, growth, and allocation at different nitrogen levels. *Plant Physiol*. doi:10.1104/pp.119.3.1125.

Bansal, M., Belcastro, V., Ambesi-Impiombato, A., et al. (2007) How to infer gene networks from expression profiles. *Molecular Systems Biology*.

Barbagallo, R.P., Barbagallo, R.P., Oxborough, K., et al. (2003) Rapid Noninvasive Screening for Perturbations of Metabolism and Plant Growth Using Chlotophyll Fluorescence Imaging. *Plant Physiology*. doi:10.1104/pp.102.018093.parallel.

Bassham, J., Benson, A., Calvin, M., et al. (1950) The path of carbon in photosynthesis. VIII. The role of malic acid. *Journal of Biological Chemistry*. doi:10.1101/SQB.1948.013.01.004.

Bassham, J.A. (2003) Mapping the carbon reduction cycle: A personal retrospective. *Photosynthesis Research*. doi:10.1023/A:1024929725022.

Baud, S., Wuillème, S., Dubreucq, B., et al. (2007) Function of plastidial pyruvate kinases in seeds of Arabidopsis thaliana. *Plant Journal*. doi:10.1111/j.1365-313X.2007.03232.x.

Beal, M.J., Falciani, F., Ghahramani, Z., et al. (2005) A Bayesian approach to reconstructing genetic regulatory networks with hidden factors. *Bioinformatics*, 21 (3): 349–356. doi:10.1093/bioinformatics/bti014.

Bechtold, U., Albihlal, W.S., Lawson, T., et al. (2013) Arabidopsis HEAT SHOCK TRANSCRIPTION FACTORA1b overexpression enhances water productivity, resistance to drought, and infection. *Journal of Experimental Botany*. doi:10.1093/jxb/ert185.

Bechtold, U., Lawson, T., Mejia-Carranza, J., et al. (2010) Constitutive salicylic acid defences do not compromise seed yield, drought tolerance and water productivity in the Arabidopsis accession C24. *Plant, Cell and Environment*, 33 (11): 1959–1973. doi:10.1111/j.1365-3040.2010.02198.x.

Bechtold, U., Penfold, C. a, Jenkins, D.J., et al. (2016) Time-Series Transcriptomics Reveals That AGAMOUS-LIKE22 Affects Primary Metabolism and Developmental Processes in Drought-Stressed Arabidopsis. *The Plant cell*, 28 (2): 345–66. doi:10.1105/tpc.15.00910.

Begcy, K., Mariano, E.D., Mattiello, L., et al. (2011) An Arabidopsis mitochondrial uncoupling protein confers tolerance to drought and salt stress in transgenic tobacco plants. *PLoS ONE*. doi:10.1371/journal.pone.0023776.

Black, C.C. (2003) Photosynthetic Carbon Fixation in Relation to Net CO 2 Uptake . *Annual Review of Plant Physiology*. doi:10.1146/annurev.pp.24.060173.001345.

Blum, A. (2005) Drought resistance, water-use efficiency, and yield potential—are they compatible, dissonant, or mutually exclusive? *Australian Journal of Agricultural Research*. doi:10.1071/AR05069.

Boggetto, N., Gontero, B. and Maberly, S.C. (2007) Regulation of phosphoribulokinase and glyceraldehyde 3-phosphate dehydrogenase in a freshwater diatom, Asterionella formosa. *Journal of Phycology*. doi:10.1111/j.1529-8817.2007.00409.x.

Boyer, J.S. (1970) Leaf Enlargement and Metabolic Rates in Corn, Soybean, and Sunflower at Various Leaf Water Potentials. *Plant Physiology*. doi:10.1104/pp.46.2.233.

Bravo, L.A., Gallardo, J., Navarrete, A., et al. (2003) Cryoprotective activity of a cold-induced dehydrin purified from barley. *Physiologia Plantarum*, 118 (2): 262–269. doi:10.1034/j.1399-3054.2003.00060.x.

Bray, E.A. (1997) Plant responses to water deficit. *Trends in Plant Science*. doi:10.1016/S1360-1385(97)82562-9.

Breeze, E., Harrison, E., McHattie, S., et al. (2011) High-Resolution Temporal Profiling of Transcripts during Arabidopsis Leaf Senescence Reveals a Distinct Chronology of Processes and Regulation. *The Plant Cell*. doi:10.1105/tpc.111.083345.

Bruinsma, J. (2009) "The Resource Outlook to 2050 - By how much do land, water use and crop yields need to increase by 2050?" In *How to Feed the World in 2050*. 2009. doi:10.1016/B978-0-323-10199-8.00006-2.

Bustos, D.M. and Iglesias, A.A. (2002) Non-phosphorylating glyceraldehyde-3-phosphate dehydrogenase is post-translationally phosphorylated in heterotrophic cells of wheat (Triticum aestivum). *FEBS Letters*. doi:10.1016/S0014-5793(02)03455-5.

Bustos, D.M. and Iglesias, A.A. (2003) Phosphorylated non-phosphorylating glyceraldehyde-3-phosphate dehydrogenase from heterotrophic cells of wheat interacts with 14-3-3 proteins. *Plant Physiology*. doi:10.1104/pp.103.030981.

von Caemmerer, S. and Farquhar, G.D. (1981) Some relationships between the biochemistry of photosynthesis and the gas exchange of leaves. *Planta*. doi:10.1007/BF00384257.

Carmo-Silva, E., Marri, L., Sparla, F., et al. (2011) Isolation and compositional analysis of a CP12-associated complex of calvin cycle enzymes from Nicotiana tabacum. *Protein and peptide letters*.

Cerff, R. (1979) *Quaternary Structure of Higher Plant Glyceraldehyde-3-Phosphate Dehydrogenases*., 247: 243–247.

Charlton, A.J., Donarski, J.A., Harrison, M., et al. (2008) Responses of the pea (Pisum sativum L.) leaf metabolome to drought stress assessed by nuclear magnetic resonance spectroscopy. *Metabolomics*. doi:10.1007/s11306-008-0128-0.

Chaves, M.M., Flexas, J. and Pinheiro, C. (2009) *Photosynthesis under drought and salt stress : regulation mechanisms from whole plant to cell*., pp. 551–560. doi:10.1093/aob/mcn125.

Chaves, M.M., Maroco, J.P. and Pereira, J.S. (2003a) Understanding plant responses to drought - From genes to the whole plant. *Functional Plant Biology*. doi:10.1071/FP02076.

Chaves, M.M., Maroco, J.P. and Pereira, J.S. (2003b) Understanding plant responses to drought — from genes to the whole plant. *Functional Plant Biology*, 30: 239–264. doi:10.1071/fp02076.

Chen, J.Q., Meng, X.P., Zhang, Y., et al. (2008) Over-expression of OsDREB genes lead to enhanced drought tolerance in rice. *Biotechnology Letters*. doi:10.1007/s10529-008-9811-5.

Chida, H., Nakazawa, A., Akazaki, H., et al. (2007) Expression of the algal cytochrome c6 gene in Arabidopsis enhances photosynthesis and growth. *Plant and Cell Physiology*, 48 (7): 948–957. doi:10.1093/pcp/pcm064.

Chuong, S.D.X., Good, A.G., Taylor, G.J., et al. (2004) Large-scale Identification of Tubulin-binding Proteins Provides Insight on Subcellular Trafficking, Metabolic Channeling, and Signaling in Plant Cells. *Molecular & Cellular Proteomics*. doi:10.1074/mcp.M400053-MCP200.

Claeys, H. and Inze, D. (2013) The Agony of Choice: How Plants Balance Growth and Survival under Water-Limiting Conditions. *PLANT PHYSIOLOGY*. doi:10.1104/pp.113.220921.

Claeys, H., Van Landeghem, S., Dubois, M., et al. (2014) What Is Stress? Dose-Response Effects in Commonly Used in Vitro Stress Assays. *PLANT PHYSIOLOGY*. doi:10.1104/pp.113.234641.

CLASPER, S., EASTERBY, J.S. and POWLS, R. (1991) Properties to two high???molecular???mass forms of glyceraldehyde???3???phosphate dehydrogenase from spinach leaf, one of which also possesses latent phosphoribulokinase activity. *European Journal of Biochemistry*. doi:10.1111/j.1432-1033.1991.tb16496.x.

Clough, S.J. and Bent, A.F. (1998) Floral dip: A simplified method for Agrobacterium-mediated transformation of Arabidopsis thaliana. *Plant Journal*. doi:10.1046/j.1365-313X.1998.00343.x.

Clough SJ und Bent A (1998) Floral dip: a simplified method for \textit{Agrobacterium}-mediated transformation of \textit{Arabidopsis thaliana}. *The Plant Journal*, 16 (June 1998): 735–743. Available at: http://www.ncbi.nlm.nih.gov/pubmed/10069079.

Cockburn, W. (1983) C3C4: MECHANISMS, AND CELLULAR AND ENVIRONMENTAL REGULATION, OF PHOTOSYNTHESIS (Book). *Plant, Cell & Environment*. doi:10.1111/1365-3040.ep11589371.

Deyholos, M.K. (2010) Making the most of drought and salinity transcriptomics. *Plant, Cell and Environment*. doi:10.1111/j.1365-3040.2009.02092.x.

Ecker, J.R. and Davis, R.W. (1986) Inhibition of gene expression in plant cells by expression of antisense RNA. *Proceedings of the National Academy of Sciences*. doi:10.1073/pnas.83.15.5372.

Edwards, K., Johnstone, C., Thompson, C., et al. (1991) A simple and rapid method for the preparation of plant genomic DNA for PCR analysis. *Nucleic Acids Research*, 19 (6): 1349. doi:10.1093/nar/19.6.1349.

Erales, J., Lignon, S. and Gontero, B. (2009) CP12 from Chlamydomonas reinhardtii, a permanent specific “chaperone-like” protein of glyceraldehyde-3-phosphate dehydrogenase. *Journal of Biological Chemistry*. doi:10.1074/jbc.M808254200.

Erales, J., Mekhalfi, M., Woudstra, M., et al. (2011) Molecular mechanism of NADPH-glyceraldehyde-3-

phosphate dehydrogenase regulation through the C-terminus of CP12 in chlamydomonas reinhardtii. *Biochemistry*. doi:10.1021/bi1020259.

FAO (2013) The state of food and agriculture, 2013. *Lancet*. doi:ISBN: 978-92-5-107671-2 I.

FAO (Food & Agriculture Organisation) (2012) *The State of World Fisheries and Aquaculture 2012*. doi:10.5860/CHOICE.50-5350.

Farquhar, G.D., von Caemmerer, S. and Berry, J.A. (1980) A biochemical model of photosynthetic CO2 assimilation in leaves of C3 species. *Planta*. doi:10.1007/BF00386231.

Feng, L., Han, Y., Liu, G., et al. (2007) Overexpression of sedoheptulose-1,7-bisphosphatase enhances photosynthesis and growth under salt stress in transgenic rice plants. *Functional Plant Biology*. doi:10.1071/FP07074.

Fermani, S., Sparla, F., Falini, G., et al. (2007) Molecular mechanism of thioredoxin regulation in photosynthetic A2B2-glyceraldehyde-3-phosphate dehydrogenase. *Proceedings of the National Academy of Sciences of the United States of America*, 104 (26): 11109–14. doi:10.1073/pnas.0611636104.

Fernie, A.R., Carrari, F. and Sweetlove, L.J. (2004) Respiratory metabolism: Glycolysis, the TCA cycle and mitochondrial electron transport. *Current Opinion in Plant Biology*. doi:10.1016/j.pbi.2004.03.007.

Fischer, R.A. and Edmeades, G.O. (2010) Breeding and cereal yield progress. *Crop Science*, 50: S-85-S-98. doi:10.2135/cropsci2009.10.0564.

Franks, S.J. (2011) Plasticity and evolution in drought avoidance and escape in the annual plant Brassica rapa. *New Phytologist*. doi:10.1111/j.1469-8137.2010.03603.x.

Fujita, Y., Nakashima, K., Yoshida, T., et al. (2009) Three SnRK2 protein kinases are the main positive regulators of abscisic acid signaling in response to water stress in arabidopsis. *Plant and Cell Physiology*. doi:10.1093/pcp/pcp147.

Fukao, T., Yeung, E. and Bailey-Serres, J. (2011) The Submergence Tolerance Regulator SUB1A Mediates Crosstalk between Submergence and Drought Tolerance in Rice. *The Plant Cell*. doi:10.1105/tpc.110.080325.

Gardner, T.S. and Faith, J.J. (2005) Reverse-engineering transcription control networks. *Physics of Life Reviews*. doi:10.1016/j.plrev.2005.01.001.

Geigenberger, P. (2003) Response of plant metabolism to too little oxygen. *Current Opinion in Plant Biology*. doi:10.1016/S1369-5266(03)00038-4.

Geiger, D.R. and Servaites, J.C. (1994) Diurnal Regulation of Photosynthetic Carbon Metabolism in C3 Plants. *Annual Review of Plant Physiology and Plant Molecular Biology*. doi:10.1146/annurev.pp.45.060194.001315.

Gibbs, D.J., Lee, S.C., Md Isa, N., et al. (2011) Homeostatic response to hypoxia is regulated by the N-end rule pathway in plants. *Nature*. doi:10.1038/nature10534.

Gibbs, D.J., MdIsa, N., Movahedi, M., et al. (2014) Nitric Oxide Sensing in Plants Is Mediated by Proteolytic Control of Group VII ERF Transcription Factors. *Molecular Cell*, 53 (3): 369–379. doi:10.1016/j.molcel.2013.12.020.

Giege, P. (2003) Enzymes of Glycolysis Are Functionally Associated with the Mitochondrion in Arabidopsis Cells. *THE PLANT CELL ONLINE*. doi:10.1105/tpc.012500.

Gómez Casati, D.F., Sesma, J.I. and Iglesias, A.A. (2000) Structural and kinetic characterization of NADP-dependent, non- phosphorylating glyceraldehyde-3-phosphate dehydrogenase from celery leaves. *Plant Science*. doi:10.1016/S0168-9452(99)00241-1.

Gowik, U. and Westhoff, P. (2011) The Path from C3 to C4 Photosynthesis. *PLANT PHYSIOLOGY*. doi:10.1104/pp.110.165308.

Graciet, E., Gans, P., Wedel, N., et al. (2003a) The small protein CP12: A protein linker for

supramolecular complex assembly. *Biochemistry*. doi:10.1021/bi034474x.

Graciet, E., Lebreton, S., Camadro, J.M., et al. (2003b) Characterization of native and recombinant A4 glyceraldehyde 3-phosphate dehydrogenase: Kinetic evidence for conformation changes upon association with the small protein CP12. *European Journal of Biochemistry*, 270 (1): 129–136. doi:10.1046/j.1432-1033.2003.03372.x.

Graciet, E., Lebreton, S., Camadro, J.M., et al. (2003c) Characterization of native and recombinant A4glyceraldehyde 3-phosphate dehydrogenase: Kinetic evidence for conformation changes upon association with the small protein CP12. *European Journal of Biochemistry*. doi:10.1046/j.1432-1033.2003.03372.x.

Graciet, E., Lebreton, S. and Gontero, B. (2004) "Emergence of new regulatory mechanisms in the Benson-Calvin pathway via protein-protein interactions: A glyceraldehyde-3-phosphate dehydrogenase/CP12/ phosphoribulokinase complex." In *Journal of Experimental Botany*. 2004. doi:10.1093/jxb/erh107.

Grant, J.J., Yun, B.W. and Loake, G.J. (2000) Oxidative burst and cognate redox signalling reported by luciferase imaging: Identification of a signal network that functions independently of ethylene, SA and Me-JA but is dependent on MAPKK activity. *Plant Journal*. doi:10.1046/j.1365-313X.2000.00902.x.

Greco, M., Chiappetta, A., Bruno, L., et al. (2013) *Genetic engineering to cadmium improve plant performance under In Posidonia oceanica induces changes in DNA drought : physiological evaluation of achievements , methylation and chromatin patterning limitations , and possibilities*., 64 (1): 83–108. doi:10.1093/jxb/err313.

Gregis, V., Andrés, F., Sessa, A., et al. (2013) Identification of pathways directly regulated by SHORT VEGETATIVE PHASE during vegetative and reproductive development in Arabidopsis. *Genome Biology*. doi:10.1186/gb-2013-14-6-r56.

Haake, V., Geiger, M., Walch-Liu, P., et al. (1999) Changes in aldolase activity in wild-type potato plants are important for acclimation to growth irradiance and carbon dioxide concentration, because plastid aldolase exerts control over the ambient rate of photosynthesis across a range of growth condition. *Plant Journal*. doi:10.1046/j.1365-313X.1999.00391.x.

Haake, V., Zrenner, R., Sonnewald, U., et al. (1998) A moderate decrease of plastid aldolase activity inhibits photosynthesis, alters the levels of sugars and starch, and inhibits growth of potato plants. *Plant Journal*. doi:10.1046/j.1365-313X.1998.00089.x.

Habash, D.Z., Parry, M.A.J., Parmar, S., et al. (1996) The regulation of component processes of photosynthesis in transgenic tobacco with decreased phosphoribulokinase activity. *Photosynthesis Research*. doi:10.1007/BF00117666.

Habenicht, A. (1997) The non-phosphorylating glyceraldehyde-3-phosphate dehydrogenase: biochemistry, structure, occurrence and evolution. *Biol Chem*. doi:10.1016/j.addr.2013.03.005.

Habenicht, A., Hellman, U. and Cerff, R. (1994) Non-phosphorylating GAPDH of higher plants is a member of the aldehyde dehydrogenase superfamily with no sequence homology to phosphorylating GAPDH. *Journal of Molecular Biology*. doi:10.1006/jmbi.1994.1217.

Hajirezaei, M.R., Biemelt, S., Peisker, M., et al. (2006) The influence of cytosolic phosphorylating glyceraldehyde 3-phosphate dehydrogenase (GAPC) on potato tuber metabolism. *Journal of Experimental Botany*. doi:10.1093/jxb/erj207.

Hancock, J.T., Henson, D., Nyirenda, M., et al. (2005) Proteomic identification of glyceraldehyde 3-phosphate dehydrogenase as an inhibitory target of hydrogen peroxide in Arabidopsis. *Plant Physiology and Biochemistry*. doi:10.1016/j.plaphy.2005.07.012.

Harb, A., Krishnan, A., Ambavaram, M.M.R., et al. (2010) Molecular and Physiological Analysis of Drought Stress in Arabidopsis Reveals Early Responses Leading to Acclimation in Plant Growth. *PLANT*

PHYSIOLOGY. doi:10.1104/pp.110.161752.

Harrison, E.P., Willingham, N.M., Lloyd, J.C., et al. (1998) Reduced sedoheptulose-1,7-bisphosphatase levels in transgenic tobacco lead to decreased photosynthetic capacity and altered carbohydrate accumulation. *Planta*. doi:10.1007/s004250050226.

Hattori, Y., Nagai, K., Furukawa, S., et al. (2009) The ethylene response factors SNORKEL1 and SNORKEL2 allow rice to adapt to deep water. *Nature*. doi:10.1038/nature08258.

Heldt, H.W., Werdan, K., Milovancev, M., et al. (1973) Alkalization of the chloroplast stroma caused by light-dependent proton flux into the thylakoid space. *BBA - Bioenergetics*. doi:10.1016/0005-2728(73)90137-0.

Hernández, J.A., Corpas, F.J., Gómez, M., et al. (1993) Salt-induced oxidative stress mediated by activated oxygen species in pea leaf mitochondria. *Physiologia Plantarum*. doi:10.1111/j.1399-3054.1993.tb01792.x.

Hinz, M., Wilson, I.W., Yang, J., et al. (2010) Arabidopsis RAP2.2: An Ethylene Response Transcription Factor That Is Important for Hypoxia Survival. *PLANT PHYSIOLOGY*. doi:10.1104/pp.110.155077.

Ho, C.L. and Saito, K. (2001) Molecular biology of the plastidic phosphorylated serine biosynthetic pathway in Arabidopsis thaliana. *Amino Acids*. doi:10.1007/s007260170042.

Holtgräwe, D., Scholz, A., Altmann, B., et al. (2005) Cytoskeleton-associated, carbohydrate-metabolizing enzymes in maize identified by yeast two-hybrid screening. *Physiologia Plantarum*. doi:10.1111/j.1399-3054.2005.00548.x.

Horton, P. (2000) Prospects for crop improvement through the genetic manipulation of photosynthesis: morphological and biochemical aspects of light capture. *Journal of Experimental Botany*. doi:10.1093/jexbot/51.suppl_1.475.

Howard, T.P., Fryer, M.J., Singh, P., et al. (2011a) Antisense Suppression of the Small Chloroplast Protein

CP12 in Tobacco Alters Carbon Partitioning and Severely Restricts Growth. *PLANT PHYSIOLOGY*. doi:10.1104/pp.111.183806.

Howard, T.P., Lloyd, J.C. and Raines, C.A. (2011b) Inter-species variation in the oligomeric states of the higher plant Calvin cycle enzymes glyceraldehyde-3-phosphate dehydrogenase and phosphoribulokinase. *Journal of Experimental Botany*, 62 (11): 3799–3805. doi:10.1093/jxb/err057.

Howard, T.P., Metodiev, M., Lloyd, J.C., et al. (2008) Thioredoxin-mediated reversible dissociation of a stromal multiprotein complex in response to changes in light availability. *Proceedings of the National Academy of Sciences*, 105 (10): 4056–4061. doi:10.1073/pnas.0710518105.

Iglesias, A.A., Vicario, L.R., Gómez-Casati, D.F., et al. (2002) On the interaction of substrate analogues with non-phosphorylating glyceraldehyde-3-phosphate dehydrogenase from celery leaves. *Plant Science*. doi:10.1016/S0168-9452(02)00015-8.

Kasuga, M., Liu, Q., Miura, S., et al. (1999) Improving plant drought, salt, and freezing tolerance by gene transfer of a single stress-inducible transcription factor. *Nature Biotechnology*. doi:10.1038/7036.

Kasuga, M., Miura, S., Shinozaki, K., et al. (2004) A combination of the Arabidopsis DREB1A gene and stress-inducible rd29A promoter improved drought- and low-temperature stress tolerance in tobacco by gene transfer. *Plant and Cell Physiology*. doi:10.1093/pcp/pch037.

Kawaguchi, R., Girke, T., Bray, E.A., et al. (2004) Differential mRNA translation contributes to gene regulation under non-stress and dehydration stress conditions in Arabidopsis thaliana. *Plant Journal*. doi:10.1111/j.1365-313X.2004.02090.x.

Kelly, G.J. and Gibbs, M. (1973) A mechanism for the indirect transfer of photosynthetically reduced nicotinamide adenine dinucleotide phosphate from chloroplasts to the cytoplasm. *Plant physiology*. doi:10.1104/pp.52.6.674.

Kilian, J., Whitehead, D., Horak, J., et al. (2007) The AtGenExpress global stress expression data set:

Protocols, evaluation and model data analysis of UV-B light, drought and cold stress responses. *Plant Journal*. doi:10.1111/j.1365-313X.2007.03052.x.

Kosmacz, M., Parlanti, S., Schwarzländer, M., et al. (2015) The stability and nuclear localization of the transcription factor RAP2.12 are dynamically regulated by oxygen concentration. *Plant, Cell and Environment*, 38 (6): 1094–1103. doi:10.1111/pce.12493.

Koßmann, J., Sonnewald, U. and Willmitzer, L. (1994) Reduction of the chloroplastic fructose-1,6-bisphosphatase in transgenic potato plants impairs photosynthesis and plant growth. *The Plant Journal*. doi:10.1046/j.1365-313X.1994.6050637.x.

Kramer, D.M. and Evans, J.R. (2011) The Importance of Energy Balance in Improving Photosynthetic Productivity. *PLANT PHYSIOLOGY*. doi:10.1104/pp.110.166652.

Kreps, J.A. (2002) Transcriptome Changes for Arabidopsis in Response to Salt, Osmotic, and Cold Stress. *PLANT PHYSIOLOGY*. doi:10.1104/pp.008532.

Larkindale, J. (2002) Protection against Heat Stress-Induced Oxidative Damage in Arabidopsis Involves Calcium, Abscisic Acid, Ethylene, and Salicylic Acid. *PLANT PHYSIOLOGY*. doi:10.1104/pp.128.2.682.

Lawlor, D.W. (2002) Limitation to photosynthesis in water-stressed leaves: Stomata vs. Metabolism and the role of ATP. *Annals of Botany*. doi:10.1093/aob/mcf110.

Lawlor, D.W. (2013a) Genetic engineering to improve plant performance under drought: Physiological evaluation of achievements, limitations, and possibilities. *Journal of Experimental Botany*. doi:10.1093/jxb/ers326.

Lawlor, D.W. (2013b) Genetic engineering to improve plant performance under drought: Physiological evaluation of achievements, limitations, and possibilities. *Journal of Experimental Botany*. 64 (1) pp. 83–108. doi:10.1093/jxb/ers326.

Lawlor, D.W. and Cornic, G. (2002) *Photosynthetic carbon assimilation and associated metabolism in*

relation to water deficits in higher plants., 44 (Evans 1998): 275–294.

Lefebvre, S., Lawson, T., Fryer, M., et al. (2005a) Increased sedoheptulose-1, 7-bisphosphatase activity in transgenic tobacco plants stimulates photosynthesis and growth from an early stage in development. *Plant Physiology*. doi:10.1104/pp.104.055046.1.

Lefebvre, S., Lawson, T., Fryer, M., et al. (2005b) Increased sedoheptulose-1, 7-bisphosphatase activity in transgenic tobacco plants stimulates photosynthesis and growth from an early stage in development. *Plant Physiology*, 138 (1): 451–460. doi:10.1104/pp.104.055046.1.

Levitt, J. (1985) Responses of Plants to Environmental Stresses. *Journal of Range Management*. doi:10.2307/3899731.

Licausi, F., Kosmacz, M., Weits, D.A., et al. (2011a) Oxygen sensing in plants is mediated by an N-end rule pathway for protein destabilization. *Nature*. doi:10.1038/nature10536.

Licausi, F., Kosmacz, M., Weits, D.A., et al. (2011b) Oxygen sensing in plants is mediated by an N-end rule pathway for protein destabilization. *Nature*. doi:10.1038/nature10536.

Lichtenthaler, H.K. (1999) THE 1-DEOXY-D-XYLULOSE-5-PHOSPHATE PATHWAY OF ISOPRENOID BIOSYNTHESIS IN PLANTS. *Annual Review of Plant Physiology and Plant Molecular Biology*. doi:10.1146/annurev.arplant.50.1.47.

Lin, R.-C., Park, H.-J. and Wang, H.-Y. (2008) Role of Arabidopsis RAP2.4 in regulating light- and ethylene-mediated developmental processes and drought stress tolerance. *Molecular plant*. doi:10.1093/mp/ssm004.

Lobell, D.B., Bänziger, M., Magorokosho, C., et al. (2011) Nonlinear heat effects on African maize as evidenced by historical yield trials. *Nature Climate Change*. doi:10.1038/nclimate1043.

Lobell, D.B. and Field, C.B. (2007) Global scale climate-crop yield relationships and the impacts of recent warming. *Environmental Research Letters*. doi:10.1088/1748-9326/2/1/014002.

Long, S.P., Marshall-Colon, A. and Zhu, X.G. (2015) Meeting the global food demand of the future by engineering crop photosynthesis and yield potential. *Cell*. doi:10.1016/j.cell.2015.03.019.

López-Calcagno, P.E., Abuzaid, A.O., Lawson, T., et al. (2017) Arabidopsis CP12 mutants have reduced levels of phosphoribulokinase and impaired function of the Calvin-Benson cycle. *Journal of Experimental Botany*. doi:10.1093/jxb/erx084.

Maberly, S.C., Courcelle, C., Groben, R., et al. (2010) Phylogenetically-based variation in the regulation of the Calvin cycle enzymes, phosphoribulokinase and glyceraldehyde-3-phosphate dehydrogenase, in algae. *Journal of Experimental Botany*. doi:10.1093/jxb/erp337.

Marri, L., Pesaresi, A., Valerio, C., et al. (2010) In vitro characterization of Arabidopsis CP12 isoforms reveals common biochemical and molecular properties. *Journal of Plant Physiology*. doi:10.1016/j.jplph.2010.02.008.

Marri, L., Sparla, F., Pupillo, P., et al. (2005a) Co-ordinated gene expression of photosynthetic glyceraldehyde-3-phosphate dehydrogenase, phosphoribulokinase, and CP12 in Arabidopsis thaliana. *Journal of Experimental Botany*. doi:10.1093/jxb/eri020.

Marri, L., Thieulin-Pardo, G., Lebrun, R., et al. (2014) CP12-mediated protection of Calvin-Benson cycle enzymes from oxidative stress. *Biochimie*. doi:10.1016/j.biochi.2013.10.018.

Marri, L., Trost, P., Pupillo, P., et al. (2005b) Reconstitution and properties of the recombinant glyceraldehyde-3-phosphate dehydrogenase/CP12/phosphoribulokinase supramolecular complex of Arabidopsis. *Plant Physiol*. doi:10.1104/pp.105.068445.

Marri, L., Trost, P., Trivelli, X., et al. (2008) Spontaneous assembly of photosynthetic supramolecular complexes as mediated by the intrinsically unstructured protein CP12. *Journal of Biological Chemistry*. doi:10.1074/jbc.M705650200.

Marri, L., Zaffagnini, M., Collin, V., et al. (2009) Prompt and easy activation by specific thioredoxins of

calvin cycle enzymes of arabidopsis thaliana associated in the GAPDH/CP12/PRK supramolecular complex. *Molecular Plant*. doi:10.1093/mp/ssn061.

Medrano, H., Parry, M.A.J., Socias, X., et al. (1997) Long term water stress inactivates Rubisco in subterranean clover. *Annals of Applied Biology*. doi:10.1111/j.1744-7348.1997.tb05176.x.

Méndez-Vigo, B., Martínez-Zapater, J.M. and Alonso-Blanco, C. (2013) The Flowering Repressor SVP Underlies a Novel Arabidopsis thaliana QTL Interacting with the Genetic Background. *PLoS Genetics*. doi:10.1371/journal.pgen.1003289.

Michels, A.K. (2005) Diatom Plastids Possess a Phosphoribulokinase with an Altered Regulation and No Oxidative Pentose Phosphate Pathway. *PLANT PHYSIOLOGY*. doi:10.1104/pp.104.055285.

Mizoguchi, M., Umezawa, T., Nakashima, K., et al. (2010) Two closely related subclass II SnRK2 protein kinases cooperatively regulate drought-inducible gene expression. *Plant and Cell Physiology*. doi:10.1093/pcp/pcq041.

Moparthi, S.B., Thieulin-Pardo, G., Mansuelle, P., et al. (2014) Conformational modulation and hydrodynamic radii of CP12 protein and its complexes probed by fluorescence correlation spectroscopy. *FEBS Journal*. doi:10.1111/febs.12854.

Moparthi, S.B., Thieulin-Pardo, G., De Torres, J., et al. (2015) FRET analysis of CP12 structural interplay by GAPDH and PRK. *Biochemical and Biophysical Research Communications*. doi:10.1016/j.bbrc.2015.01.135.

Moran, J., Becana, M., Iturbe-ormaetxe, I., et al. (1994) Drought induces oxidative stress in pea plants. *Planta*. doi:10.1007/BF00197534.

Muñoz-Bertomeu, J., Cascales-Miñana, B., Alaiz, M., et al. (2010) A critical role of plastidial glycolytic glyceraldehyde-3-phosphate dehydrogenase in the control of plant metabolism and development. *Plant Signaling and Behavior*. doi:10.4161/psb.5.1.10200.

Munoz-Bertomeu, J., Cascales-Minana, B., Mulet, J.M., et al. (2009) Plastidial Glyceraldehyde-3-Phosphate Dehydrogenase Deficiency Leads to Altered Root Development and Affects the Sugar and Amino Acid Balance in Arabidopsis. *PLANT PHYSIOLOGY*. doi:10.1104/pp.109.143701.

Murata, Y., Pei, Z., Mori, I.C., et al. (2001) Abscisic Acid Activation of Plasma Membrane Ca 2 ⁒ Channels in Guard Cells Requires Cytosolic NAD (P) H and Is Differentially Disrupted Upstream and Downstream of Reactive Oxygen Species Production in abi1-1 and abi2-1 Protein Phosphatase 2C Mutants. *The Plant cell*, 13 (November): 2513–2523. doi:10.1105/tpc.010210.2514.

Murchie, E.H. and Lawson, T. (2013) Chlorophyll fluorescence analysis: A guide to good practice and understanding some new applications. *Journal of Experimental Botany*. doi:10.1093/jxb/ert208.

Murphy, K. and Mian, S. (1999) Modelling gene expression data using dynamic Bayesian networks. *Graphical Models*. doi:10.1.1.30.9391.

Nakagawa, T., Kurose, T., Hino, T., et al. (2007) Development of series of gateway binary vectors, pGWBs, for realizing efficient construction of fusion genes for plant transformation. *Journal of bioscience and bioengineering*, 104 (1): 34–41. doi:10.1263/jbb.104.34.

Nakano, T., Suzuki, K., Fujimura, T., et al. (2006) Genome-wide analysis of the ERF gene family in Arabidopsis and rice. *Plant Physiology*. doi:10.1104/pp.105.073783.currently.

Nelson, D.E., Repetti, P.P., Adams, T.R., et al. (2007) Plant nuclear factor Y (NF-Y) B subunits confer drought tolerance and lead to improved corn yields on water-limited acres. *Proceedings of the National Academy of Sciences*. doi:10.1073/pnas.0707193104.

Nishizawa, A.N. and Buchanan, B.B. (1981) Enzyme Regulation in C4 Photosynthesis. *Biological Chemistry*, 256 (12): 6119–6126.

Oesterhelt, C., Klocke, S., Holtgrefe, S., et al. (2007) Redox regulation of chloroplast enzymes in Galdieria sulphuraria in view of eukaryotic evolution. *Plant and Cell Physiology*. doi:10.1093/pcp/pcm108.

Orozco-Cardenas, M. and Ryan, C.A. (1999) Hydrogen peroxide is generated systemically in plant leaves by wounding and systemin via the octadecanoid pathway. *Proceedings of the National Academy of Sciences*. doi:10.1073/pnas.96.11.6553.

Ort, D.R., Merchant, S.S., Alric, J., et al. (2015) Redesigning photosynthesis to sustainably meet global food and bioenergy demand. *Proceedings of the National Academy of Sciences*. doi:10.1073/pnas.1424031112.

Ozfidan, C., Turkan, I., Sekmen, A.H., et al. (2012) Abscisic acid-regulated responses of aba2-1 under osmotic stress: The abscisic acid-inducible antioxidant defence system and reactive oxygen species production. *Plant Biology*. doi:10.1111/j.1438-8677.2011.00496.x.

Papdi, C., Pérez-Salamõ, I., Joseph, M.P., et al. (2015) The low oxygen, oxidative and osmotic stress responses synergistically act through the ethylene response factor VII genes RAP2.12, RAP2.2 and RAP2.3. *Plant Journal*. doi:10.1111/tpj.12848.

Park, H.Y., Seok, H.Y., Woo, D.H., et al. (2011) AtERF71/HRE2 transcription factor mediates osmotic stress response as well as hypoxia response in Arabidopsis. *Biochemical and Biophysical Research Communications*, 414 (1): 135–141. doi:10.1016/j.bbrc.2011.09.039.

Passioura, J. (2007) "The drought environment: Physical, biological and agricultural perspectives." In *Journal of Experimental Botany*. 2007. doi:10.1093/jxb/erl212.

Paul, M.J., Knight, J.S., Habash, D., et al. (1995) Reduction in phosphoribulokinase activity by antisense RNA in transgenic tobacco: effect on CO2 assimilation and growth in low irradiance. *The Plant Journal*. doi:10.1046/j.1365-313X.1995.7040535.x.

Petersen, J., Brinkmann, H. and Cerff, R. (2003) Origin, evolution, and metabolic role of a novel glycolytic GAPDH enzyme recruited by land plant plastids. *Journal of Molecular Evolution*. doi:10.1007/s00239-002-2441-y.

Petersen, J., Teich, R., Becker, B., et al. (2006) The GapA/B gene duplication marks the origin of streptophyta (charophytes and land plants). *Molecular Biology and Evolution*, 23 (6): 1109–1118. doi:10.1093/molbev/msj123.

Pinheiro, C. and Chaves, M.M. (2011) Photosynthesis and drought: Can we make metabolic connections from available data? *Journal of Experimental Botany*. doi:10.1093/jxb/erq340.

Plaxton, W.C. (1996) THE ORGANIZATION AND REGULATION OF PLANT GLYCOLYSIS. *Annual Review of Plant Physiology and Plant Molecular Biology*. doi:10.1146/annurev.arplant.47.1.185.

Pohlmeyer, K., Paap, B.K., Soll, J., et al. (1996) CP12: A small nuclear-encoded chloroplast protein provides novel insights into higher-plant GAPDH evolution. *Plant Molecular Biology*. doi:10.1007/BF00020493.

Poolman, M.G., Fell, D. a and Thomas, S. (2000) Modelling photosynthesis and its control. *Journal of experimental botany*. doi:10.1093/jexbot/51.suppl_1.319.

Price, G., Yu, J., vonCaemmerer, S., et al. (1995a) Chloroplast Cytochrome B(6)/F and Atp Synthase Complexes in Tobacco - Transformation with Antisense Rna Against Nuclear-Encoded Transcripts for the Rieske Fes and Atp-Delta Polypeptides. *Australian Journal Of Plant Physiology*. doi:10.1093/plankt/24.9.889.

Price, G.D., Evans, J.R., von Caemmerer, S., et al. (1995b) Specific reduction of chloroplast glyceraldehyde-3-phosphate dehydrogenase activity by antisense RNA reduces CO2 assimilation via a reduction in ribulose bisphosphate regeneration in transgenic tobacco plants. *Planta*. doi:10.1007/BF00202594.

Quan, R., Hu, S., Zhang, Z., et al. (2010) Overexpression of an ERF transcription factor TSRF1 improves rice drought tolerance. *Plant Biotechnology Journal*. doi:10.1111/j.1467-7652.2009.00492.x.

Raines, C. a (2011a) Increasing photosynthetic carbon assimilation in C3 plants to improve crop yield:

current and future strategies. *Plant physiology*. doi:10.1104/pp.110.168559.

Raines, C.A. (2003a) The Calvin cycle revisited. *Photosynthesis Research*. 75 (1) pp. 1–10. doi:10.1023/A:1022421515027.

Raines, C.A. (2003b) The Calvin cycle revisited. *Photosynthesis Research*. doi:10.1023/A:1022421515027.

Raines, C.A. (2006) Transgenic approaches to manipulate the environmental responses of the C3 carbon fixation cycle. *Plant, Cell and Environment*, 29 (3): 331–339. doi:10.1111/j.1365-3040.2005.01488.x.

Raines, C.A. (2011b) Increasing Photosynthetic Carbon Assimilation in C3 Plants to Improve Crop Yield: Current and Future Strategies. *Plant Physiology*, 155 (January): 36–42. doi:10.1104/pp.110.168559.

Raines, C.A., Lloyd, J.C. and Dyer, T.A. (1999) New insighits into the structure and function of sedoheptulose-1,7-bisphosphatase; an important but neglected Calvin cycle enzyme. *Journal of Experimental Botany*. doi:10.1093/jxb/50.330.1.

Raines, C.A. and Paul, M.J. (2006) "Products of leaf primary carbon metabolism modulate the developmental programme determining plant morphology." In *Journal of Experimental Botany*. 2006. doi:10.1093/jxb/erl011.

Rangel, C., Angus, J., Ghahramani, Z., et al. (2004) Modeling T-cell activation using gene expression profiling and state-space models. *Bioinformatics (Oxford, England)*, 20 (9): 1361–72. doi:10.1093/bioinformatics/bth093.

Ray, D.K., Mueller, N.D., West, P.C., et al. (2013) Yield Trends Are Insufficient to Double Global Crop Production by 2050. *PLoS ONE*. doi:10.1371/journal.pone.0066428.

Rius, S.P., Casati, P., Iglesias, A.A., et al. (2006) Characterization of an Arabidopsis thaliana mutant lacking a cytosolic non-phosphorylating glyceraldehyde-3-phosphate dehydrogenase. *Plant Molecular Biology*. doi:10.1007/s11103-006-0060-5.

Rius, S.P., Casati, P., Iglesias, A.A., et al. (2008a) Characterization of Arabidopsis Lines Deficient in GAPC-1, a Cytosolic NAD-Dependent Glyceraldehyde-3-Phosphate Dehydrogenase. *PLANT PHYSIOLOGY*. doi:10.1104/pp.108.128769.

Rius, S.P., Casati, P., Iglesias, A.A., et al. (2008b) Characterization of Arabidopsis Lines Deficient in GAPC-1, a Cytosolic NAD-Dependent Glyceraldehyde-3-Phosphate Dehydrogenase. *Plant Physiology*, 148 (3): 1655–1667. doi:10.1104/pp.108.128769.

Roberts, M.J. and Schlenker, W. (2009) World supply and demand of food commodity calories. *American Journal of Agricultural Economics*, 91 (5): 1235–1242. doi:10.1111/j.1467-8276.2009.01290.x.

Rosenthal, D.M., Locke, A.M., Khozaei, M., et al. (2011) Over-expressing the C3photosynthesis cycle enzyme Sedoheptulose-1-7 Bisphosphatase improves photosynthetic carbon gain and yield under fully open air CO2fumigation (FACE). *BMC Plant Biology*. doi:10.1186/1471-2229-11-123.

Rumpho, M.E., Edwards, G.E. and Loescher, W.H. (1983) A Pathway for Photosynthetic Carbon Flow to Mannitol in Celery Leaves : Activity and Localization of Key Enzymes. *PLANT PHYSIOLOGY*. doi:10.1104/pp.73.4.869.

Sakuma, Y. (2006) Functional Analysis of an Arabidopsis Transcription Factor, DREB2A, Involved in Drought-Responsive Gene Expression. *THE PLANT CELL ONLINE*. doi:10.1105/tpc.105.035881.

Sambrook, J. and Russell, D.W. (2001) *Molecular cloning: a laboratory manual*.

Scagliarini, S., Trost, P. and Pupillo, P. (1998) The non-regulatory isoform of NAD(P)-glyceraldehyde-3-phosphate dehydrogenase from spinach chloroplasts. *Journal of Experimental Botany*, 49 (325): 1307–1315. doi:10.1093/jxb/49.325.1307.

Scheibe, R., Wedel, N., Vetter, S., et al. (2002) Co-existence of two regulatory NADP-glyceraldehyde 3-P dehydrogenase complexes in higher plant chloroplasts. *European Journal of Biochemistry*. doi:10.1046/j.1432-1033.2002.03269.x.

Seki, M., Narusaka, M., Ishida, J., et al. (2002) Monitoring the expression profiles of 7000 Arabidopsis genes under drought, cold and high-salinity stresses using a full-length cDNA microarray. *Plant Journal*. doi:10.1046/j.1365-313X.2002.01359.x.

Serraj, R. and Sinclair, T.R. (2002) Osmolyte accumulation: Can it really help increase crop yield under drought conditions? *Plant, Cell and Environment*, 25 (2): 333–341. doi:10.1046/j.1365-3040.2002.00754.x.

Sharkey, T.D., Bernacchi, C.J., Farquhar, G.D., et al. (2007) Fitting photosynthetic carbon dioxide response curves for C3 leaves. *Plant, Cell and Environment*. doi:10.1111/j.1365-3040.2007.01710.x.

Sharma, P. and Dubey, R.S. (2005) Drought induces oxidative stress and enhances the activities of antioxidant enzymes in growing rice seedlings. *Plant Growth Regulation*, 46 (3): 209–221. doi:10.1007/s10725-005-0002-2.

Shinozaki, K. and Yamaguchi-Shinozaki, K. (2007) "Gene networks involved in drought stress response and tolerance." In *Journal of Experimental Botany*. 2007. doi:10.1093/jxb/erl164.

Simkin, A.J., McAusland, L., Headland, L.R., et al. (2015) Multigene manipulation of photosynthetic carbon assimilation increases CO2 fixation and biomass yield in tobacco. *Journal of experimental botany*, 66 (13): 4075–90. doi:10.1093/jxb/erv204.

Simkin, A.J., McAusland, L., Lawson, T., et al. (2017) Over-expression of the RieskeFeS protein increases electron transport rates and biomass yield. *Plant Physiology*. doi:10.1104/pp.17.00622.

Singh, D., Nath, K. and Sharma, Y.K. (2007) Response of wheat seed germination and seedling growth under copper stress. *Journal of environmental biology / Academy of Environmental Biology, India*. doi:10.5829/idosi.ijmr.2013.4.3.81228.

Singh, P., Kaloudas, D. and Raines, C.A. (2008) Expression analysis of the Arabidopsis CP12 gene family suggests novel roles for these proteins in roots and floral tissues. *Journal of Experimental Botany*.

doi:10.1093/jxb/ern236.

Skirycz, A., De Bodt, S., Obata, T., et al. (2010) Developmental Stage Specificity and the Role of Mitochondrial Metabolism in the Response of Arabidopsis Leaves to Prolonged Mild Osmotic Stress. *PLANT PHYSIOLOGY*. doi:10.1104/pp.109.148965.

Skirycz, A., Vandenbroucke, K., Clauw, P., et al. (2011) Survival and growth of Arabidopsis plants given limited water are not equal. *Nature Biotechnology*. doi:10.1038/nbt.1800.

Someren, E. van, Wessels, L., Backer, E., et al. (2005) Genetic network modeling. *Pharmacogenomics*. doi:10.1517/14622416.3.4.507.

South, P.F., Cavanagh, A.P., Liu, H.W., et al. (2019) Synthetic glycolate metabolism pathways stimulate crop growth and productivity in the field. *Science*. doi:10.1126/science.aat9077.

Sparla, F., Pupillo, P. and Trost, P. (2002) The C-terminal extension of glyceraldehyde-3-phosphate dehydrogenase subunit B acts as an autoinhibitory domain regulated by thioredoxins and nicotinamide adenine dinucleotide. *Journal of Biological Chemistry*, 277 (47): 44946–44952. doi:10.1074/jbc.M206873200.

Stitt, M., Lunn, J. and Usadel, B. (2010) Arabidopsis and primary photosynthetic metabolism - More than the icing on the cake. *Plant Journal*. doi:10.1111/j.1365-313X.2010.04142.x.

STITT, M. and SCHULZE, D. (1994) Does Rubisco control the rate of photosynthesis and plant growth? An exercise in molecular ecophysiology. *Plant, Cell & Environment*. doi:10.1111/j.1365-3040.1994.tb00144.x.

Sytar, O., Kumar, A., Latowski, D., et al. (2013) Heavy metal-induced oxidative damage, defense reactions, and detoxification mechanisms in plants. *Acta Physiologiae Plantarum*. doi:10.1007/s11738-012-1169-6.

Takahashi, Y., Ebisu, Y., Kinoshita, T., et al. (2013) BHLH transcription factors that facilitate k+uptake

during stomatal opening are repressed by abscisic acid through phosphorylation. *Science Signaling*. doi:10.1126/scisignal.2003760.

Tamoi, M., Miyazaki, T., Fukamizo, T., et al. (2005) The Calvin cycle in cyanobacteria is regulated by CP12 via the NAD(H)/NADP(H) ratio under light/dark conditions. *Plant Journal*. doi:10.1111/j.1365-313X.2005.02391.x.

Tang, Y., Liu, M., Gao, S., et al. (2012) Molecular characterization of novel TaNAC genes in wheat and overexpression of TaNAC2a confers drought tolerance in tobacco. *Physiologia Plantarum*, 144 (3): 210–224. doi:10.1111/j.1399-3054.2011.01539.x.

Tezara, W., Mitchell, V.J., Driscoll, S.D., et al. (1999) Water stress inhibits plant photosynthesis by decreasing coupling factor and ATP. *Nature*. doi:10.1038/44842.

Trost, P., Fermani, S., Marri, L., et al. (2006) Thioredoxin-dependent regulation of photosynthetic glyceraldehyde-3- phosphate dehydrogenase: Autonomous vs. CP12-dependent mechanisms. *Photosynthesis Research*, 89 (3): 263–275. doi:10.1007/s11120-006-9099-z.

Trost, P., Scagliarini, S., Valenti, V., et al. (1993) Activation of spinach chloroplast glyceraldehyde 3-phosphate dehydrogenase: effect of glycerate 1,3-bisphosphate. *Planta*. doi:10.1007/BF00196960.

Ueguchi, C., Koizumi, H., Suzuki, T., et al. (2001) Novel family of sensor histidine kinase genes in Arabidopsis thaliana. *Plant and Cell Physiology*. doi:10.1093/pcp/pce015.

Uematsu, K., Suzuki, N., Iwamae, T., et al. (2012) Increased fructose 1,6-bisphosphate aldolase in plastids enhances growth and photosynthesis of tobacco plants. *Journal of Experimental Botany*. doi:10.1093/jxb/ers004.

Valverde, F., Ortega, J.M., Losada, M., et al. (2005) Sugar-mediated transcriptional regulation of the Gap gene system and concerted photosystem II functional modulation in the microalga Scenedesmus vacuolatus. *Planta*. doi:10.1007/s00425-005-1501-0.

Verelst, W., Bertolini, E., De Bodt, S., et al. (2013) Molecular and physiological analysis of growth-limiting drought stress in brachypodium distachyon leaves. *Molecular Plant*. doi:10.1093/mp/sss098.

Wang, X., Chen, Y., Zou, J., et al. (2007) Involvement of a cytoplasmic glyceraldehyde-3-phosphate dehydrogenase GapC-2 in low-phosphate-induced anthocyanin accumulation in Arabidopsis. *Chinese Science Bulletin*. doi:10.1007/s11434-007-0277-y.

Wedel, N. and Soll, J. (1998a) Evolutionary conserved light regulation of Calvin cycle activity by NADPH-mediated reversible phosphoribulokinase/CP12/ glyceraldehyde-3-phosphate dehydrogenase complex dissociation. *Proceedings of the National Academy of Sciences of the United States of America*, 95 (16): 9699–9704. doi:10.1073/pnas.95.16.9699.

Wedel, N. and Soll, J. (1998b) Evolutionary Conserved Light Regulation of Calvin Cycle Activity by NADPH-mediated Reversible Phosphoribulokinase/CP12/Glyceraldehyde-3-phosphate Dehydrogenase Complex Dissociation. *Proceedings of the National Academy of Sciences*. doi:10.1073/pnas.95.16.9699.

Wedel, N., Soll, J. and Paap, B.K. (1997a) CP12 provides a new mode of light regulation of Calvin cycle activity in higher plants. *Proceedings of the National Academy of Sciences of the United States of America*. doi:10.1073/pnas.94.19.10479.

Wedel, N., Soll, J. and Paap, B.K. (1997b) CP12 provides a new mode of light regulation of Calvin cycle activity in higher plants. *Proceedings of the National Academy of Sciences of the United States of America*, 94 (19): 10479–10484. doi:10.1073/pnas.94.19.10479.

Wedel, N., Soll, J. and Paap, B.K. (1997c) CP12 provides a new mode of light regulation of Calvin cycle activity in higher plants. *Proceedings of the National Academy of Sciences*. doi:10.1073/pnas.94.19.10479.

Wenderoth, I., Scheibe, R. and Von Schaewen, A. (1997) Identification of the cysteine residues involved in redox modification of plant plastidic glucose-6-phosphate dehydrogenase. *Journal of Biological*

Chemistry. doi:10.1074/jbc.272.43.26985.

Werdan, K., Heldt, H.W. and Milovancev, M. (1975) The role of pH in the regulation of carbon fixation in the chloroplast stroma. Studies on CO2 fixation in the light and dark. *BBA - Bioenergetics*. doi:10.1016/0005-2728(75)90041-9.

Weston, D.J., Gunter, L.E., Rogers, A., et al. (2008) Connecting genes, coexpression modules, and molecular signatures to environmental stress phenotypes in plants. *BMC Systems Biology*. doi:10.1186/1752-0509-2-16.

Wilkins, O., Bräutigam, K. and Campbell, M.M. (2010) Time of day shapes Arabidopsis drought transcriptomes. *Plant Journal*. doi:10.1111/j.1365-313X.2010.04274.x.

Wohlbach, D.J., Quirino, B.F. and Sussman, M.R. (2008) Analysis of the Arabidopsis Histidine Kinase ATHK1 Reveals a Connection between Vegetative Osmotic Stress Sensing and Seed Maturation. *THE PLANT CELL ONLINE*. doi:10.1105/tpc.107.055871.

Wolosiuk, R. a and Buchanan, B.B. (1978) Activation of chloroplast NADP-linked glyceraldehyde-3-phosphate dehydrogenase by the ferredoxin/thioredoxin system. *Plant physiology*, 61 (4): 669–671. doi:10.1104/pp.61.4.669.

Xu, K., Xu, X., Fukao, T., et al. (2006) Sub1A is an ethylene-response-factor-like gene that confers submergence tolerance to rice. *Nature*. doi:10.1038/nature04920.

Xue, G.P., McIntyre, C.L., Glassop, D., et al. (2008) Use of expression analysis to dissect alterations in carbohydrate metabolism in wheat leaves during drought stress. *Plant Molecular Biology*. doi:10.1007/s11103-008-9311-y.

Yamori, W., Takahashi, S., Makino, A., et al. (2011) The Roles of ATP Synthase and the Cytochrome b6/f Complexes in Limiting Chloroplast Electron Transport and Determining Photosynthetic Capacity. *PLANT PHYSIOLOGY*. doi:10.1104/pp.110.168435.

Yoshida, T., Fujita, Y., Maruyama, K., et al. (2015) Four Arabidopsis AREB/ABF transcription factors function predominantly in gene expression downstream of SnRK2 kinases in abscisic acid signalling in response to osmotic stress. *Plant, Cell and Environment*. doi:10.1111/pce.12351.

Zeng, L., Deng, R., Guo, Z., et al. (2016) Genome-wide identification and characterization of Glyceraldehyde-3-phosphate dehydrogenase genes family in wheat (Triticum aestivum). *BMC Genomics*. doi:10.1186/s12864-016-2527-3.

Zhao, Y., Wei, T., Yin, K.Q., et al. (2012) Arabidopsis RAP2.2 plays an important role in plant resistance to Botrytis cinerea and ethylene responses. *New Phytologist*. doi:10.1111/j.1469-8137.2012.04160.x.

Zhu, X.-G., Long, S.P. and Ort, D.R. (2010) Improving Photosynthetic Efficiency for Greater Yield. *Annual Review of Plant Biology*. doi:10.1146/annurev-arplant-042809-112206.

Zhu, X.-G., de Sturler, E. and Long, S.P. (2007) Optimizing the Distribution of Resources between Enzymes of Carbon Metabolism Can Dramatically Increase Photosynthetic Rate: A Numerical Simulation Using an Evolutionary Algorithm. *Plant Physiology*, 145 (2): 513–526. doi:10.1104/pp.107.103713.